SYNTHESIS OF ZEOLITIC IMIDAZOLATE FRAMEWORK ZIF-8 THIN FILMS AND MEMBRANES ON POLYMER SUBSTRATES FOR PROPYLENE/PROPANE SEPARATION

A Dissertation

by

MOHAMAD REZI BIN ABDUL HAMID

Submitted to the Office of Graduate and Professional Studies of
Texas A&M University
in partial fulfillment of the requirements for the degree of

DOCTOR OF PHILOSOPHY

Chair of Committee,	Hae-Kwon Jeong
Committee Members,	Mustafa Akbulut
	Yossef Elabd
	Hongchai Zhou
Head of Department,	Arul Jayaraman

December 2019

Major Subject: Chemical Engineering

ABSTRACT

Propylene is one of the most important chemical feedstock for the production of a variety of polymers and intermediates. The conventional thermally-driven distillation method to separate propylene, typically from propane, unfortunately are capital and energy intensive. Membrane-based system has emerged as an energy efficient alternative to the traditional distillation process. Although polymer membranes have dominated gas separation industries for over three decades, there are no commercially available polymer membranes for propylene/propane separation due to fundamental limitation of polymer such as poorly defined free volume, plasticization, etc.

Zeolitic imidazolate framework ZIF-8 with sodalite topology has been heavily investigated as propylene-selective membranes due to its well-fitted effective pore apertures (~4.0 Å), which are in between the van der Waals diameter of propylene and propane. Despite ZIF-8 potential for propylene/propane separation, their large scale applications unfortunately are impeded by the lack of simple and cost effective processing to prepare ultrathin membranes on scalable substrates. Other than inexpensive membrane processing, it is also important to increase productivity of ZIF-8 membranes by reducing membrane thickness (i.e., < 1 μm) and synthesizing the membrane on high surface-to-volume ratio (i.e., HFs) substrates.

In this dissertation, we developed two state of the art membrane processing techniques to prepare ultrathin ZIF-8 membranes on polymer HFs. PMMOF seeding and KOH-assisted solvothermal seeding process, which are based on polymer modification

strategy, enables high quality ZIF-8 seed layers to be deposited selectively on the bore side of polymer HFs. Relevant properties of ZIF-8 seed layers such as seed crystal density and seed layer thickness can be tailored through simple manipulation of alkali treatment time. Subsequent microfluidic secondary growth led to a formation of continuous and defect-free ZIF-8 membranes. The resulting ZIF-8 membranes on polymer HFs, after post-treatment, displayed propylene/propane separation factor as high as 55, satisfying the commercial requirement for propylene-selective membranes.

ACKNOWLEDGEMENTS

I would like to thank my committee chair, Professor Hae-Kwon Jeong, and my committee members, Professor Mustafa Akbulut, Professor Yossef Elabd, and Professor Hongchai Zhou for kindly offering their support and guidance throughout the course of this research.

Thanks also go to my friends and colleagues and the department faculty and staff for making my time at Texas A&M University a worthwhile experience.

Finally, thanks to my father, mother, as well as my siblings for providing me with word of encouragements throughout the entire years of my doctoral study. Without their supports, this work would not have been possible.

CONTRIBUTORS AND FUNDING SOURCES

Contributors

This work was supervised by a dissertation committee consisting of Professor Hae-Kwon Jeong [advisor] and Professor Mustafa Akbulut and Professor Yossef Elabd of the Department of Chemical Engineering and Professor Hongchai Zhou of the Department of Chemistry.

The X-ray photoelectron spectra shown in Chapter 3 was collected and analyzed by Mr. Sunghwan Park and Dr. Kieyong Cho. The polymer HFs used in Chapter 3 and 4 were fabricated by Dr. Jongmyeong Lee and Mr. Jusung Kim at Hanyang University, Republic of Korea. The rest of the work presented in this dissertation was completed by the student independently.

Funding Sources

This work was supported by the National Science Foundation (CBET-1510530 and DBI-0116835), the Qatar National Research Fund (NRRP grant #8-001-2-001), the VP for Research Office, and the Texas A&M Engineering Experimental Station.

NOMENCLATURE

ATR-FTIR	Attenuated total reflectance Fourier transform infrared
EDX	Energy dispersive X-ray spectroscopy
GPU	Gas permeation unit
HF	Hollow fiber
ID	Inner diameter
MMM	Mixed matrix membrane
MOF	Metal organic framework
OD	Outer diameter
PDMS	Polydimethylsiloxane
PMMOF	Polymer modification enabled *in-situ* MOF formation
PXRD	Powder X-ray diffraction
PVDF	Polyvinylidene fluoride
SEM	Scanning electron microscopy
TEM	Transmission electron microscopy
XPS	X-ray photoelectron spectroscopy
ZIF	Zeolitic imidazolate framework

TABLE OF CONTENTS

Page

LIST OF FIGURES

LIST OF TABLES

1. INTRODUCTION AND OVERVIEW

Propylene is the second largest chemical feedstock used in petrochemical industry behind ethylene, typically separated from propane via distillation process. Due to similarities in their physicochemical properties (e.g., boiling point and molecule size), propylene/propane fractionator (i.e., C_3 splitter) uses large number of stages (up to 200 stages or more) and operates under high reflux ratio, making it one of the most capital and energy intensive separations.[1, 2] Membrane-based system has emerged as a promising alternative to the traditional distillation process.[3] However, there are no commercially available membranes for propylene/propane separation due to limited capability of current membrane materials to provide high resolution separation and/or lack of simple and cost effective processing to prepare advanced materials into thin films and membranes on large scale.[4]

Recently, metal organic frameworks (MOFs),[5, 6] a class of porous crystalline materials have been heavily investigated for separation applications. Zeolitic imidazolate frameworks (ZIFs), a sub-family of MOFs, have shown great potential as molecular sieve membranes owing to their uniform pore sizes, permanent porosities, and exceptional chemical and thermal stabilities.[7-9] A prototypical ZIF, ZIF-8 is composed of Zn atoms connected by 2-methylimidazolate linkers, forming an open structure resembling sodalite structure of zeolite. ZIF-8 possess cavity of ~11.4 Å connected by 6-membered ring apertures of ~3.4 Å.[10] ZIF-8 is known to possess an effective pore aperture of ~4.0 Å,[11]

due to flexibility of the ZIF-8 linkers, rendering the kinetic separation of propylene from propane possible.[12]

For propylene/propane separation, the separation performances of most ZIF-8 membranes synthesized either via *in-situ* or secondary growth method reported in literature so far, outperformed that of polymer and carbon molecular sieve membranes as illustrated in Figure 1.1. In addition, their separation performances are within the 'commercially attractive' region, which is minimum propylene permeability of 1 Barrer and propylene/propane separation factor of 35 required for a commercial propylene-selective membranes as proposed by Colling et al.[13] in their patent.

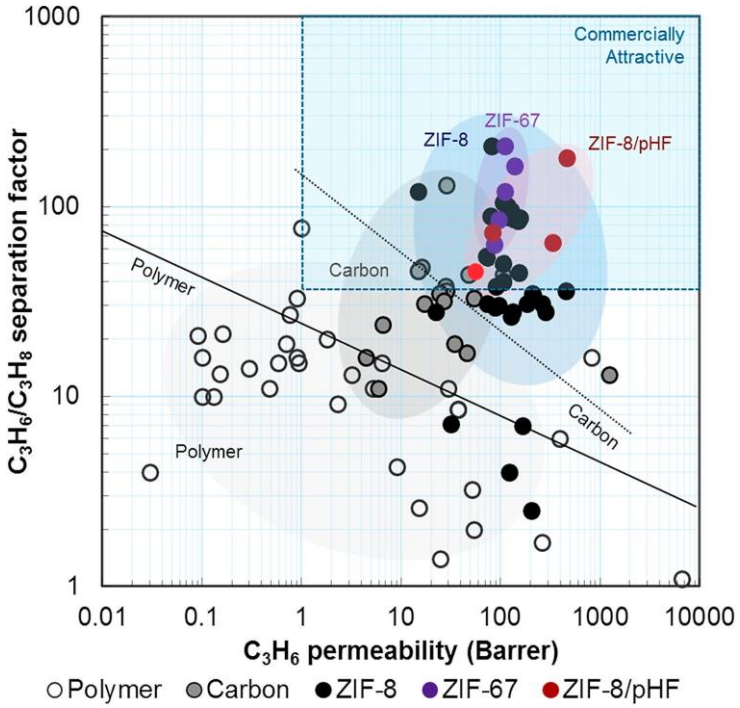

Figure 1.1 Propylene/propane separation performances of ZIF-8 membranes reported in literature. 1 Barrer = 3.348×10^{-16} mol•m/(m^2•Pa•s). The data includes polymer, carbon, and ZIF membranes (ZIF-8 and iso-structural ZIF-67 membranes grown on either organic or inorganic substrates). Modified based on ref.[10] Copyright 2018 Elsevier

Despite showing attractive propylene/propane separation performances, most of ZIF-8 membranes are grown on ceramic flat discs having low packing density. Ceramic HFs offer greater packing density, but they are fairly expensive. Inherent brittleness of ceramic HFs makes them difficult to handle and to be assembled into membrane modules. In contrast, polymer substrates are inexpensive (< $50 per sq. meter), easy to form high surface-to-volume ratio modules (i.e., HFs), and prevalent in commercial market, thereby more attractive as substrates for the synthesis of ZIF-8 membranes.[14] However, preparing high quality ZIF-8 membranes on polymer HFs especially on the bore side, intended for the challenging propylene/propane separation is a non-trivial task as evidenced by limited number of scientific works available in literature.

While using cheap and scalable substrates for the synthesis of ZIF-8 membranes is important, an equally important factor to consider is propylene throughput (i.e. productivity) of the ZIF-8 membranes. Given the sheer volume of propylene gas to be processed on industrial scale, preparing highly productive ZIF-8 membranes would definitely give the membranes competitive advantages over different types of membranes. The membrane productivity is represented by the following expression:

$$Q_A = F_A \cdot A = \frac{P_A \cdot \Delta p_A \cdot A}{l} \rightarrow (1)$$

Where F_A, P_A, and Δp_A are the molar flux of gas A, permeability of gas A, and partial pressure difference of gas A between feed and permeate sides, respectively. In above expression, membrane productivity, Q_A, that is the amount of gas A that a

membrane module element can process per unit time, depends on membrane thickness, l, and membrane surface area, A. Therefore, to obtain high throughput ZIF-8 membranes, increasing membrane surface area (i.e., using substrates with high surface-to-volume ratio such as HFs) and reducing membrane thickness are necessary.

In this dissertation, we focused on the development of new synthesis strategy to prepare ultrathin ZIF-8 membranes on polymer HFs for high performance propylene/propane separation and explored the prospect of scaling the membrane up. Two new ZIF-8 seeding strategies, namely PMMOF seeding and KOH-assisted solvothermal seeding were developed for deposition of densely packed ZIF-8 seed layers on the bore side of polymer HFs prior to secondary growth. Important synthesis variables were carefully manipulated and their effects on membrane microstructures and membrane separation performances were thoroughly studied.

This dissertation is composed of a six chapters. Chapter 2 provides introductory review of membranes for gas separation and summary of current progress in ZIF-8 membranes for propylene/propane separation. Chapter 3 is dedicated for the development of new synthetic strategies, namely PMMOF method to prepare ZIF thin films on flat polymer (i.e., polyimide) substrates. A number of characterization tools were used to understand polymer modification and ZIF formation mechanism by the PMMOF method. Important synthesis variables were manipulated and their effect on microstructures of ZIF thin films were analyzed. ZIF thin films were successfully synthesized on a variety of polyimide substrates, showing that the PMMOF method could be general.

The following Chapter 4 looks into the possibility of preparing high quality ZIF-8 membranes on a more scalable polymer HFs. PMMOF method was slightly improvised with an aim to prepare thin layer of ZIF-8 seed crystals selectively on the bore side of HFs. Subsequent microfluidic secondary growth led to a formation of well-intergrown ZIF-8 membranes. The membranes displayed excellent propylene/propane separation performances and long term stability, which are important prerequisites for their practical applications. Chapter 5 introduces a much simpler and a more scalable KOH-assisted solvothermal seeding method to deposit high quality ZIF-8 seed layers on polymer HFs prior to microfluidic secondary growth. Optimization of both seeding and microfluidic secondary growth steps were performed to improve performances of the membrane performances. Post-synthetic defect sealing with PDMS minimize membrane grain boundary defects, thereby improving membrane separation performances.

The final chapter, Chapter 6 provides conclusions and suggestion for future works.

2. BACKGROUND*

2.1. Propylene industry

Propylene is one the key component in petrochemical industry with an annual production of approximately 80 million tons and the annual production is expected to grow to 100 million tons in 2020 (Figure 2.1).[15] Propylene is used in a number of important intermediates such as polypropylene, cumene, isopropyl alcohol, acrylonitrile, propylene oxide, and other industrially relevant chemicals with polypropylene being the largest end use of propylene (55%).[16]

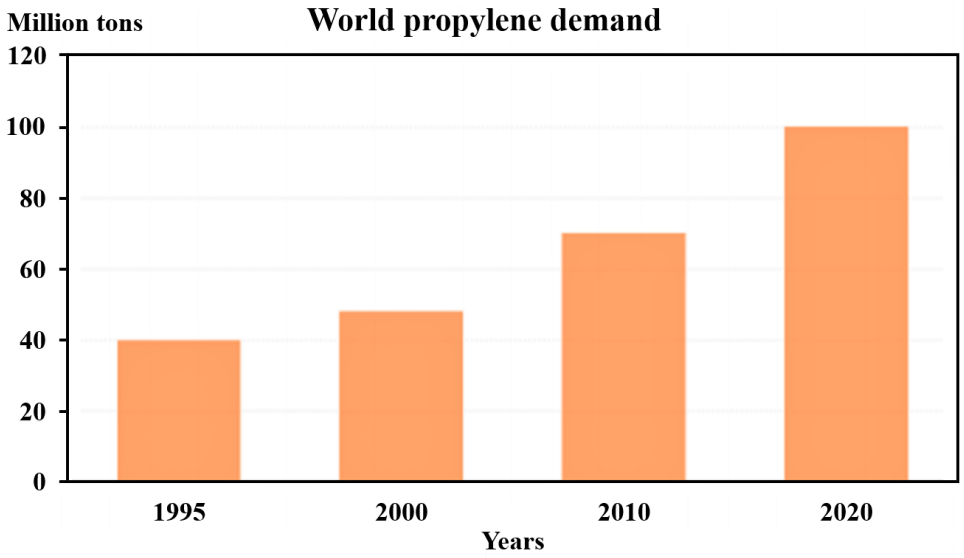

Figure 2.1 Global production of propylene. Reproduced and modified based on ref.[17] Copyright 2015 American Chemical Society

**Part of this chapter was adapted and modified with permission from Mohamad Rezi Abdul Hamid and Hae-Kwon Jeong, Korean Journal of Chemical Engineering, 2018, 35, 1577 - 1600. Copyright 2018 Springer US*

The majority of propylene is produced by steam cracking and fluidized catalytic cracking. Fluidized catalytic cracking and steam cracking account for roughly 90% of global propylene production.[18] Remaining of the supply is met by propylene on-purpose technologies such as propane dehydrogenation, methanol to propene, etc.[18, 19] Separation of propylene from propane is traditionally performed by a highly energy intensive distillation process. The low temperature distillation are performed at elevated pressure in propylene/propane fractionator that contain more than 200 trays.[1] Propylene are marketed by purity: polymer grade (minimum 99.5%), chemical grade (minimum 92% - 96%), and refinery grade (minimum 70%).[20]

2.2. Membrane materials for gas separations, which direction?

Recent study estimates that light olefin/paraffin separation (e.g., propylene/ propane) through distillation consumes approximately 120×10^{12} Btu of energy per year.[1] Given the commercial importance of propylene in chemical and petrochemical industries, a more energy efficient separation processes such as membrane, adsorption, and absorption have been proposed as alternatives to replace or augment distillation process.[21] Membrane technology in particular is promising for gas separation applications due to its inherent advantages: high stability and efficiency, low energy consumption, and easy scale-up. Sholl and Lively estimate that membrane-based system can provide up to 90% of energy saving as compared to distillation process.[22] Compact membrane modules offer operational flexibility, thereby allowing them either to function as a standalone unit or to be retrofitted into existing process units.[23-25]

Prior to considering manufacturing cost competitiveness, the most important aspect to consider in gas separation membranes is the choice of membrane materials. Economics of membrane systems are highly dependent on membrane material properties: permeability and selectivity.[26] Gas permeability determines the required membrane area for separation, whereas selectivity determines the purity and recovery of end products. Furthermore, membrane materials should be chemically, thermally, and mechanically stable.[27] Membrane robustness guarantees stable long term performances under chemically aggressive and high temperature conditions. Most importantly, membrane materials must be processible to form stable thin separating layers often supported on macroporous sub-layers that can be packaged into high surface-to-volume modules.[4] Developing next generation membranes is a subject of ongoing research and it generally falls into two categories: organic and inorganic.

2.2.1. Polymer membranes

First commercial success in gas separation membranes dates back to the 1970s. PRISM® separator, developed by Permea (currently owned by Air Products and Chemicals) is multistage polysulfone HFs membrane system designed to separate H_2 from ammonia purge gas stream.[28] This membrane technology was then extended for several different applications such as H_2 recovery in refineries and H_2/CO_2 or H_2/CH_4 syngas ratio adjustments. In the 1980s, companies like Separex (currently part of Honeywell) and Cynara (currently part of Schlumberger) started developing cellulose acetate-based membrane systems for CO_2 removal from natural gas.[4] Since then, membrane-based gas

separation has blossomed into a billion dollar industry with current market projected in the range of $1.5 billion per year and polymer membranes dominating 80 - 90% of the total membrane market sales.[29]

Polymer membranes are commercially attractive mainly due to their economic and engineering advantages. Typical fabrication cost for polymer membranes is $5 - 10 per sq. meter and $5 - 200 per sq. meter for HFs and spiral wounds, respectively.[30] Scaling-up and commercialization are not an issue because polymeric membrane fabrication technologies such as melt spinning for dense membranes and solution spinning (phase inversion) for asymmetric membranes have already reached a mature stage.[31] One of the biggest pitfalls for polymer membranes however are swelling and plasticization. Under high feed pressure, polarizable gases such as CO_2 tend to swell and plasticize the membranes, causing substantial drop in their permselectivity.[32]

Another fundamental challenge of polymer is their gas separation performances are limited by the so called 'Robeson upper bound', tradeoff between permeability and selectivity (Figure 2.2). The Robeson upper bound is a major setback in developing high-permeability-high-selectivity polymer membranes because simultaneous improvement in both selectivity and permeability is restricted. Despite extensive research to improve separation performances of polymer membranes beyond the Robeson upper bound, surprisingly, the improvement is marginal.

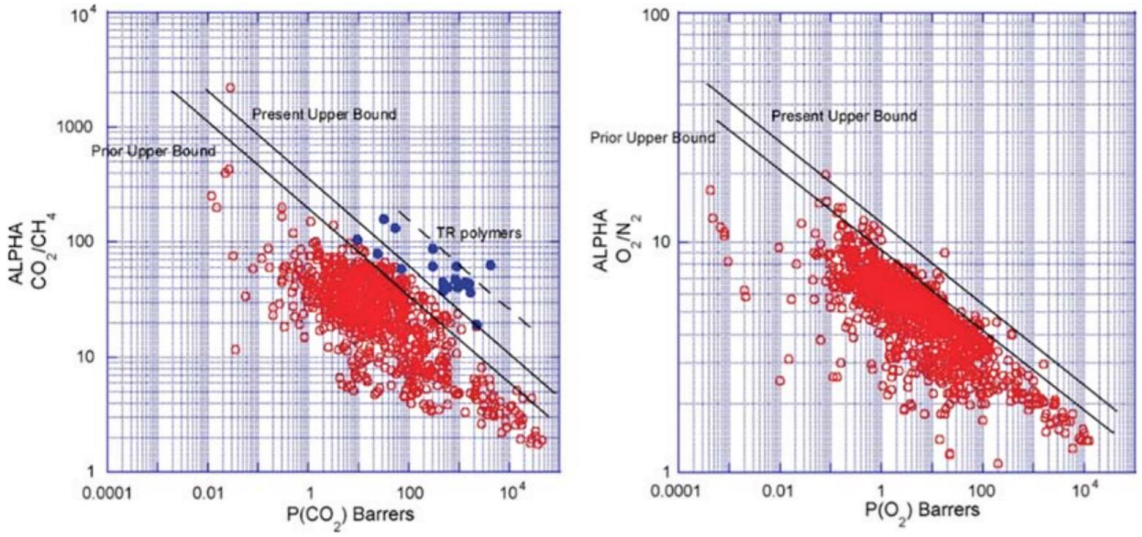

Figure 2.2 Robeson upper bound for CO_2/CH_4 and O_2/N_2 gas pairs obtained from various polymer membranes. TR represent thermally rearranged polymer. Reproduced with permission from ref.[33] Copyright 2008 Elsevier

2.2.2. Mixed matrix membranes

Other than polymer membranes, a great deal of research has been undertaken on MMMs which have the potential to overcome limitations of polymer. MMMs are composite membranes, consisting of nano-sized inorganic particles homogenously dispersed in continuous organic polymer phases. By merging desirable properties of both inorganic and organic phases, the hybrid membranes are expected to possess better gas separation performances than those of neat polymer membranes, but still maintain economic and processing convenience of polymers.[34] As shown in Figure 2.3, MMMs possess better permeability and selectivity than that of polymers, therefore could be used as a short term solution for gas separation application. However, as mentioned by Koros and co-workers[35] the ultimate solution for gas separation applications would be an evolution from current generation organic membrane materials (i.e., polymer) to next

generation inorganic membrane materials (i.e., zeolites, MOFs, metal, etc.). Successful transition from current generation to next generation membrane materials will lead to significant breakthrough in gas separation industries.

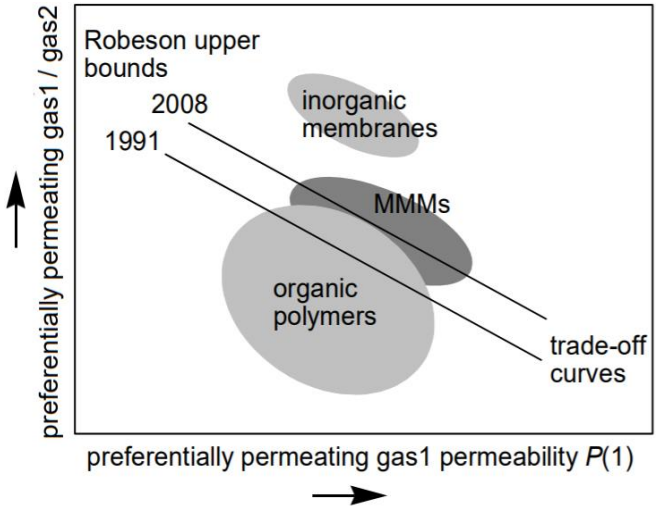

Figure 2.3 Comparison between different types of gas separation membranes - polymer, MMMs, and inorganic membranes. The actual value for the Robeson upper bound and commercially attractive region vary depending on types of gas mixture. Reproduced and modified based on ref.[36]

2.2.3. Inorganic membranes

Despite their widespread uses in gas separation industry, the majority of polymer membranes are limited to operation temperatures of 120 ^{o}C. Inorganic membranes, on the other hand, are operable at even higher temperature (e.g., between 500 ^{o}C to 900 ^{o}C for carbon and ceramic membranes).[37, 38] Despite being more expensive, chemical and thermal stability of inorganic membranes makes them a more attractive choice compared to polymer membranes for separation applications under demanding conditions.[39] Microporous zeolites with uniform sub-nanometer pores are capable of separating small gases based on size exclusion principle. Zeolites are thermally stable to over 500 ^{o}C and

chemically stable in acidic or alkaline conditions, making them an ideal membrane material for high temperature applications.[40]

Polycrystalline zeolite membranes are commonly grown on stainless steel or porous alumina supports by *in-situ* or secondary growth method.[41, 42] Numerous successful fabrication of polycrystalline zeolite membranes of CHA,[43] DDR,[44] FAU,[45] and MFI[46] types have been reported, showing promising separation performance. CMS prepared by carbonization of different polymer precursor are highly porous with open micropores interconnected with rigid slit-like ultramicropores. The ultramicropores 0.35 - 1.0 nm (depending on synthesis condition) offer enhanced entropic selectivity, while the open micropores provide relatively high diffusion coefficient.[47, 48] Gas transport mechanism in CMS membranes is predominantly via molecular sieving. CMS membranes prepared from various engineering polymers have been tested for many gas pairs, including CO_2/CH_4,[49] O_2/N_2,[50] and CO_2/N_2.[51] Other than zeolites and CMS, other inorganic membranes such as silica, metals, etc. are also heavily investigated for separation applications.

Despite the promising separation performances of inorganic membranes on laboratory scale, scaling-up inorganic membranes faces a number of challenges. First, synthesis of continuous and defect-free polycrystalline membranes is not straightforward, especially in controlling membrane microstructures and suppressing cracks and grain boundary defects.[52, 53] Second, inorganic membranes tend to be prohibitively expensive. A rough estimate of supported zeolite membranes is of the order of $1,000 per sq. meter.[54] On the other hand, cost of metal palladium membranes is around $5,000 per sq. meter.[30] Since free standing inorganic membranes are inherently brittle, rather expensive porous

inorganic supports are required, adding more cost to the membrane system.[55] Issues mentioned above along with other issues such as reproducibility greatly limit application of inorganic membranes in industrial scale membrane modules.

2.3. Zeolitic Imidazolate Frameworks (ZIFs)

2.3.1. What is ZIFs?

ZIFs,[7, 9] a sub-family of MOFs, are microporous crystalline materials comprised of tetrahedral metal centers (e.g., Zn and Co) bridged with imidazolate-based linkers forming various types of three dimensional frameworks. The metal-imidazole-metal (M-Im-M) bond angles of ZIFs are ~145°, coincidently similar to Si-O-Si bond angle of most zeolites. This has led to formation of a variety of ZIFs with zeolite type topologies (several examples are shown in Figure 2.4).[7, 8, 56] In fact, over 100 ZIF topologies have been discovered and the number is expected to keep rising in the future. Most ZIFs are thermally stable up to 500°C and displayed excellent chemical stability in many organic solvents.[7, 56] ZIFs exhibit sharp molecular sieving properties from their well-defined angstrom size pores (typically < 5 Å), making them attractive as molecular sieve membranes.[57] Several ZIF materials including ZIF-7,[58] ZIF-8,[59] ZIF-22,[60] ZIF-69,[61] and ZIF-90,[62] have been successfully fabricated as thin films or membranes, showing good separation performance for various gas pairs.

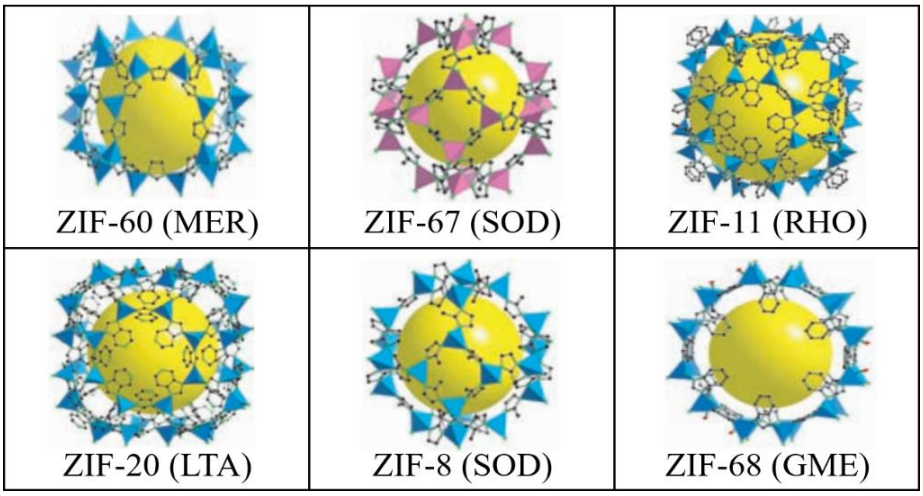

Figure 2.4 Example of crystal structures of ZIFs (three capital letters in the parenthesis correspond to zeolite structure code). Modified based on ref.[9] Copyright 2008 American Association for the Advancement of Science

2.3.2. ZIF-8 materials

ZIF-8 is constructed by linking divalent Zn ions with 2-methylimidazolate linkers forming an open structure with SOD topology. As illustrated in Figure 2.4, SOD cages (~11.4 Å) of ZIF-8 consist of six 4-membered ring apertures (~0.8 Å)[63] and eight 6-membered ring apertures (~3.4 Å).[7] It is worth mentioning that the 4-membered ring of ZIF-8 are too small for even the smallest gas molecules to pass through. Well-defined microporous cavities in ZIF-8 offer high gas diffusion coefficients, whereas their ultramicroporous 6-membered ring apertures contribute to high diffusion selectivity, making ZIF-8 an ideal candidate for molecular sieve membranes.[47]

2.3.3. ZIF-8 for propylene/propane separation

The potential of ZIF-8 for propylene/propane separation was first recognized by Li et al.[12] In their study, they found that under equilibrium condition, adsorption capacities

for both propylene and propane in ZIF-8 were identical. However, their diffusion rate coefficients were noticeably different, where the diffusion rate coefficient of propylene in ZIF-8 is 125 larger than that of propane (Figure 2.5a). Their findings suggest that ZIF-8 has potential for kinetic separation of propylene from propane. Koros and co-workers[11] later showed that effective pore apertures of ZIF-8 are larger than its crystallographically defined apertures (~3.4 Å vs. ~4.0 Å) due to linker flexibility. Based on the measured corrected diffusivities of propylene and propane in ZIF-8 (Figure 2.5b), pure ZIF-8 membranes (assuming ZIF-8 could be fabricated as defect-free membranes) theoretically will have propylene/propane selectivity of 130.

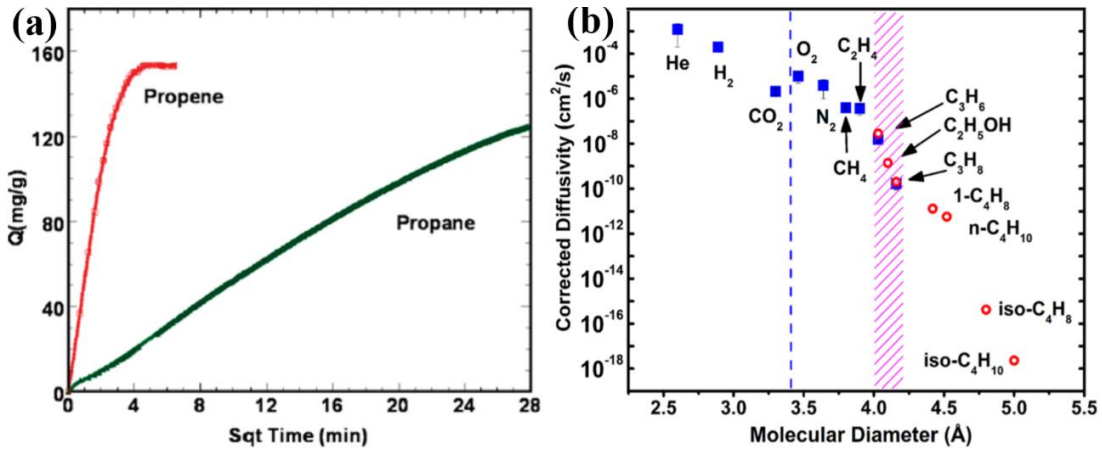

Figure 2.5 (a) propylene and propane uptake of ZIF-8 (b) corrected diffusivity of various probe gas in ZIF-8 at 35°C. Reproduced with permission from ref.[11, 12] Copyright 2009 and Copyright 2012 American Chemical Society

2.4. Membrane configuration and modules for synthesis of ZIF-8 membranes

Commercial gas separation plants require several hundred thousand sq. meter of membrane area to meet the required separation needs. Large membrane area need to be packaged efficiently into specific membrane modules depending on end uses. Plate and frame modules are among the first to be utilized for gas separations, but have been slowly

displaced by a more competitive design such as HF modules or spiral wound modules. In plate and frame modules, flat membranes and membrane spacers are alternately stacked and held together in a frame. HF modules on the other hand are made from a bundle of HFs housed inside a closed vessel.[64] Finally spiral wound modules are made from several flat sheet membrane envelopes wrapped around a central pipe core.[65]

The nature of polycrystalline membranes (i.e., brittleness) prevented them from being packaged into spiral wound modules, leaving HF modules and plate and frame modules as viable options for ZIF-8 membranes. Packing density of plate and frame modules is relatively low about 100 - 400 m^2/m^3. HF modules on the other hand offer a much higher packing density up to 10,000 m^2/m^3. In addition, HF module is a more popular choice for gas separation application as they represent up to 80% of total membrane modules used in commercial gas separation industry.[64] Therefore, using HF configuration and packaging the membrane into HF modules are likely the best way forward for commercialization of ZIF-8 membranes.

2.5. Polymer HF as substrates for synthesis of ZIF-8 membranes

An estimated price ceiling of any membranes for commercial application is approximately $200 per sq. meter.[39] In contrast, current cost of zeolite membranes is approximately $1,000 per sq. meter. It is important to note that more than 75% of zeolite membranes cost is from the use of porous ceramic supports.[54] In order for polycrystalline membranes, including ZIF-8 membranes to compete with other types of membranes on commercial scale, current cost of zeolite and ZIF-8 membranes need to be further reduced.

One way to reduce membrane overall cost is to substitute expensive ceramic supports with polymer supports. The price range of polymer supports is considerably lower: $10 for flat sheet supports and $5 for HF supports.[3] Therefore, replacing expensive ceramic substrates with HF substrates could be a better option for the synthesis of ZIF-8 membranes.

2.6. Synthesis of polycrystalline ZIF-8 membranes on polymer HFs

Regardless of substrates (i.e., flat discs or HFs), synthesis of polycrystalline membranes can be broadly classified by *in-situ* and secondary growth.

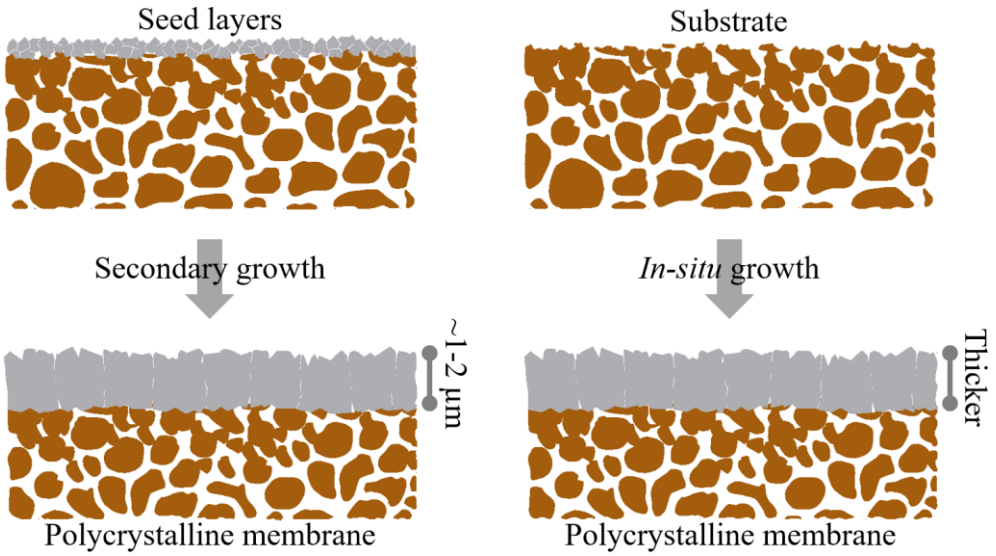

Figure 2.6 Comparison between *in-situ* and secondary growth used in the synthesis of polycrystalline ZIF-8 membranes

2.6.1. *In-situ* method

As depicted in Figure 2.6, *in-situ* growth is a one pot hydrothermal or solvothermal membrane synthesis on substrates without pre-attached seed crystals.[66] Single step synthesis offers processing convenience, making *in-situ* method a popular choice among researchers to prepare polycrystalline membranes. However, *in-situ* crystallization relies

heavily on high heterogeneous nucleation density on support surfaces in order to successfully form uniform and continuous membrane layers.[56] In some cases, substrate modification steps were performed to enhance heterogeneous nucleation on substrate surfaces. For example, Huang et al.[67] prepared continuous ZIF-8 membranes on porous α-Al_2O_3 substrates by using 3-aminopropyltriethoxysilane to promote heterogeneous nucleation and growth of ZIF-8 crystals.

2.6.2. Secondary growth method

As oppose to *in-situ* method, secondary growth method is more complicated as it involve two steps. The first step is deposition of densely packed seed crystals on substrate surfaces. The second step is solvothermal or hydrothermal growth where the seed crystals are grown into well-intergrown films or membranes.[66] In secondary growth method, seeding and growth step are decoupled, allowing each step to be optimized independently. By controlling important seed layer properties such as crystal density, crystal orientation, seed layer thickness, and seed interaction with substrates, ultrathin membranes with enhanced grain boundary structures can be prepared.[68, 69] For example, Yang and co-workers[46] have demonstrated the synthesis of *b*-oriented MFI films on planar substrates by depositing *b*-oriented MFI seed layers prior to hydrothermal growth.

In general, high quality ZIF-8 membranes can be synthesized using this method, provided that densely packed ZIF-8 seed layers were successfully deposited on the substrates prior to solvothermal or hydrothermal growth. High quality seed layers consist of densely packed seed nanocrystals uniformly covering the substrates surfaces. In

addition to high seed crystal density, strong attachment of the seed to substrates is also important to enhance mechanical stability of ZIF-8 membranes.[70] A number of seeding strategies have been proposed such as microwave assisted seeding[70] and slip/dip coating[71] to list a few. Figure 2.7 summarized criteria for high quality seed layers required for the synthesis of ZIF-8 membranes using secondary growth.

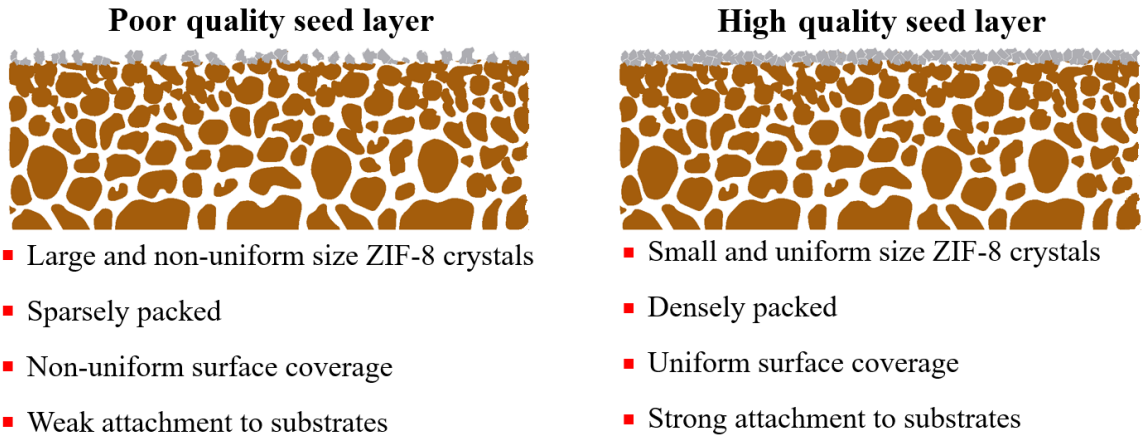

Figure 2.7 Comparison between poor quality and high quality seed layers

2.7. Different synthesis strategy to prepare ZIF-8 membranes on polymer HFs

2.7.1. Direct immersion in synthesis solution

Direct immersion of polymer HFs in ZIF-8 synthesis solution is probably the simplest method to prepare ZIF-8 membranes. In typical synthesis, pristine HF is immersed in ZIF-8 synthesis solution inside an autoclave. Temperature of the synthesis solution is tightly regulated throughout membrane synthesis. In most cases, surface functionalization/modification or additional coating layer is applied on the substrates to promote heterogeneous nucleation of ZIF-8. For example, Zhang and co-workers[72] performed ammoniation reaction on PVDF HFs (OD, 1100 µm) to introduce abundance of -NH_2 groups. Chen and co-workers[73, 74] on the other hand functionalized the PVDF HF

(OD, 1100 µm) surfaces with APTES (APTES, 3-aminopropyl-triethoxysilane) or polydopamine to form continuous ZIF-8 membranes. Terminal amine groups on the surface of PVDF react with Zn ions to form metal complex, thereby enhances heterogeneous nucleation density of ZIF-8.[74, 75] Even though both research groups use similar synthesis strategies, thicknesses of the ZIF-8 membranes were noticeably different (43 µm vs. 1 µm). Due to nature of direct immersion synthesis, nucleation and growth of ZIF-8 are mostly concentrated on shell side of HFs, rendering the synthesis of ZIF-8 membrane on confined space (i.e., bore side) of HFs challenging.

2.7.2. Continuous flow processing

In continuous flow processing, ZIF-8 precursor solutions are continuously fed through either bore or shell side of HFs for a predetermined period of time. A number of flow protocols have been developed to prepare ZIF-8 membranes on polymer HFs. To form ZIF-8 membranes on bore side of polysulfone (ID 315 µm) HFs, Coronas and co-workers[76] mixed both metal and linker precursor solutions and later fed them through the bore side at flow rate of 100 µL/min for 75 min. The as-synthesized ZIF-8 membranes (3.6 µm thick) were then tested for CO_2/CH_4 and H_2/CH_4 separations.

Marti et al.[77] on the other hand flow metal and linker precursor solutions separately to form ZIF-8 membranes on shell side of Torlon® polyamide-imide HFs (OD, 400 µm). Zn precursor solution was fed through the shell side at flow rate of 0.25 ml/min while linker precursor solution was fed through the bore side at flow rate of 0.13 ml/min. The as-synthesized ZIF-8 membranes were tested for post-combustion CO_2 capture

application. The 8.8 µm thick ZIF-8 membranes displayed CO_2 permeance of 22 GPU and CO_2/N_2 separation factor of 52.

2.7.3. Interfacial synthesis

The basic idea behind interfacial synthesis is to guide and confine ZIF-8 crystallization only at the interface between two immiscible solvents. Brown and co-workers[78] developed what they refer to as IMMP (interfacial microfluidic membrane processing) to synthesize ZIF-8 membranes on Torlon® polyamide-imide HFs for propylene/propane separation. Two immiscible precursor solutions (Zn/1-octanol and 2-methylimidazolate/water) were passed through bore and shell side of HFs housed inside a custom made reactor as shown in Figure 2.8. Total of eight flow protocols were investigated with an aim to grow ZIF-8 membranes on the bore side of Torlon® HFs but only five were found promising to prepare well-intergrown membranes.[79] Two synthesis variables were found important to prepare defect-free membranes: location of precursor solutions and flow configurations of precursor solutions (static, continuous, or combination of both). Their ~8.0 µm thick ZIF-8 membranes displayed an average propylene permeance and propylene/propane separation factor of 27 GPU and 12, respectively. In their later works, membrane microstructure optimization were carried out and the resulting ZIF-8 membranes exhibited superior performances with propylene permeance of 45 GPU and separation factor of 180.[80, 81]

Biswal et al.[82] on the other hand used isobutyl alcohol/water interfacial system to prepare ZIF-8 membranes on polybenzimidazole-based HFs (PBI-BuI HFs) for

helium/propane separation. Isobutyl alcohol with low boiling temperature allow for easier removal from the membranes and mild activation temperature. Similar to works by Brown and co-workers,[78] they can also grow the membrane selectively on preferred surface (i.e., bore or shell side) by adjusting the location of Zn and linker precursor solutions inside membrane synthesis module. The as-synthesized ZIF-8 membranes were relatively thick: 10 µm thick for ZIF-8 membrane grown on bore side and 20 µm thick for ZIF-8 membrane grown on shell side. Their membranes showed helium permeance and helium/propane separation factor of 6 GPU and 8, respectively.

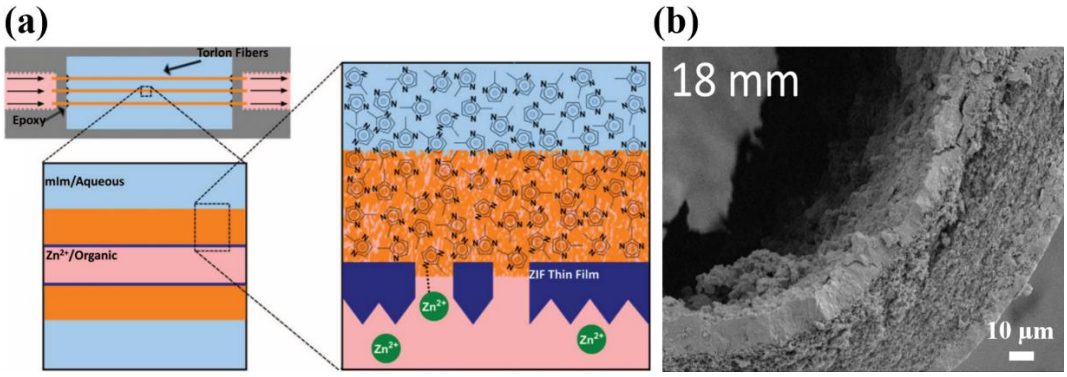

Figure 2.8 (a) schematic of IMMP approach to synthesize ZIF-8 membranes on polymer HF (b) cross sectional SEM image of the ZIF-8 membranes prepared using IMMP. Adapted from ref.[78] Copyright 2014 American Association of the Advancement of Science

2.7.4. Vapor phase synthesis

A number ultrathin ZIF-8 membranes on polymer HFs have been successfully prepared using vapor phase synthesis. In typical processing, metal precursors such as metal-oxide clusters[83] and metal-based gel[84] are deposited on substrates. Then, the substrates are exposed to ligand vapor to convert the metal precursors to ZIF-8. Relatively high temperature is required to provide sufficient ligand vapor to complete the crystallization process. Solvent free processing eliminate the use of large volume of

solvents, making vapor phase synthesis an environmentally friendly method. Li et al.[84] have successfully grown continuous and defect-free ZIF-8 layers as thin as 87 nm using gel-vapor deposition method as illustrated in Figure 2.9. Their ultrathin membranes displayed propylene permeance up to 840 GPU. In addition, they also have successfully demonstrated the formation of multiple HF membranes (30 HFs) inside membrane module. The use of solid state metal precursor to prepare ultrathin ZIF-8 membranes can be quite challenging due to high viscosity of gel. Therefore, regulating gel concentration is crucial to obtain thin and continuous gel layer prior to ligand treatment.[85, 86]

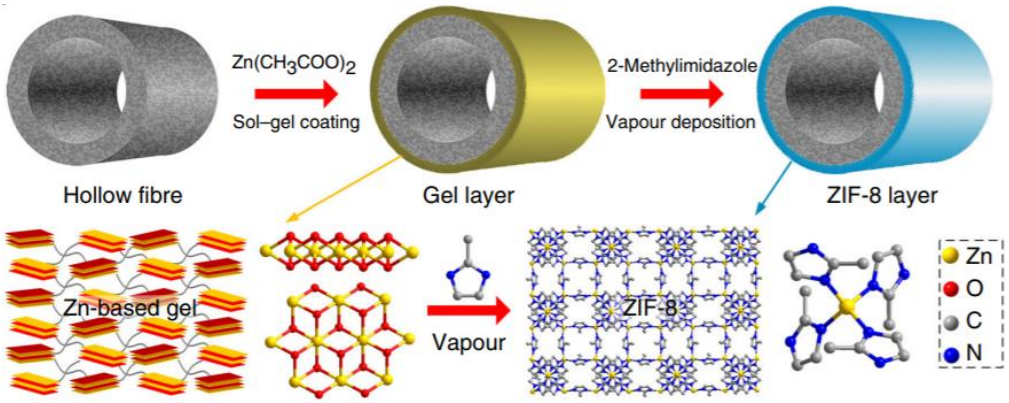

Figure 2.9 Schematic of membrane fabrication process via gel-vapor deposition method. Reproduced with permission from ref.[84] Copyright 2017 Springer Nature

2.7.5. Secondary growth

With exception of a few reports,[73, 74, 84] ZIF-8 membranes on polymer HFs synthesized using *in-situ* method mentioned above are relatively thick. For practical application, it is crucial to synthesize ultrathin ZIF-8 membranes to increase propylene throughput. Secondary growth method is attractive to prepare ultrathin ZIF-8 membranes due to decoupling between ZIF-8 nucleation and growth. To the best of our knowledge,

Jeong's group[10] is the only group to have successfully synthesized ZIF-8 membranes on bore side of polymer HFs via secondary growth.

As shown in Figure 2.10, high quality ZIF-8 seed layers were rapidly deposited on bore side of Matrimid® HFs (ID, 344 μm) under microwaves. First, Zn precursor solution was passed through bore side at flow rate of 0.33 ml/min to saturate the substrates. Then, the HFs were subjected to microwave irradiation for 90 s while flowing linker precursor solution through the bore side of HFs. Increasing linker concentration was found important to synthesize uniform nanometer-sized ZIF-8 seed crystals. Microfluidic secondary growth conducted at room temperature led to formation of defect-free ZIF-8 membranes strongly attached to Matrimid® HF surfaces. The as-synthesized membranes were relatively thin (~800 nm) and showed decent propylene permeance (55 GPU) and propylene/propane separation factor (46).

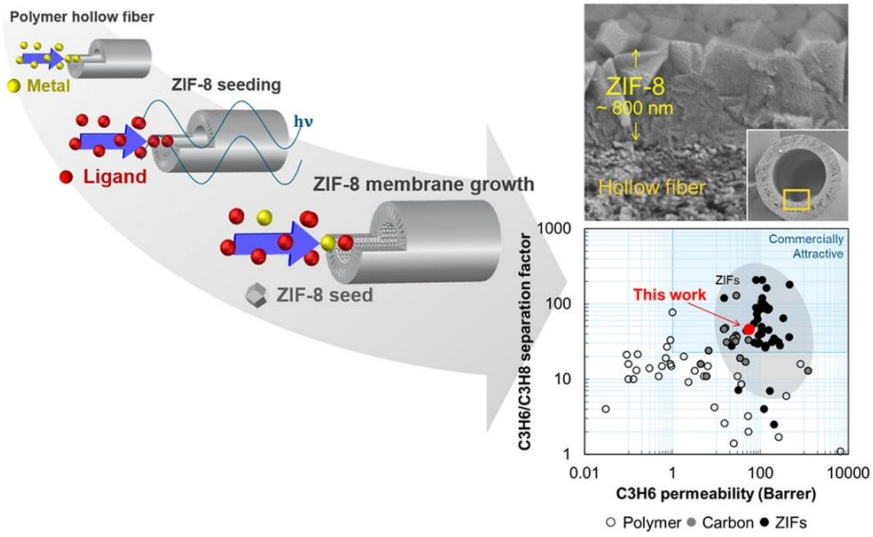

Figure 2.10 Schematic illustration of microwave assisted seeding and microfluidic secondary growth to prepare ultrathin ZIF-8 membranes on Matrimid® HFs. Reproduced from ref.[10] Copyright 2018 Elsevier

2.8. Repairing ZIF-8 membrane defects

Gas transport through the polycrystalline ZIF-8 membranes are dominated by selective diffusion through ZIF-8 crystal grains and non-selective diffusion through ZIF-8 grain boundary (considered as defects).[87] Grain boundary structures of each membrane, even though the membranes were synthesized using similar synthesis protocol could be drastically different. This is attributed to the fact that controlling grain boundary structures and defect density of polycrystalline membranes is challenging. This is a huge issue that need to be addressed before consider membrane scale-up. A sufficiently poor grain boundary structures can be disastrous to ZIF-8 membrane separation performances. Facile post-treatment of ZIF-8 is useful to minimize the defects, thereby restoring/improving the performances of the membranes.

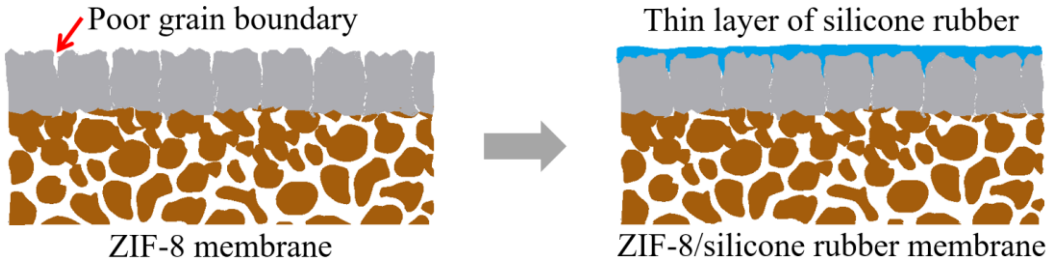

Figure 2.11 Schematic of silicone rubber coating strategy to minimize micro-defects in ZIF-8 membranes

A common engineering practice to eliminate micro-defects in membranes is through caulking method as demonstrated by Henis and Tripodi in their patent.[88] This method has been used by a number of researchers to seal grain boundary defects polycrystalline membranes. As presented in Figure 2.11, a thin layer of highly permeable material such as silicone rubber is coated on top of ZIF-8 membrane layer to plug possible micro-defects. Sheng and co-workers[87] applied a thin layer of polydimethylsiloxane

(PDMS) on top of ZIF-8 membrane layer to improve separation performances of the membranes, making them more selective towards propylene. PDMS is more permeable towards propylene than ZIF-8 (7,200 Barrer vs. 390 Barrer measured at 35^{o}C) but not selective towards propylene.[11, 89]

A sufficiently thin PDMS layer deposited on top of ZIF-8 membrane layer will not significantly affect propylene flux and propylene/propane separation factor of the membranes. However, the PDMS can block poor inter-crystalline defects of ZIF-8 membranes, resulting in improvement in separation factor. ZIF-8 is inherently hydrophobic with abundance of organic linkers. Therefore, ZIF-8 is expected to form an intimate interface with hydrophobic PDMS.[90] In their work, Sheng et al.[87] observed significant improvement in propylene/propane separation factor after PDMS coating step. For example, propylene/propane separation factor of ZIF-8 membranes as low as 2 increased to 45 after PDMS coating layer was applied.

2.9. Imide ring opening of polyimide

Polyimides is an engineering polymers characterized by the presence of imide groups in polymer backbone. Polyimides are generally synthesized through poly-condensation reaction between dianhydrides and diamines.[32] Polyimides have high T_g (> 250 ^{o}C) and chemically stable.[28, 91] Basic chemistry behind imide ring opening of polyimide is illustrated in Figure 2.12. Imide rings of polyimide (i.e., PMDA-ODA) are hydrolyzed with KOH to form carboxylic acid groups complexed with K ions. Imide ring opening reactions can be confirmed using FTIR spectroscopy. The FTIR spectra of

hydrolyzed polyimides shows disappearance of carbonyl bands of imide groups and appearance of new bands in the region of 1500 cm^{-1} - 1700 cm^{-1} of amide groups.[92] It is found that the K ions complexed with carboxyl groups can be ion-exchanged with metal ion of interest.[92-94] K ions in modified polymer layer can be replaced with another ions such as Ag, Cu, and Co ions, while maintaining electroneutrality of the system. By using inductive coupled plasma atomic emission spectroscopic measurements, Akamatsu et al.[92] have demonstrated that the ion exchange between K ions in the KOH-modified polyimides and Cu ions in aqueous solution proceed in a stoichiometric manner (1:2 ratio).

In the past, imide ring opening of polyimide using base (e.g., KOH, NaOH, etc.) were performed to modify surface properties or deposit thin metal films on polyimide surfaces.[95] For example, Lee et al.[96] hydrolyzed the surface of BPDA-PDA polyimide with KOH to increase surface wettability of the polyimide. After modification by KOH, water contact angle decrease from 79^{o} to 49^{o}, indicating that the surface become more hydrophilic. Yin and co-workers[93] on the other hand explored the formation of highly reflective and conductive Ag thin films on polyimide substrates by annealing the Ag-doped polyimide substrate at 250^{o}C for 30 min. During annealing process, the Ag ions complexed with carboxyl groups of polymer were reduced to form continuous Ag clusters on the surface. More recently, Tsuruoka et al.[97] used imide ring opening chemistry to form MIL-53 (Al) thin films on PMDA-ODA substrates under microwaves. In their works, the Al ions immobilized in KOH-modified polyimide layer were liberated using counter ions and the Al ions later reacted with organic linkers to form MIL-53 (Al) thin films.

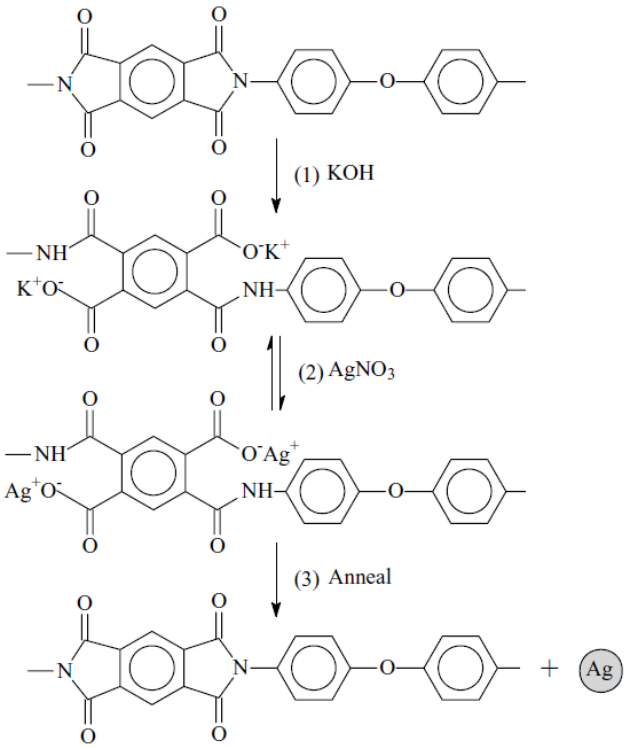

Figure 2.12 Imide ring opening of PMDA-ODA polyimide using aqueous KOH solution. Reproduced with permission from ref.[93] Copyright 2004 Elsevier

2.10. PVDF dehydrofluorination reactions

PVDF have excellent chemical stability against most chemicals and solvents but their chemical stability are not particularly great against strong base.[98] Reaction between PVDF and strong base led to elimination of hydrogen fluoride groups (commonly referred as PVDF dehydrofluorination) and formation of carbon carbon double bonds and hydroxyl bonds. Figure 2.13 shows the generally accepted PVDF dehyrofluorination reaction pathway.[99] Formation of C=C and -OH bonds are confirmed by FTIR spectroscopy. The base-modified PVDF exhibit two broad FTIR peaks between 1650 cm^{-1} - 1550 cm^{-1} and 3300 cm^{-1} - 3500, that can be assigned to C=C and -OH bonds, respectively.[100]

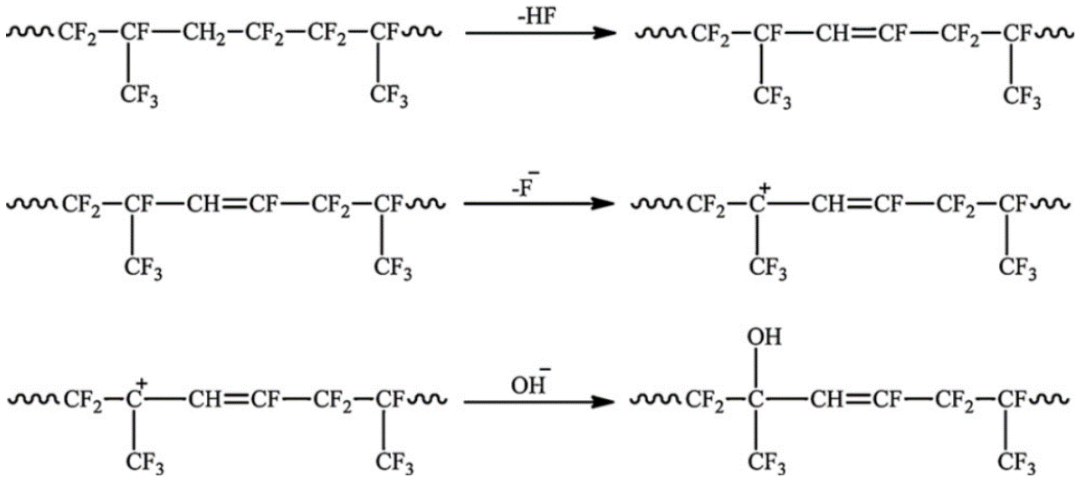

Figure 2.13 Possible PVDF dehydrofluorination reaction pathway. Reproduced with permission from ref.[99] Copyright 2011 Elsevier

Dehydrofluorination of PVDF polymer chain led to discoloration from white to brown and later to dark brown upon immersion in hot alkaline solution for several hours.[101-103] The PVDF dehydrofluorination reactions can be accelerated by manipulating exposure time, concentration, temperature, etc. Other than enhancing polymer adhesion properties, PVDF dehydrofluorination reaction has been used to increase hydrophilicity of PVDF.[104, 105] Piaagio and co-workers[106] investigated effect of hot KOH treatment on hydrophilicity and water separation properties of flat PVDF membranes. Upon modification with KOH, the water contact angle of the modified-PVDF decrease to 68^{o} and the membranes exhibit higher water flux than those of unmodified PVDF membranes.

3. IN-SITU FORMATION OF ZIF THIN FILMS AND COMPOSITES USING MODIFIED POLYMER SUBSTRATES*

3.1. Introduction

MOFs with unique properties have drawn considerable attention for a variety of advanced applications including gas storage,[107] separation,[108] sensing,[109] and catalysis.[110] ZIFs,[7, 111] a sub-class of MOFs, are one of the most widely studied MOFs on account for their ultramicroporosities (< 5.0 Å) and chemical/thermal stabilities relative to other MOFs. ZIFs are typically constructed by linking divalent metal ions (e.g., Zn and Co ions) with imidazolate-based linkers forming open structures analogous to those of zeolites. While MOF materials are readily applicable in bulk/powder forms as adsorbents and catalysts,[112, 113] advanced applications including film-based sensors and separation membranes require them to be fabricated as thin films typically supported on substrates[114, 115] or composites with other materials.[3]

To date, MOF thin films have been predominantly grown on inorganic ceramic supports especially for membrane applications.[59, 116-118] Ceramic supports are, however, relatively expensive, thereby increasing the cost of MOF thin films. In contrast, polymer substrates are cheap, scalable, and more readily available in commercial market, thereby

**This chapter was adapted and modified with permission from Mohamad Rezi Abdul Hamid, Sunghwan Park, Jusung Kim, Young Moo Lee, and Hae-Kwon Jeong, Journal of Materials Chemistry A, 2019, 7, 9680 - 9689. Copyright 2019 Royal Society of Chemistry*

more attractive for MOF thin films and composites. Nevertheless, there are only a limited number of reports on the synthesis of MOF thin films on either dense or porous polymer substrates. Typical synthesis methods to form MOF thin films include *in-situ*,[119-121] secondary growth,[122-125] layer-by-layer,[126] and interfacial growth.[80, 127] Centrone et al.[128] were the first to report MOF thin films on polymer supports under microwave irradiation. They found that conversion of the nitrile groups of polyacrylonitrile substrates to carboxylic acid groups was a requisite for nucleation and growth of MIL-47 crystals on the substrates.

Wang and co-workers[129] reported synthesis of ZIF-8 thin films on porous nylon substrates using counter-diffusion method. Nagaraju et al.[130] have demonstrated the formation of Cu-BTC and ZIF-8 thin films on porous asymmetric ultrafiltration polymer membranes using *in-situ* crystallization, followed by layer-by-layer deposition to form continuous MOF layers. Nair and co-workers[78] reported synthesis of ZIF-8 membranes on Torlon® HFs using the interfacial microfluidic membrane processing where two immiscible solvents (octanol-water) interfacial approach can be precisely controlled to achieve a positional control over ZIF-8 membrane formation. To enhance heterogeneous nucleation of MOFs on polymer substrates, intermediate coating layers such as 3-aminopropyl-triethoxysilane-functionalized TiO_2[74] or Zn-based gel[84] were often utilized, resulting in ultrathin ZIF-8 membranes.

Although these reports demonstrate successful preparation of MOF thin films and membranes on polymer substrates, multiple synthesis steps (e.g., repeated growth cycles, substrate functionalization, intermediate coating layers, etc.) add a degree of complexity,

thereby increase the cost of resulting membranes. In addition, most of literature report on the synthesis of MOF thin films on polymer flat sheets that have low packing density. Furthermore, with a few exceptions,[10, 76, 78, 80] deposition of MOF thin films were typically performed on and limited to easily accessible external surfaces only. For practical applications especially in separation, it is critical to synthesize MOF thin films on substrates with high surface-to-volume ratio (i.e., HFs) to provide high packing density. In addition, MOF thin films grown on the bore side of HFs have advantage where these fibers can be bundled together in close proximity without compromising the relatively fragile MOF layers, to form membrane modules with high packing density. However, synthesizing MOF thin films in a confined space (i.e., bore side) of the HFs is more challenging than growing on easily accessible external surface (i.e., shell side), as evidenced by the very limited number of scientific works available in literature.

Recently, Tsuruoka et al.[97] reported a general methodology for the formation of Al-based MOF (MIL-53) films on pyromellitic dianhydrides oxidianiline (PMDA-ODA, trademarked as Kapton®) polymer substrates based on an interfacial reaction approach using metal-doped polymers as substrates under microwave irradiation. A PMDA-ODA polyimide film was first hydrolyzed in aqueous KOH solution, resulting in a potassium polyamate salt containing potassium carboxylate groups. Potassium ions were then ion-exchanged with aluminum ions. Subsequent microwave heating of the Al ion-exchanged polyamate salt in a 1,4-benzenedicarboxylic acid linker solution led to interfacial self-assembly of MIL-53 crystals on the modified polymer substrate. Thickness and crystal density of the resulting MOF thin films were readily controlled by manipulating alkali

treatment time and Al ion elution rate, respectively. In their later works,[131, 132] they were able to control the morphology and anisotropic growth of Cu-based MOF (Cu-based MOF = $[Cu_2(ndc)_2(dabco)]_n$, ndc = 1,4-naphthalene dicarboxylate, dabco = 1,4-diazabicyclo (2.2.2) octane) thin films on PMDA-ODA substrates by controlling linker concentration in synthesis solution. Although interfacial growth approach is expected to be a versatile strategy for the construction of MOF films on polymer substrates, there are no reports on successful fabrication of ZIF thin films using a similar approach. Moreover, the current interfacial reaction approach by Tsuruoka and co-workers[97] resulted only in MOF film formation on polymer surfaces. It is often desirable to form MOF crystals inside polymer substrates (i.e., mixed matrix composite films) as the resulting composites offer new features and functionalities that can be applied for advanced applications such as mixed matrix membranes.[3]

Herein, we report facile *in-situ* preparation of well-intergrown ZIF thin films on polyimide surfaces as well as well-dispersed ZIF nanoparticles inside the polymers (i.e., ZIF/polymer composites) using a modified interfacial reaction approach. Instead of relying on combination of counter ions and high temperature condition (enabled by microwave heating) to liberate the strongly coordinated Zn ions with carboxylic groups in modified polymer layer, our method takes advantage of free Zn ions present in polymer free volume, thereby enabling the formation of ZIF thin films and composites at a relatively lower temperature without using counter ion species in the linker solution. In addition, it is found that one can form ZIF-8 thin films on different polyimide substrates with various geometries including HFs. In this work, we focus primarily on ZIF-8, ZIF-

67 (Co-substituted ZIF-8), and Zn/Co mixed metal ZIF-8 analogues which are of particular interest for gas separation applications. Using ZIF-8 thin films on Matrimid® HF as seed layers, well-intergrown ZIF-8 membranes were prepared by secondary growth and tested for propylene/propane separation.

3.2. Experimental section

3.2.1. Materials

Kapton® films (PMDA-ODA, 50 µm thick, DuPont) were purchased and used as received. Matrimid® 5218 powder was kindly provided by Huntsman Advanced Materials. Potassium hydroxide (KOH, reagent grade, VWR International) was used as a hydrolyzing agent. Zinc nitrate hexahydrate ($Zn(NO_3)_2 \cdot 6H_2O$, 98%, Sigma-Aldrich), cobalt nitrate hexahydrate ($Co(NO_3)_2 \cdot 6H_2O$, 98%, Sigma-Aldrich), and 2-methylimidazole ($C_4H_6N_2$, 99%, Sigma-Aldrich, hereafter HmIm) were used as metal and linker sources, respectively. Sodium formate (HCOONa, 99%, Sigma-Aldrich) was used as a deprotonating agent. Methanol (CH_3OH, > 99%, Alfa-Aesar), ethanol (C_2H_5OH, 94 - 96%, Alfa-Aesar), dimethylformamide (C_3H_7NO, > 99%, Alfa-Aesar, hereafter DMF), tetrahydrofuran (C_4H_8O, > 99%, Alfa-Aesar, hereafter THF), hexane (C_6H_{14}, ACS grade, VWR International), and deionized water were used as solvents. All chemicals were used as received without further purification.

3.2.2. Methods

3.2.2.1. Preparation of porous Matrimid® flat sheets and HFs

Porous Matrimid® HFs were fabricated by a dry-wet jet spinning process following a procedure previously optimized and reported.[133] Dope and bore solution compositions as well as spinning parameters were appropriately manipulated to obtain HFs with porous structure on both bore and shell side. Asymmetric Matrimid® flat sheet substrates were prepared by the dry-wet phase inversion method. The polymer dope solutions were prepared by dissolving Matrimid® 5218 powder (1.25 g, 25.0 wt.%) in a THF (0.86 g, 17.2 wt.%) and DMF (2.59 g, 51.8 wt.%) co-solvent mixture.

The co-solvent of volatile THF and nonvolatile DMF with 1:3 ratio was used to increase local polymer concentration at polymer surface during drying step, forming asymmetric structures. A non-solvent, ethanol (0.30 g, 6.0 wt.%) was added to the mixture to increase phase inversion rate. Mixing process was done at room temperature overnight. The dope solution was poured on a flat glass substrate and casted using a film casting knife with clearance of 346 µm. The volatile components were evaporated for 15 s in air. Then, the as-casted film was immediately immersed in water at 25^{o}C for 24 hrs. The film was solvent exchanged in ethanol for 30 min and then in hexane for 30 min. Finally, the film was dried at room temperature in air for 1 hr and further dried at 60^{o}C for 2 hrs.

3.2.2.2. Surface modification and metal doping of polymer substrates

Modification and ion-exchange of Kapton® and Matrimid® films were performed following a procedure reported by Tsuruoka et al.[97] with a slight adjustment. Pristine

Kapton® and Matrimid® films (2.5 × 2.5 cm^2) were treated in a 5 M aqueous KOH solution at 50°C for different periods of time and then rinsed with deionized water. One sides of the films were sealed with epoxy to ensure surface modification take place only on the exposed sides. Next, the films were immersed in a 100 mM aqueous zinc nitrate hexahydrate solution for 1 hr. The films were then rinsed with deionized water. Excess metal solution and deionized water on the films were carefully removed using Kimwipes.

3.2.2.3. Solvothermal formation of ZIF-8 crystals on and in polymer substrates

To form ZIF-8 crystals on and inside polymer substrates, the Zn-doped polymer films were solvothermally treated in a linker solution based on our previously reported recipe with a minor modification.[118] Briefly, a linker precursor solution was prepared by dissolving 2.59 g of HmIm and 0.125 g of sodium formate in 30 ml of methanol (hereafter, linker solution). A Zn-doped polymer film was positioned vertically in a Teflon-lined autoclave containing the linker solution. The autoclave was kept in a convection oven at 120°C for 2 hrs. The sample was then rinsed with methanol several times and washed with fresh methanol overnight.

3.2.2.4. Characterization

PXRD patterns were collected using a Rigaku Miniflex II powder X-ray diffractometer with Cu-Kα radiation (λ = 1.5406 Å). ATR-FTIR spectra were obtained using a Thermo Nicolet iS5 with a diamond ATR sampling accessory, accumulating total of 16 scans from 400 cm^{-1} to 4000 cm^{-1} with a resolution of 0.241 cm^{-1}. XPS spectra were

collected on an Omicron XPS system with a DAR 400 dual Mg/Al X-ray source. SEM micrographs were obtained using a JEOL JSM-7500F operating at 5 keV acceleration voltage and 15 mm working distance. EDX line profile analysis was performed using an Oxford EDS system operated at 20 keV acceleration voltage and 8 mm working distance. TEM micrographs were obtained using a FEI Tecnai F20 electron microscope equipped with a thermal (Schottky) field-emission gun. Electron transparent specimens were prepared prior to imaging. Briefly, the samples were embedded in an epoxy resin and allowed to cure for 24 hrs. under heat. The resin block was then silver sectioned (i.e., 60 - 90 nm thick) using a Leica UC7 ultramicrotome. Then, the thin sections were collected and transferred directly on a 300 mesh copper grid.

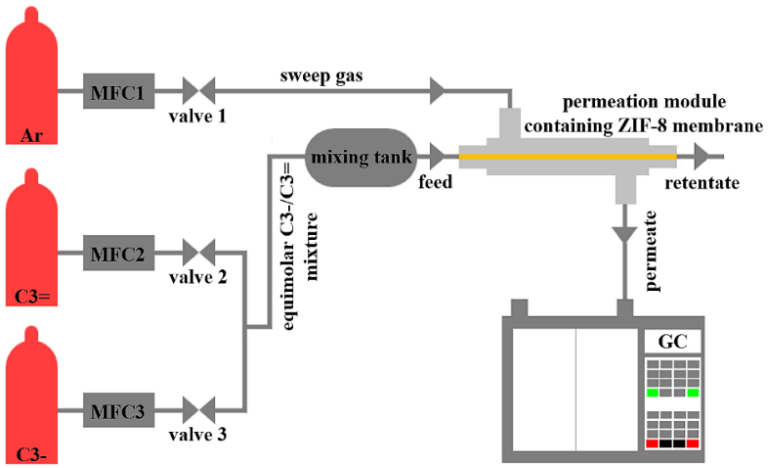

Figure 3.1 Schematic illustration of the Wicke-Kallenbach setup for binary propylene/propane permeation measurements

The gas separation properties of ZIF-8 membranes on Matrimid® HFs were determined using the Wicke-Kallenbach technique carried out at room temperature (~22°C) under atmospheric pressure (setup for permeation measurement is shown in Figure 3.1). An equal molar propylene/propane mixture was supplied to bore side while

argon sweeping gas was flowed to shell side. Volumetric flow rates of both feed and sweep gases were set at 3.33×10^{-1} ml/s. The composition of the permeate stream was analyzed using a gas chromatography (Agilent GC 7890 A) equipped with a HP-PLOT/Q column.

3.3. Result and discussion

Figure 3.2 presents a schematic illustration of the modified interfacial reaction process, what we refer to as the PMMOF process. As shown in the illustration, the process starts with alkali induced cleavage of imide rings of a pristine Kapton® polyimide (hereafter, KAP) or any polyimides, forming carboxylates which can serve as ion-exchangeable sites. It is noted that as illustrated in Figure 3.2, only a part of the polyimide (typically less than 5 μm) was hydrolyzed. Immersion of the KOH-modified film into an aqueous metal solution (e.g., Zn, Co, Ag, etc.) initiates ion-exchange of K ions with the metal ions of interest. It is noted that the formation of a polyamic acid potassium salt enhances the hydrophilicity of the film, facilitating the diffusion of Zn ions into and inside the film.[134]

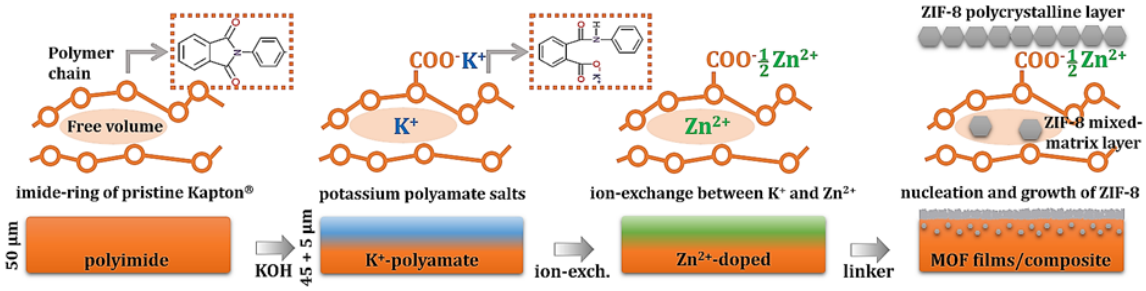

Figure 3.2 Schematic illustration of the PMMOF approach enabling the solvothermal formation of ZIF-8 thin films on polymer substrates. It is noted that ZIF-8 crystals also form inside polymer substrates, depending on processing conditions

As depicted in Figure 3.2, there are two different type of Zn ions: those relatively strongly coordinated with carboxyl groups as well as those free (i.e., unbound) in the hydrophilic free volume. Upon the *in-situ* solvothermal treatment of the Zn-polyamate salt in a HmIm linker solution, only free Zn ions elude from the free volume, resulting in the formation of continuous ZIF-8 layers on polymer surface as well as ZIF-8 crystals inside the polymer. The coordinated Zn ions on the other hand do not seem to participate in the formation of the ZIF-8 crystals (will be discussed in later section). It is noted that even after extensive attempts, it was not possible to obtain ZIF-8 thin films using microwave heating as reported by Tsuruoka et al.[97] PMMOF process is expected to be readily extended for the fabrication of MOF thin films on any polymer substrates, provided that the substrates are capable of undergoing similar chemistry.

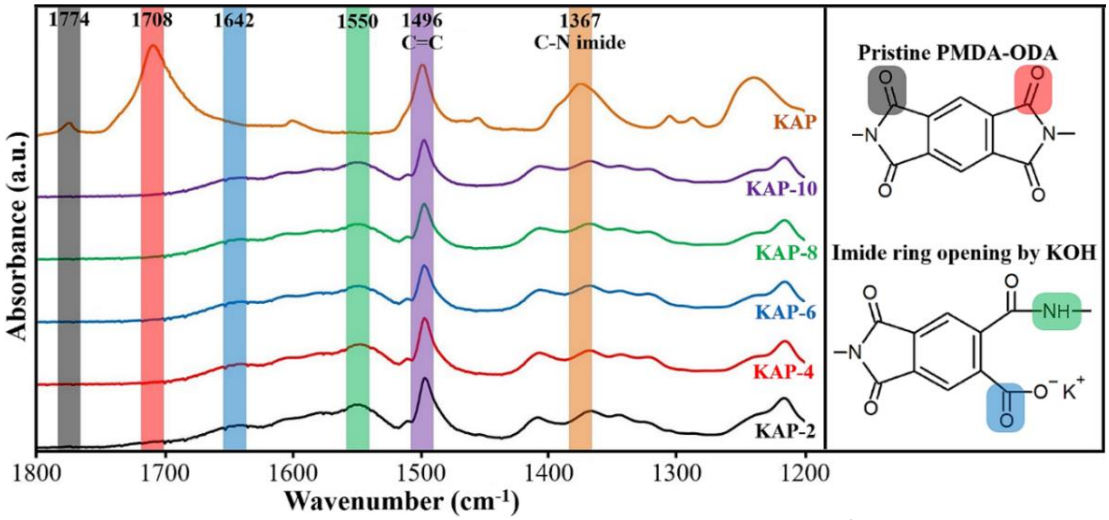

Figure 3.3 ATR-FTIR spectra of a pristine and hydrolyzed Kapton® films

Figure 3.3 and Figure 3.4 presents the ATR-FTIR spectra of pristine Kapton®, KOH-treated Kapton® (hereafter, KAP-X, X represents KOH treatment time in minutes), Zn ion-exchanged Kapton®, and ZIF-8 crystals grown on the KOH-modified Kapton®.

The pristine film exhibited characteristic absorption bands at wavenumbers of 1774 cm^{-1}, 1708 cm^{-1}, and 1367 cm^{-1}, which correspond to symmetric C=O, asymmetric C=O, and C-N-C vibration modes, respectively. The hydrolysis reaction by aqueous KOH led to imide ring cleavage, thus resulting in significant reduction of the C=O imide absorption bands (1774 cm^{-1} and 1708 cm^{-1}). There appeared new broad peaks at 1500 cm^{-1} - 1700 cm^{-1}, which were superposition of carboxyl groups complexed with K ions (1500 cm^{-1} - 1600 cm^{-1}), C=O amide (1642 cm^{-1}), and N-H amide (1550 cm^{-1}) modes of the resulting polyamic metal salt.[92, 94, 135]

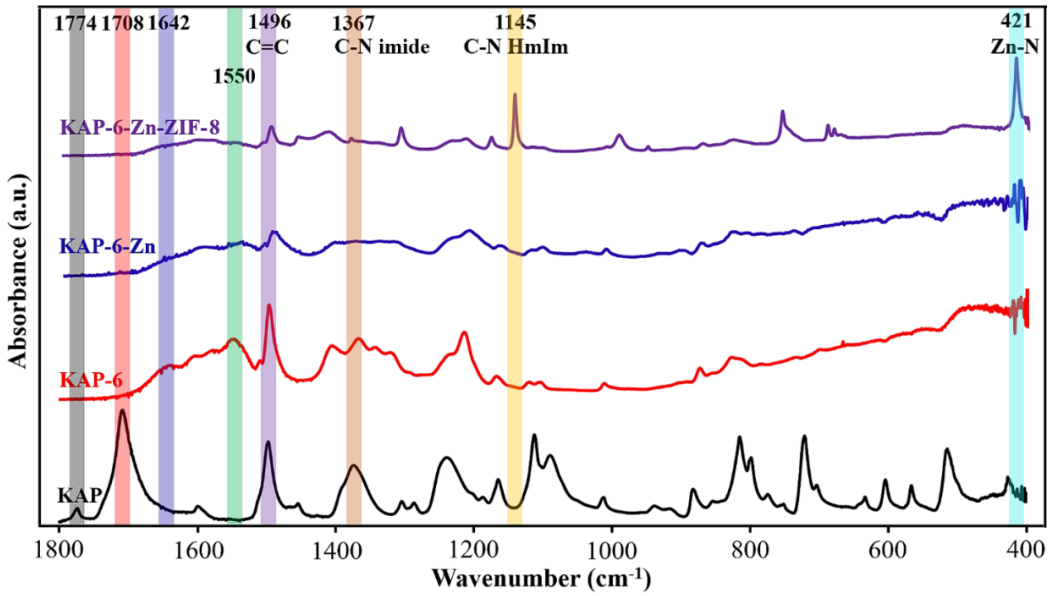

Figure 3.4 ATR-FTIR spectra of a pristine Kapton® film (KAP), hydrolyzed film for 6 min (KAP-6), Zn ion-exchanged film (KAP-6-Zn), and ZIF-8 crystals grown on modified Kapton® films (KAP-6-Zn-ZIF-8)

A prolonged alkali hydroxylation reaction greater than 15 min led to degradation of the substrates, thereby compromising their physical properties.[136] Immersion of the KOH-treated films in aqueous Zn solution resulted in ion-exchange between K and Zn ions and diffusion of Zn ions into the hydrophilic free volume. Although the ATR-FTIR

spectra of both KOH-treated and Zn ion-exchanged film (hereafter, KAP-X-Zn for X min in KOH) were mostly indistinguishable, a decrease in absorption intensity of the spectra and formation of complex features in the region between 1500 cm^{-1} - 1600 cm^{-1} suggest the existence of several coordination states around Zn ion complexes.

The KAP-X-Zn was then solvothermally treated in a HmIm linker solution to form continuous ZIF-8 layers (hereafter, KAP-X-Zn-ZIF-8). As shown in Figure 3.4, two new bands at 1145 cm^{-1} and 421 cm^{-1} appear, that can be assigned to the C-N and Zn-N bands of ZIF-8. Formation of ZIF-8 crystal layers on the polymer substrates were also confirmed by PXRD patterns shown in Figure 3.5. All samples exhibit superimposed diffraction patterns of ZIF-8 and pristine Kapton® film. Interestingly, diffraction intensities of the characteristic ZIF-8 peaks increase with hydrolysis time. The samples exhibit relatively similar degree of peak broadening, indicating the formation of ZIF-8 nanoparticles regardless of hydrolysis time.

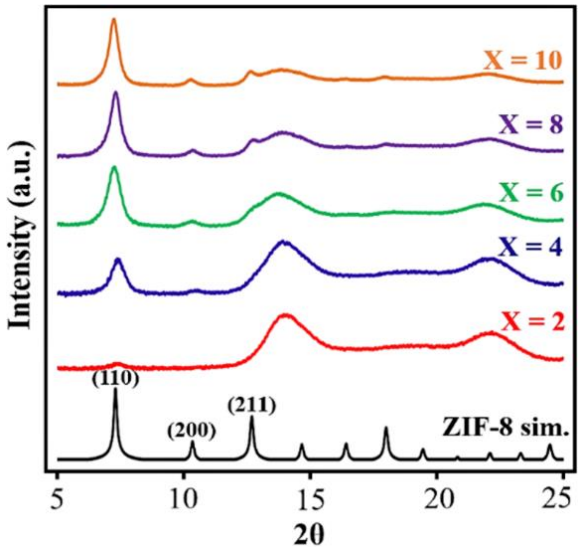

Figure 3.5 PXRD patterns of ZIF-8 films synthesized over different KOH treatment time in comparison with the simulated one (KAP-X-Zn-ZIF-8)

A plot of the relative (110) intensity provides a preliminary mean to estimate relative increment in the amount of ZIF-8 nanocrystals formed as hydrolysis time increases. Since the concentration of Zn ions in the polymer is relatively low as compared to that of the linker, the number of ZIF-8 nanocrystals formed is expected to be limited by concentration of Zn ions. The relative intensities of the (110) reflection are, therefore, directly related to the relative increment in Zn ion content in the modified polymer layer with respect to KOH treatment time. As shown in Figure 3.6, relative (110) intensity increases linearly with degree of KOH hydrolysis, suggesting a systematic increment in Zn ion content in polymer substrates. This result agrees well with those previously reported.[92, 97, 134]

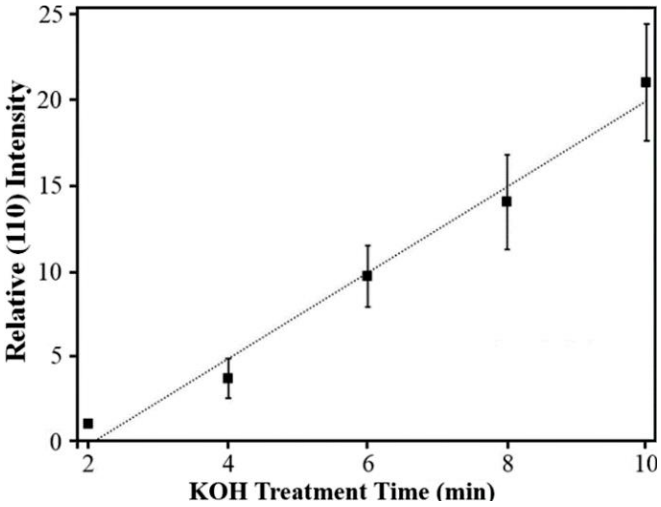

Figure 3.6 Relative (110) intensity of KAP-X-Zn-ZIF-8 (X represents KOH treatment time in minutes) with respect to that of KAP-2-Zn-ZIF-8

Extending hydrolysis reaction increases the number of K ions in modified polymer layer. During ion-exchange process, the monovalent K ions were replaced with divalent Zn ions. Also, the presence of more carboxylates due to longer KOH treatment enhances

hydrophilicity of the substrates, which later facilitates mobility and amount of free Zn ions into the polymer free volume. It is also worth mentioning that films not subjected to KOH treatment did not result in ZIF-8 crystals. This highlights the importance of imide ring opening through hydrolysis reaction and subsequent ion-exchange with Zn ions required for nucleation and growth of ZIF-8 crystals.

To identify Zn bonding environments present in the polymer modified layer, XPS analysis was performed on the Zn-doped films. Figure 3.7a shows XPS spectra of Zn $2p_{3/2}$ core level of the Zn-doped films. Deconvolution of the Zn $2p_{3/2}$ core level gives out two separate peaks at 1022.5 eV and 1023.1 eV that can be assigned to Zn-polymer (i.e., coordinated ions) and Zn-water (i.e., free ions) interaction, respectively.[137, 138] Control experiments were performed to gain insight into which of these Zn ions (coordinated vs. free) are most likely to participate in ZIF-8 crystal formation. A Zn-doped film was washed with copious amount of deionized water sufficiently long to remove free Zn ions from polymer free volume, leaving only coordinated Zn ions in polymer modified layer. Elution of free Zn ions from the film was monitored by periodically measuring electrical conductivity of the deionized water during washing process.

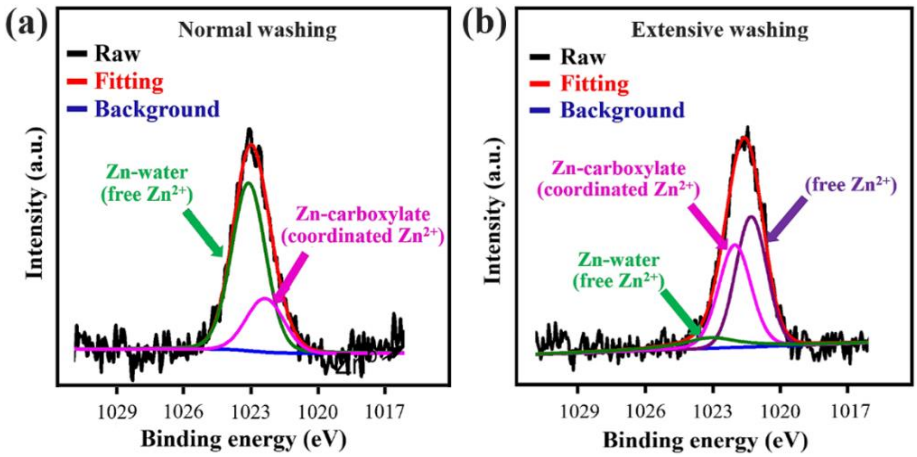

Figure 3.7 High resolution XPS spectra of the Zn ion-exchanged Kapton® film subjected to (a) normal washing (b) extensive washing

Washing step was terminated once electrical conductivity of the deionized water reaches steady states (result not shown). At this point, elution of free Zn ions from hydrophilic free volume was assumed to have completed and most of the free Zn ions have been removed. After extensive deionized water washing, significant reduction in XPS peak intensity at binding energy of 1023.1 eV was observed, suggesting that most of the free Zn ions have been successfully removed (Figure 3.7b). To our surprise, we observed a new XPS peak at 1021 eV binding energy, also assigned to free Zn ions. We believe the formation of this new peak may originate from the remaining free Zn ions present in polymer free volume but they experience new binding environment due to longer contact in deionized water. Nevertheless, ratio between free and coordinated Zn has been decreased from 3.0 (rapid washing) to 1.4 (extensive washing).

Based on this evidence, it is therefore not surprising that after solvothermal reaction in HmIm solution, the Zn-doped films subjected to extensive washing showing significantly weaker ZIF-8 diffraction peak than that with quick washing (result not

shown). This observation strongly suggests that Zn ions coordinating with carboxylic groups do not participate in the formation of ZIF-8 crystals. This is attributed to the fact that the coordinated Zn ions cannot be easily liberated possibly due to relatively low concentration of counter ions (i.e., H^+) present in linker solution (pH ~9.9) and use of relatively mild reaction temperature (120°C).[97, 139] It is noted that Tsuruoka et al.[97] used microwave heating where strong interaction between microwaves and coordinated Al ions inside the polymer led to a rapid increase in local temperature, thereby liberating the coordinated Al ions.

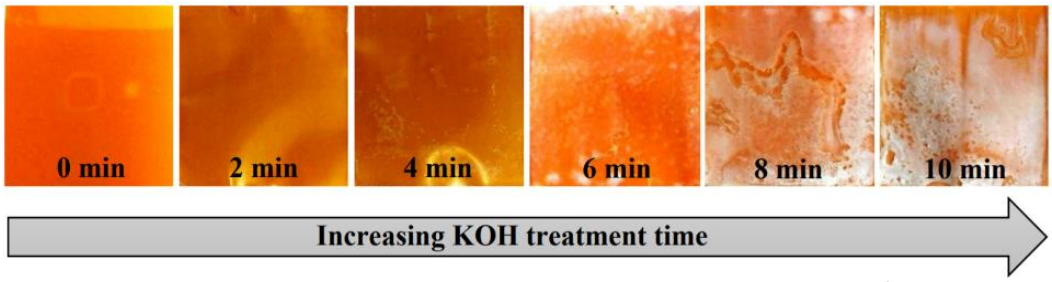

Figure 3.8 Optical images of ZIF-8 thin films synthesized using Kapton® films subjected to different degree of hydrolysis

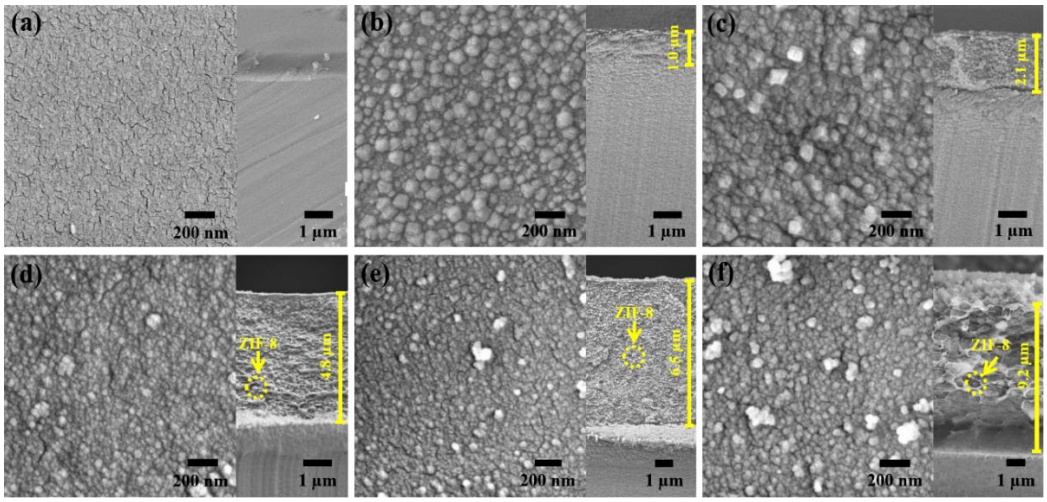

Figure 3.9 Top and cross sectional SEM images of (a) pristine films and ZIF-8 thin films synthesized using polymer substrates immersed in KOH for (b) 2 min (c) 4 min (d) 6 min (e) 8 min and (f) 10 min

Optical images in Figure 3.8 and electron micrographs in Figure 3.9 display the temporal evolution of KAP-X-Zn-ZIF-8 as a function of KOH treatment time. With an exception of KAP-2-Zn-ZIF-8, the samples formed continuous ZIF-8 crystal layers on top, implying that there exists a minimum amount of metal ion dopants required to form continuous ZIF-8 films on the substrate surfaces. The crystallite sizes were determined approximately 40.3 ± 7.6 nm, which is comparable with the crystallite sizes calculated using the Scherer equation (33.7 ± 7.0 nm). Cross sectional SEM images, however, revealed a very interesting morphology which has never been previously observed. As shown in inset cross section images, ZIF-8 crystals appeared to be embedded (shown in yellow circles) and uniformly distributed in polymer matrix and the composite layer thickness increased linearly with KOH treatment time. Linear depth modification profile observed in this study is consistent with past observation by Stoffel et al.[140] and Lee et al.[95] As mentioned by Stoffel and co-workers,[140] growth rate of KOH-modified layer was governed by kinetics of hydrolysis of imide rings at the modified and unmodified layer interface. In their study, they found that the kinetics of hydrolysis at the interface were constant regardless of modification depth. Constant hydrolysis kinetics led to constant growth kinetics, and this result in a linear depth modification profile of the polymer as a function of KOH treatment time.

To confirm the formation of ZIF-8 crystals inside the polymers, a quick acid treatment was performed to remove surface bound crystals from the samples. KAP-6-Zn-ZIF-8 samples were subjected to a diluted acid wipe (0.05 M HNO_3) for several cycles

and PXRD patterns were collected after each cycle. A plot of the relative (110) intensity with the number of acid treatment cycles was constructed, serving as indirect indicator of the relative amount of ZIF-8 formed inside vs. outside the polymer. After five acid treatment cycles, the relative (110) intensity remains almost constant at 60%. After initial removal of the surface bound crystals, further removal of ZIF-8 by dilute HNO_3 are thwarted as the remaining ZIF-8 crystals are embedded and protected inside the polymer.

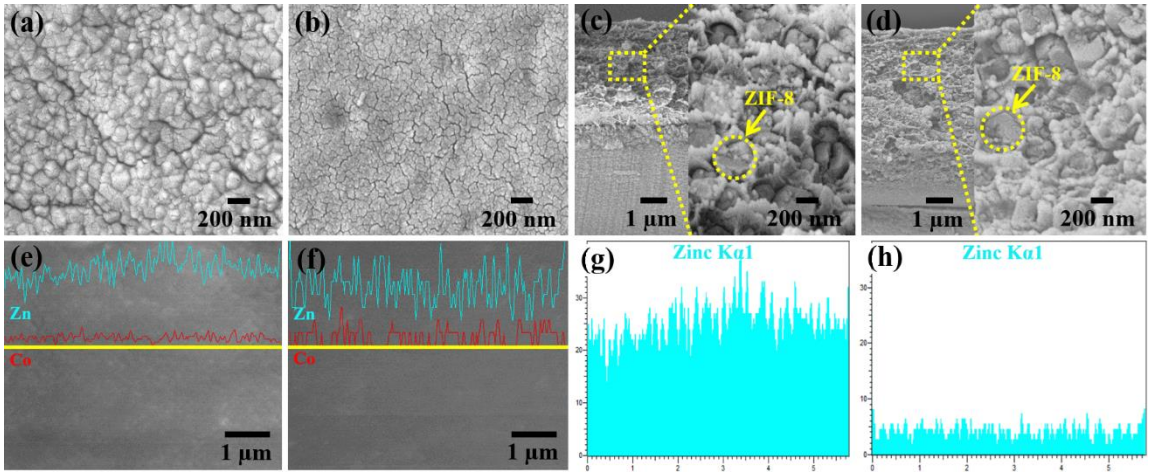

Figure 3.10 (a - d) top and cross sectional SEM images and (e - h) EDX line scan analysis of film surfaces before and after acid treatment

Figure 3.10 shows top and cross section electron micrographs of the samples before and after acid treatment. The SEM micrographs, in addition with the EDX line scan analysis confirmed a complete removal of surface bound ZIF-8 crystals. On the other hand, cross sectional SEM images revealed that most of the ZIF-8 crystals formed inside the polymer remained intact even after subjected to eight acid treatment cycles. As opposed to KAP-6-Zn-ZIF-8, relative (110) intensity of KAP-2-Zn-ZIF-8 was reduced to 0% after subjected to similar acid treatment cycles, suggesting ZIF-8 crystals formed

mostly on the polymer surface. This strongly indicates that one can control the location of ZIF-8 crystals by simply adjusting the hydrolysis time.

Figure 3.11 presents microstructure of a representative KAP-6-Zn-ZIF-8 sample, showing that the size of embedded ZIF-8 particles detected under SEM (Figure 3.11b) and TEM (Figure 3.11c) was comparable. Although the observed particle shown in Figure 3.11c appears to be a ZIF-8 single crystal, inset electron diffraction suggests that the particle consist of several smaller ZIF-8 crystals but of unknown sizes. To the best of our knowledge, *in-situ* formation of ZIF-8 inside the polymer has never been previously reported. It is surmised that during solvothermal reaction in a linker solution, ZIF-8 crystals formed not only at the polymer/solution interface[97] but also inside the polymer possibly due to slow elution of free Zn ions from polymer free volume, thereby allowing linker molecules to diffuse deep into and consequently crystallizing inside the modified layer. Inside free volume spaces, several nuclei might form, resulting in ZIF-8 particles of several grains inside the polymer. It is worthy of noting that the ability to *in-situ* form ZIF-8 nanoparticles inside polymer substrates bears a significant implication for one step synthesis of ZIF-8/polymer composite films and membranes.

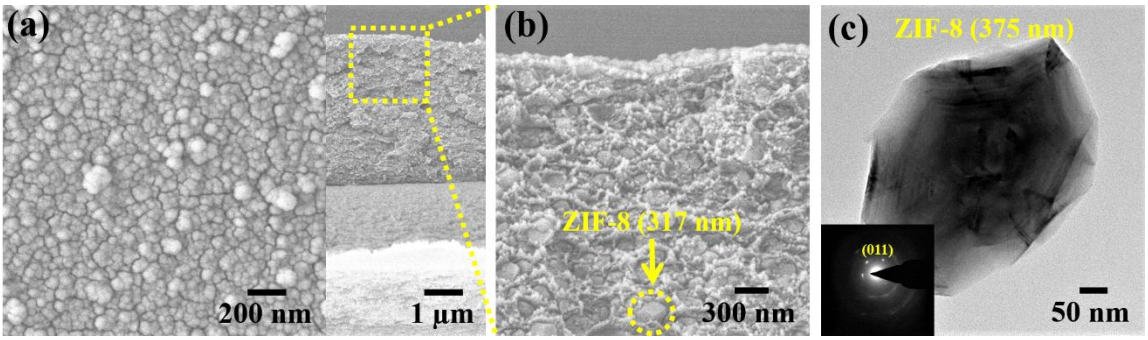

Figure 3.11 (a) top and cross sectional SEM images of KAP-6-Zn-ZIF-8 (b) magnified view of the selected area (c) cross sectional TEM image of ZIF-8 crystals with electron diffraction pattern (inset)

In addition to ZIF-8, the PMMOF process was also applied to synthesize thin films of ZIF-67 (Co-substituted ZIF-8) and Zn/Co mixed metal ZIFs (hereafter, Zn_xCo_{1-x}-ZIF-8). A great deal of research has been undertaken to fine tune the properties (e.g., pore aperture, pore volume, functionality, etc.) of MOFs by mixed metal[141, 142] and mixed linker[143, 144] approaches. Versatility of the PMMOF process not only allows one to use different metal dopants (i.e., Co ions) but also to tailor composition of co-dopants (i.e., Zn and Co ions) in the polymer modified layer, thereby enabling construction of monometallic and bimetallic ZIF films with rational control over metal compositions in the frameworks.

ZIF-67 films were readily prepared by simply replacing metal dopant from Zn to Co ions. On the other hand, Zn_xCo_{1-x}-ZIF-8 films were synthesized by doping the polymer substrates with a mixture of metal ions (i.e., Zn and Co ions) of known composition. As a proof of concept, an aqueous mixture of zinc nitrate hexahydrate (50 mM) and cobalt nitrate hexahydrate (50 mM) was used during ion-exchange, forming an equimolar mixture of the dopant species in the ZIF frameworks ($Zn_{0.5}Co_{0.5}$-ZIF-8). All samples were subjected to similar KOH treatment time of 6 min (KAP-6) and subsequent reaction conditions were maintained the same.

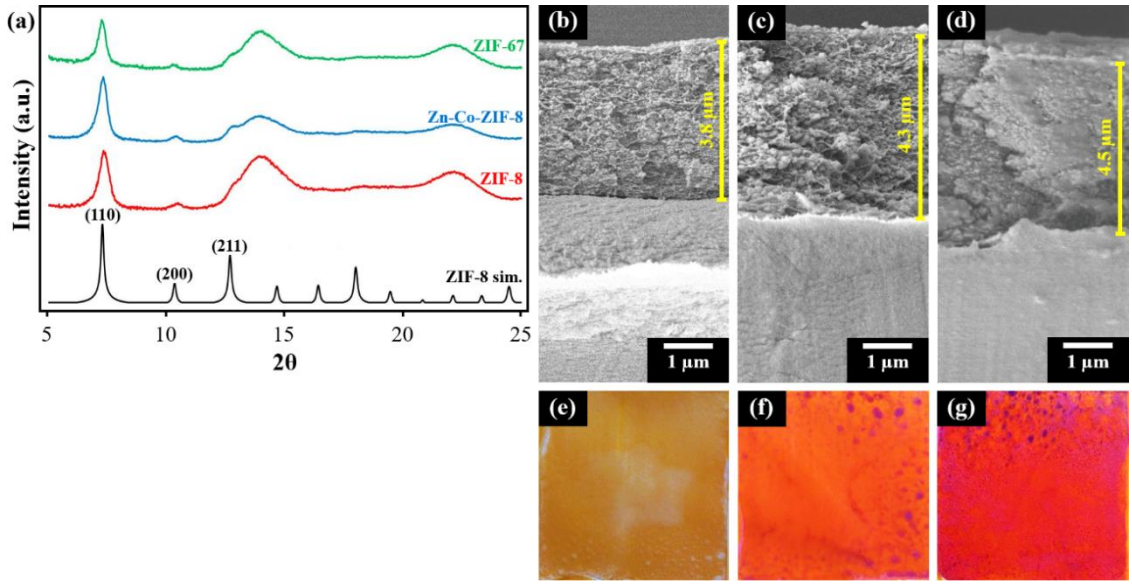

Figure 3.12 (a) PXRD patterns (b - d) cross sectional SEM images and (e - g) optical images of different ZIF thin films

The PXRD patterns shown in Figure 3.12a confirmed the formation of pure phase ZIF-8, $Zn_{0.5}Co_{0.5}$-ZIF-8, and ZIF-67 crystals. The resulting ZIF thin films are presented in Figure 3.13(c - e) where several observations can be made. First, ZIF-8, $Zn_{0.5}Co_{0.5}$-ZIF-8, and ZIF-67 crystals were densely packed, yielding continuous films on the substrates. Second, the films were made of grains with a relatively narrow size distribution and the sizes of these grains appeared to be systematically increasing in the following order, ZIF-8 < $Zn_{0.5}Co_{0.5}$-ZIF-8 < ZIF-67 (40 nm vs. 155 nm vs. 271 nm). The difference in crystallite sizes can be attributed to slower nucleation and different crystal growth kinetics upon incorporation of Co ions in the Zn-doped substrates.[142]

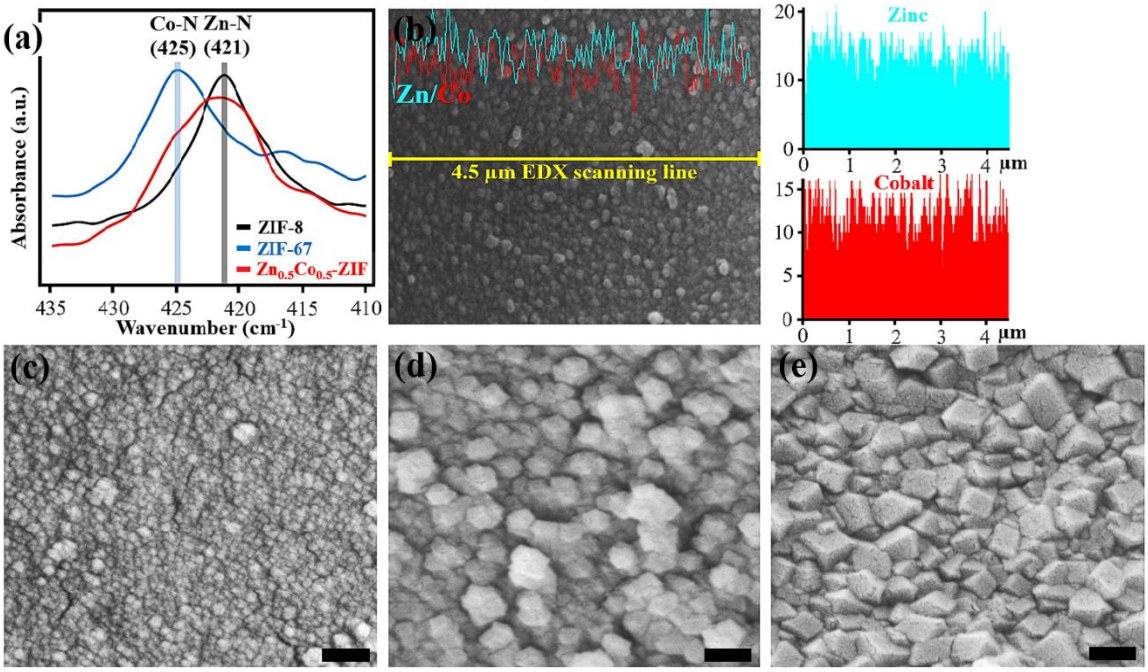

Figure 3.13 (a) ATR-FTIR spectra showing metal-to-nitrogen stretching vibrations of different ZIF thin films (b) EDX line scan analysis on $Zn_{0.5}Co_{0.5}$-ZIF-8 film surface. Top SEM images of (c) ZIF-8 (d) $Zn_{0.5}Co_{0.5}$-ZIF-8 and (e) ZIF-67 thin film on polymer substrates. Top view scale bar: 200 nm

For Zn/Co mixed metal ZIF, interestingly, incorporation of Co and Zn in ZIF framework can be monitored through direct optical observation of color change as shown in Figure 3.12(e - g). To further confirm the incorporation of Zn and Co in ZIF frameworks, EDX line profile analysis was performed. The EDX line scan analysis of $Zn_{0.5}Co_{0.5}$-ZIF-8 surfaces in Figure 3.13b shows that Zn and Co element were uniformly distributed throughout the surface. Relative amount between Zn and Co was close to unity and was found to be consistent with those of co-doped polymer substrates (Figure 3.14 vs. Figure 3.15).

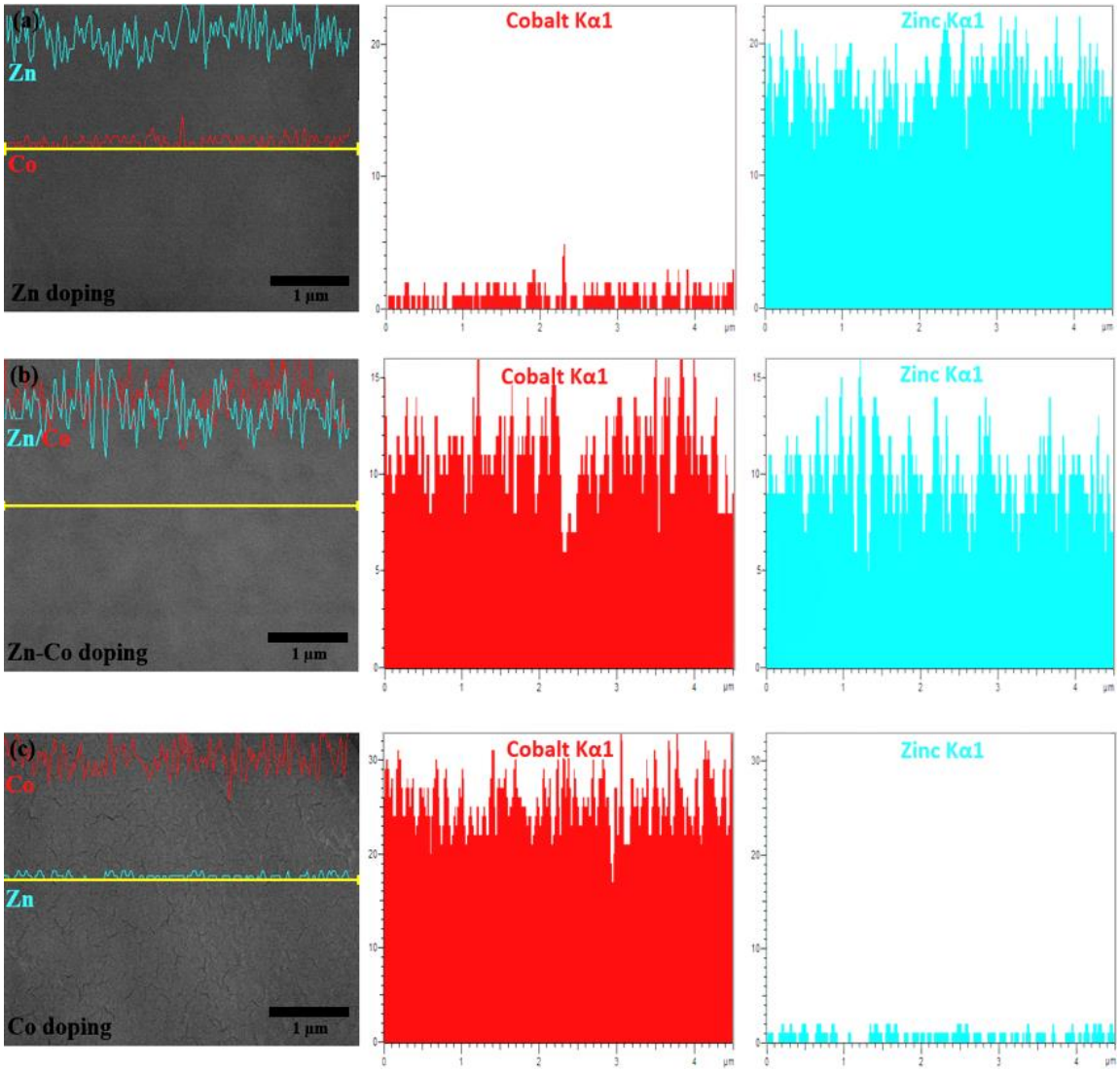

Figure 3.14 EDX line profile analysis of (a) Zn-doped (b) $Zn_{0.5}Co_{0.5}$-doped and (c) Co-doped polymer substrates

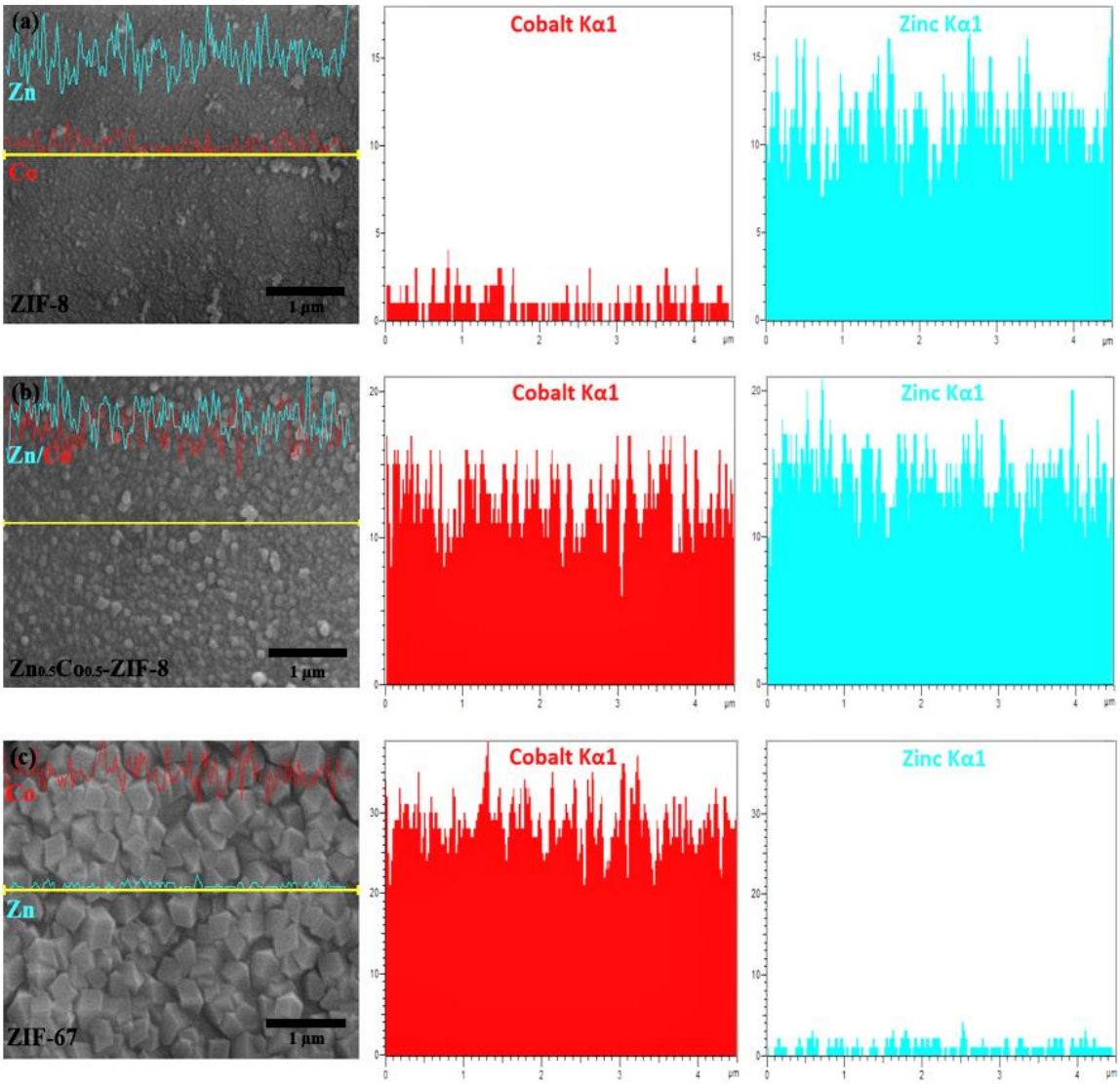

Figure 3.15 EDX line profile analysis of (a) ZIF-8 (b) $Zn_{0.5}Co_{0.5}$-ZIF-8 and (c) ZIF-67 thin films on polymer substrates

Additionally, metal-to-nitrogen absorption bands of $Zn_{0.5}Co_{0.5}$-ZIF-8 became broader and blue-shifted upon incorporation of Co element into the ZIF-8 frameworks, which agrees with the previous report.[145] $Zn_{0.5}Co_{0.5}$-ZIF-8 (Zn/Co mixed metal ZIF) consisting of more rigid Co-N (i.e., stiffer) and less rigid Zn-N bonds alter metal-to-nitrogen stretching frequency, thus leading to the blue-shift.[118] An ability to control

dopants and their compositions in polymer substrates present an unprecedented opportunity to fabricate important monometallic family of ZIFs and bimetallic ZIF films for a variety of applications. Finally, site-selective interfacial reaction allows for construction of one and/or multiple types of ZIF films grown at specific locations on polymer substrates.[146] When ion-exchanged with Co ions on one side and Zn ions on the other side, ZIF-67 and ZIF-8 films were formed on different sides (i.e., Janus MOF films) as shown in Figure 3.16.

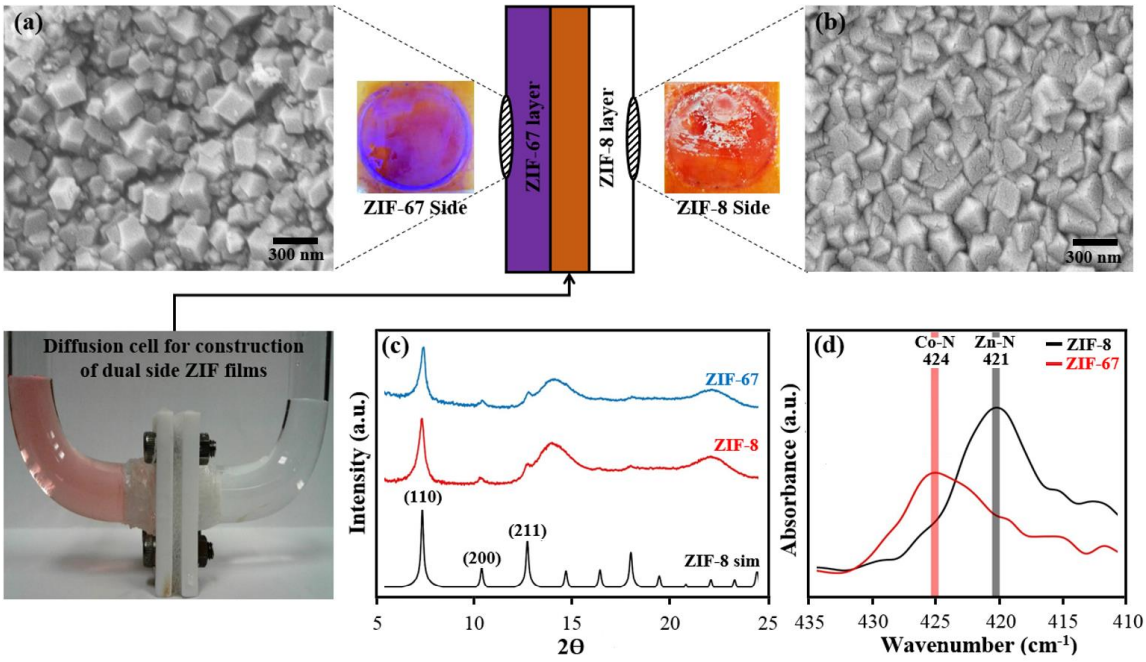

Figure 3.16 (a - b) top SEM images (c) PXRD patterns and (d) ATR-FTIR spectra of ZIF-8 and ZIF-67 Janus MOF thin films

Based on the proposed mechanism illustrated in Figure 3.2, it is postulated that the PMMOF process can be readily extended to fabricate ZIF-8 thin films on different polymer-based substrates with various geometries, provided that the substrates are able to undergone similar chemistry. To test our hypothesis, we attempted to fabricate ZIF-8 thin

films on porous Matrimid® flat sheet and HFs. Matrimid® flat sheets were prepared by a dry-wet phase inversion method while Matrimid® HFs were fabricated by a dry-wet jet spinning process. The pristine HFs were microporous (N_2 permeance ~45,594 GPU, 1 GPU = 3.348×10^{-10} mol/(m^2•Pa•s)) with ID and OD of 465 µm and 590 µm, respectively. Thin polycrystalline ZIF-8 layers were successfully grown on Matrimid® flat sheets using the PMMOF process (result not shown). Similarly, in Figure 3.17(inset images), densely packed nanometer-sized ZIF-8 crystal layers with uniform surface coverage were successfully deposited on the bore side of Matrimid® HFs using similar approach. This finding is of particular importance as the proposed approach can provide a new means to synthesize well-intergrown films and membranes on commercially available polyimide-based HFs especially for separation applications.

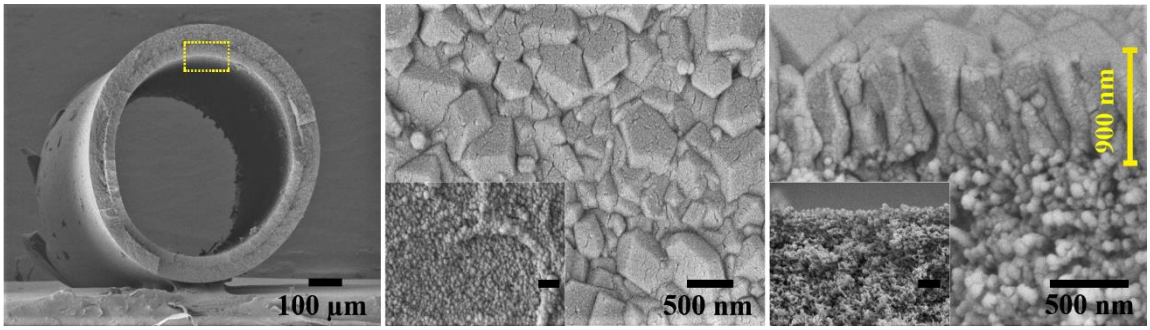

Figure 3.17 (a) cross section view of ZIF-8 membranes under low magnification (b - c) top and cross section view of the ZIF-8 membrane and seed crystals (inset) in higher magnification. Inset image scale bar: 500 nm

The ZIF-8 seed crystals layers on Matrimid® HFs obtained using the PMMOF processes were secondarily grown into ZIF-8 membranes under continuous microfluidic flow of growth solution. The resulting ZIF-8 membranes supported on Matrimid® HFs were well-intergrown without any macroscopic defects with thickness of ~900 nm. Binary

propylene/propane separation performances of the membranes were tested using the Wicke-Kallenbach technique conducted at room temperature. ZIF-8 membrane module used for propylene/propane permeation measurements has an active membrane area of 0.584 cm^2. An equimolar propylene/propane gas mixture was fed to the bore side while argon sweep gas was provided to the shell side of HFs. Volumetric flow rates of both feed and sweep gases were set at 3.33×10^{-1} ml/s. The as-prepared ZIF-8 membranes on Matrimid® HFs unfortunately did not display good propylene/propane separation performances presumably due to relatively poor grain boundary defects.

A thin PDMS coating was applied on top of the membranes to seal those defects and the resulting ZIF-8 membranes showed much improved separation performances.[87] The average propylene permeances and separation factor of the supported ZIF-8 membranes were 195×10^{-10} mol/(m^2•Pa•s) and 27, respectively, which are somewhat promising. However, the separation factor of our ZIF-8 membranes need to be further improved to a minimum separation factor of 35 required to be considered 'commercially attractive'.[13] Optimization of ZIF-8 seeding and secondary growth steps are currently underway to improve microstructures of the ZIF-8 membranes on Matrimid® HFs. Our finding regarding the optimized ZIF-8 membrane formation on Matrimid® HFs including their improved gas separation performances will be discussed in the next chapter.

3.4. Conclusions

In conclusion, we have developed and demonstrated a simple methodology (termed as PMMOF) for facile synthesis of ZIF-8 thin films and membranes on polymer

substrates and ZIF-8/polymer composites using ion-exchanged polymer substrates followed by conventional solvothermal reaction. While continuous and densely packed ZIF-8 crystal layers were observed on the polymer surfaces, ZIF-8/polymer mixed matrix layers were also observed inside the polymer substrates. Adjusting hydrolysis time was found a simple means to control the location of ZIF-8 crystals forming. PMMOF approach was applied to different ZIFs and mixed metal ZIFs as well as to different polyimide-based substrates with different geometries, showing versatility of the approach. Furthermore, PMMOF approach utilizing interfacial reaction on metal-doped polymer substrates is found location-selective, potentially enabling the construction of complex patterns of MOFs. Finally, ultrathin ZIF-8 membranes on porous Matrimid® HFs were demonstrated by secondarily growing ZIF-8 seed crystal layers deposited on the bore sides of Matrimid® HFs by the PMMOF. The membranes exhibited promising propylene/propane separation performances once coated with PDMS. It is expected that the PMMOF approach reported here can potentially open up new possibilities to readily fabricate MOF crystals on and inside polymer substrates for a variety of advanced applications including gas separation, catalysis, and sensing.

4. SYNTHESIS OF ULTRATHIN ZIF-8 MEMBRANES ON MATRIMID® HOLLOW FIBERS USING A POLYMER MODIFICATION STRATEGY*

4.1. Introduction

Polycrystalline ZIF-8 membranes (mostly grown on planar substrates) have shown excellent kinetic separation of propylene from propane due to its effective aperture ~4.0 Å, which are in between the van der Waals diameter of propylene (~4.0 Å) and propane (~4.2 Å).[11, 12] Currently, there have been no commercial polycrystalline ZIF-8 membranes. This is ultimately due to the cost of polycrystalline membranes being prohibitively high (e.g., $1,000 per sq. meter for polycrystalline zeolite membranes vs. $20 per sq. meter for polymer membranes).[3] It is, therefore, critical to reduce cost of ZIF-8 membranes by increasing membrane productivity by 1) using cost effective scalable substrates with high surface-to-volume ratio and 2) reducing membrane thickness (thickness less than 1 μm).[147]

Despite successful preparation of polycrystalline ZIF-8 membranes on inorganic substrates with high surface-to-volume ratio (i.e., HF, capillary, tubular),[148-151] inorganic substrates are not considered cost effective. For example, ceramic HFs, in particular, can provide high packing density but they are fairly expensive. Moreover, ceramic HFs are in

**This chapter was adapted and modified with permission from Mohamad Rezi Abdul Hamid, Sunghwan Park, Jusung Kim, Young Moo Lee, and Hae-Kwon Jeong, Industrial & Engineering Chemistry Research, 2019, 58, 14947 - 14953. Copyright 2019 American Chemical Society*

general quite difficult to handle due to their inherently poor mechanical properties. In contrast, polymer HFs are inexpensive and easy to form modules with high packing density, thereby more attractive as cost effective substrates for polycrystalline ZIF-8 membranes.[14]

Hou et al.[74] explored the formation of 1 μm thick ZIF-8 membranes on the shell side of 3-aminopropyltriethoxysilane-titania-functionalized PVDF HF by simply immersing the HFs in ZIF-8 synthesis solution. Biswal and co-workers[82] demonstrated a facile room temperature synthesis of ZIF-8 membranes on either shell or bore side of polybenzimidazole-based HFs (OD, 780 μm) using an interfacial synthesis method for helium separation. Venna et al.[77] utilized a simple continuous flow processing method to prepare ZIF-8 membranes on the shell side of Torlon® polyamide-imide HFs (OD, 400 μm) for post-combustion CO_2 capture application. Finally, Li and co-workers[84] reported synthesis of ultrathin ZIF-8 membranes on the shell side of Zn-based gel coated PVDF HFs via a gel-vapor deposition. The 87 nm thick ZIF-8 membranes showed propylene/propane separation factor of 73 and propylene permeance of 840 GPU

While ZIF-8 membranes grown on the shell side of polymer HFs have slightly higher surface-to-volume ratio, membranes grown on the bore side have several advantages: (1) where the relatively fragile polycrystalline ZIF-8 membranes are better protected from physical damages during handling, (2) the HFs can be packed together in a close proximity to form modules with a high fiber packing, and (3) membrane module assembly process can be performed without damaging the relatively brittle ZIF-8 layers, especially when membranes are ultrathin (i.e., < 1 μm). However, growing ZIF-8

membranes on the bore side of HFs requires synthesis in a confined space, thereby presenting several challenges such as surface accessibility, reactant availability, positional control, etc.[152]

Coronas et al.[76] were among the first to report synthesis of ZIF-8 membranes on the bore side of polysulfone HFs (ID, 315 μm) using a continuous flow processing method for CO_2/CH_4 and H_2/CH_4 separations. Nair and co-workers[78] prepared 8.8 μm thick ZIF-8 membranes on the bore side of Torlon® polyamide-imide HFs using interfacial microfluidic membrane processing, where the membranes formed at the interface between two solutions (water-octanol). The membranes exhibited propylene permeance and propylene/propane separation factor of 27 GPU and 12, respectively. Later, the same group reported improved ZIF-8 membranes with propylene permeance and separation factor of 45 GPU and 180, respectively.[80, 81] Most recently, Jeong and co-workers[10] prepared ultrathin (~800 nm thick) ZIF-8 membranes on the bore of Matrimid® HFs (ID, 344 μm) via microwave assisted seeding followed by microfluidic secondary growth. The membranes displayed an average propylene permeance of 55 GPU and propylene/propane separation factor of 46. With exception of a few groups (i.e., Nair's[78, 80, 81] and Jeong's[10] group), reports on the synthesis of ZIF-8 membranes on bore side of polymer HFs intended for the challenging propylene/propane separation are quite rare. This is unsurprising considering the challenging nature of preparing high quality ZIF-8 membranes on the confined space of HFs.

In general, polycrystalline ZIF-8 membranes can be prepared either via *in-situ* or secondary growth.[66, 153] Although not as straightforward as the *in-situ* growth, synthesis

of ZIF-8 membranes by secondary growth allows for better control over membrane microstructures (i.e., membrane thickness, crystal orientation, crystal grain size, etc.), therefore better separation performances of the resulting membranes.[154] However, the challenges here lie in obtaining high quality seed layers prior to membrane growth. Typical high quality seed layers consist of seed nanocrystals that are densely packed, uniformly distributed on surfaces, and strongly attached to the substrate surfaces.[66] In our recent contribution,[68] we have introduced the PMMOF method for the construction of ZIF/polymer composites and ZIF thin films on polyimide (i.e., Kapton® and Matrimid®) flat sheets. The method relies on targeted Zn ion doping on modified polymer substrates (i.e., partially deimidized polyimides) which enables the formation of ZIF nanoparticles at a specific location. As a proof of concept, the ZIF-8 nanocrystals deposited on Matrimid® substrates by the PMMOF were secondarily grown to form defect-free and well-intergrown membranes.[68]

Herein, we report a successful preparation of ultrathin ZIF-8 membranes with much improved propylene/propane separation performances on the bore side of Matrimid® HFs by using the PMMOF method in combination with microfluidic secondary growth. PMMOF can control the location of where the ZIF-8 polycrystalline layer is grown, owing to site-selective nature of the process. In this work, Fourier transform infrared spectroscopy was used to identify the chemical bonding environment present on the surface of Matrimid® HFs, X-ray diffraction was used to determine crystallinities and phases of ZIF-8 crystals, and electron microscopy was used to analyze microstructures of

ZIF-8 seed layers and membranes. Gas transport properties of ZIF-8 membranes on Matrimid® HFs were determined using Wicke-Kallenbach technique.

4.2. Experimental section

4.2.1. Materials

Matrimid® 5218 (Alfa-Aesar, Ward Hill, USA) and N-methyl-2-pyrolidinone (C_5H_9NO, 99.5%, Daejung Chemicals and Metals, Siheung, Korea) were used to fabricate Matrimid® HFs. Potassium hydroxide (KOH, reagent grade, VWR International) was used to hydrolyze the imide rings of Matrimid® HFs. 2-methylimidazole ($C_4H_6N_2$, 99%, Sigma-Aldrich, hereafter HmIm), zinc nitrate hexahydrate ($Zn(NO_3)_2 \cdot 6H_2O$, 98%, Sigma-Aldrich), sodium formate (HCOONa, 99%, Sigma-Aldrich), methanol (CH_3OH, > 99%, Alfa-Aesar), and deionized water were used to prepare PMMOF and secondary growth precursor solutions. PDMS (Sylgard® 184, Dow Chemical) and hexane (C_6H_{14}, ACS grade, VWR International) were used to seal defective ZIF-8 membranes.

4.2.2. Methods

4.2.2.1. Preparation of Matrimid® HFs

Porous Matrimid® HFs (Figure 4.1) were prepared using a dry-wet jet spinning process. Spinning parameters can be found in Table 4.1. As shown in Figure 4.1, pristine Matrimid® HFs were microporous (N_2 permeance ~45,594 GPU) with ID and OD of 465 µm and 590 µm, respectively. Preparation of Matrimid® HF setup (11 cm in length) used for ZIF-8 seeding and secondary growth can be found in our previous work.[10]

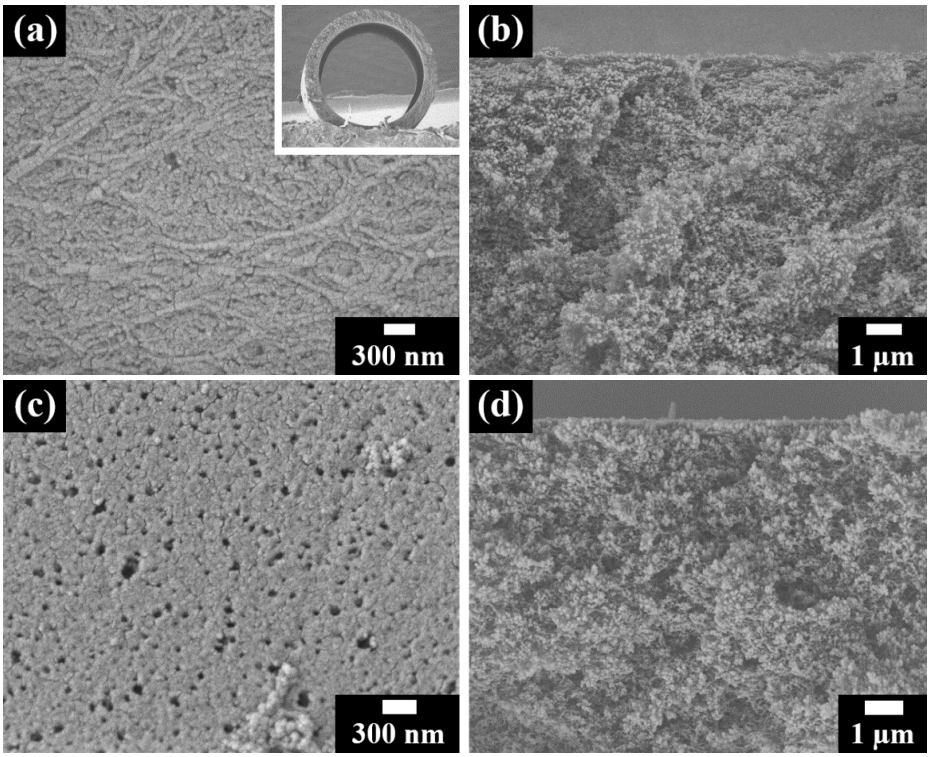

Figure 4.1 Top and cross section view of the (a - b) bore side and (c - d) shell side of pristine Matrimid® HFs. Inset SEM image shows cross section of the HFs under low magnification

Table 4.1 Spinning parameters to fabricate Matrimid® HFs

Parameter	**Values**
Dope solution composition, polymer/solvent (wt.%)	20/80
Bore solution composition, NMP/water (wt.%)	40/60
Dope and bore solution temperatures (ºC)	60
Spinneret temperature (°C)	60
Air-gap distance (m)	0.15
Dope flow rate (ml/s)	1.7×10^{-2}
Bore flow rate (ml/s)	2.5×10^{-2}
Coagulation bath temperature, water (°C)	80

4.2.2.2. Preparation of ZIF-8 seed layers on Matrimid® HFs

Surface modification and Zn ion doping on the bore side of Matrimid® HF were performed following a procedure previously reported with a slight adjustment.[68] Briefly, using a syringe pump (Harvard Model 55-4152), a 5 M aqueous KOH solution (50°C) was flowed to the bore side of HF at a flow rate of 5.50×10^{-3} ml/s for different period of time, followed by a continuous flow of 100 mM aqueous zinc nitrate hexahydrate solution with similar flow rate for 1 hr. Excess KOH and Zn solutions were purged slowly with air and dried with Kimwipes. To form ZIF-8 seed layers on the bore side, a Zn-doped HF was positioned vertically in a Teflon autoclave containing HmIm linker solution (10.36 g of HmIm and 0.5 g of sodium formate in 120 ml of methanol). Then, the autoclave was kept inside a preheated convection oven at 120°C for 1 hr, followed by 2 hrs. of cooldown to room temperature. The seeded HF was then washed with fresh methanol for 1 hr. Finally, the seeded HF sample (hereafter, ZIF-8-S/HF) was dried inside a convection oven at 60°C for 4 hrs.

4.2.2.3. Preparation of ZIF-8 membranes on Matrimid® HFs

A ZIF-8-S/HF was grown into a well-intergrown ZIF-8 membrane using a microfluidic secondary growth method. Preparation of secondary growth precursor solution is described elsewhere.[10, 71] Syringe pump was used to flow secondary growth solution through the bore side of ZIF-8-S/HF at a flow rate of 8.33×10^{-4} ml/s for 6 hrs. The membrane growth was performed inside a vacuum oven at 30°C. The resulting ZIF-8 membrane (hereafter, ZIF-8-M/HF) was thoroughly washed by flowing methanol

through the bore side at flow rate of 1.83×10^{-3} ml/s for 1 hr. Finally, the ZIF-8 membrane was dried at room temperature for 24 hrs.

4.2.2.4. Defect sealing of ZIF-8 membranes using PDMS:

Defect sealing of ZIF-8-M/HF was performed while the membrane was in the permeation module. A 5 wt.% PDMS/hexane coating solution was prepared by dissolving part A and part B of Sylgard® 184 with a 10:1 ratio in hexane under vigorous stirring at room temperature for several hours. Then, the PDMS coating solution was flowed to the bore side of a ZIF-8-M/HF sample at a flow rate of 1.83×10^{-3} ml/s for 1 min. Excess PDMS solution was slowly removed from the bore side by flowing air at a flow rate of 5.50×10^{-3} ml/s for 1 min. Finally, the PDMS coated ZIF-8 membrane (hereafter, ZIF-8-M-PDMS/HF) was dried and cured at room temperature under vacuum for 48 hrs.

4.2.2.5. Characterization

ATR-FTIR spectra (wavenumber scan range from 400 to 4000 cm^{-1}) were collected using a Thermo Scientific Nicolet iS5 FTIR Spectrometer equipped with iD7-ATR diamond accessory. PXRD patterns were collected using a Miniflex II benchtop X-ray diffractometer (Rigaku) with Cu-Kα radiation (λ = 1.5406 Å) scanning from the 2θ range of 5 - 25º. SEM images were obtained using a JEOL JSM-7500F operating at acceleration voltage of 5 keV and working distance of 15 mm. The gas separation properties of ZIF-8-M/HF and ZIF-8-M-PDMS/HF were measured using the Wicke-Kallenbach method. Propylene/propane permeation measurement were performed at room

temperature (~22°C) under atmospheric pressure. A 50:50 vol.% propylene/propane feed mixture (3.33×10^{-1} ml/s) was flowed to the bore side while argon sweeping gas (3.33×10^{-1} ml/s) was flowed through the shell side of HF. The composition of propylene and propane in argon sweep gas was analyzed using Agilent GC 7890 A gas chromatography.

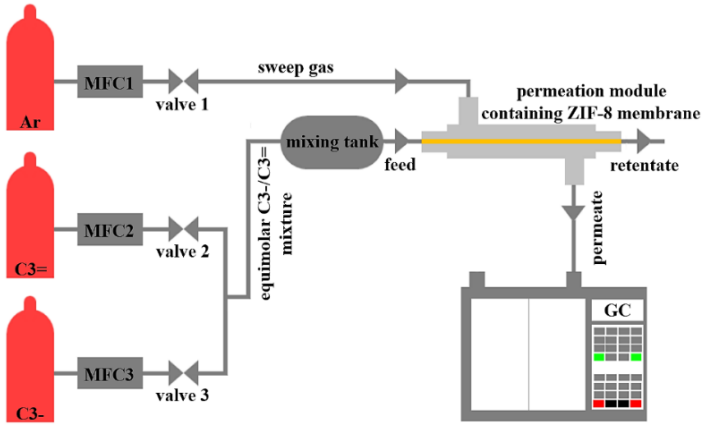

Figure 4.2 Schematic illustration of Wicke-Kallenbach setup for binary propylene/propane permeation measurements

4.3. Result and discussion

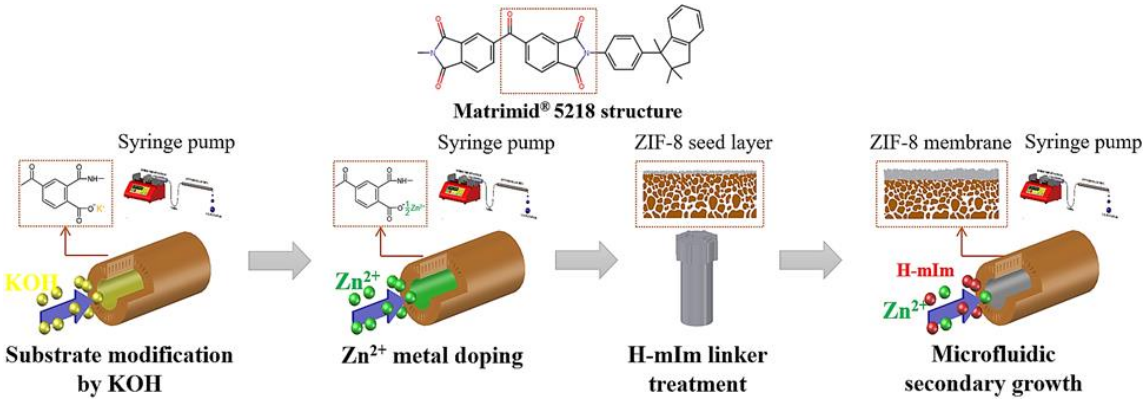

Figure 4.3 Schematic illustration of the synthesis of ZIF-8-M/HFs using combination of the PMMOF process and microfluidic secondary growth

Figure 4.3 illustrates synthesis of ZIF-8 seed layers by the PMMOF process and polycrystalline ZIF-8 membranes by subsequent secondary growth. Details about the

PMMOF process were presented in our recent report (see also previous chapter).[68] Briefly, imide rings of Matrimid® HFs were first hydrolyzed by a strong base (i.e., KOH) forming carboxylates that serve as ion-exchangeable sites and creating hydrophilic free volume.[97] The KOH-modified Matrimid® HFs were then subjected to a continuous flow of aqueous Zn solution, thereby initiating K-Zn ion-exchange reaction and diffusion of free Zn ions into hydrophilic free volume of the polymer.[68] The Zn ion-exchanged layers did not propagate through the entire thickness of the Matrimid® HFs as the shell side of Matrimid® HFs remained unchanged as compared to the bore side (Figure 4.4).

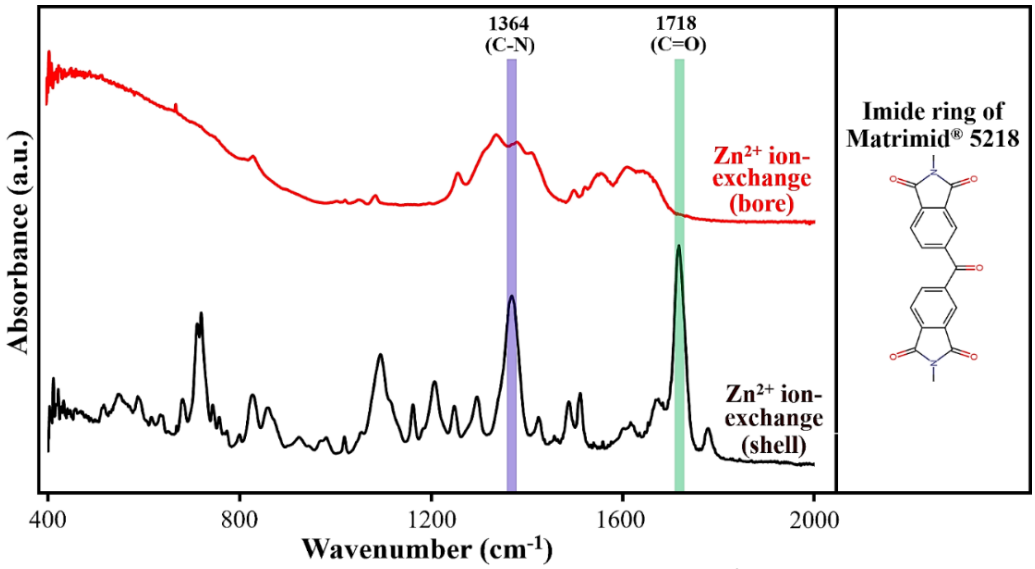

Figure 4.4 ATR-FTIR spectra of Zn ion-exchanged Matrimid® HFs on both bore and shell side

In fact, only a portion (several μm thick) of Matrimid® HFs were hydrolyzed and then ion-exchanged to form Zn polyamate salt as evidenced by a clear morphological change observed under SEM as shown in Figure 4.5. Upon *in-situ* solvothermal treatment in a HmIm ligand solution, free Zn ions diffuse from the polymer free volume and then react with HmIm to form of ZIF-8 seed layers on the bore side of the HFs. One of the

advantages of PMMOF process is a positional control over ZIF-8 seed layer formation, which depends on the location where substrate modification and Zn ion doping take place. Finally, the seeded HFs prepared by the PMMOF process were then secondarily grown under a continuous flow of a growth solution to form continuous, defect-free, and well-intergrown ZIF-8 membranes.

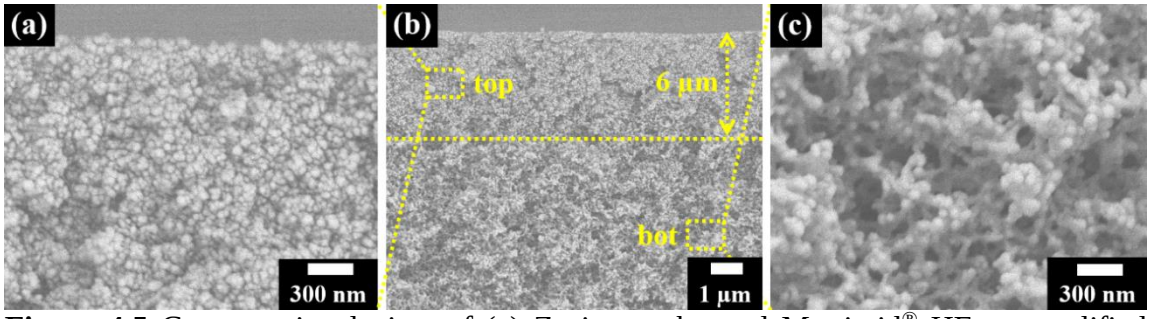

Figure 4.5 Cross sectional view of (a) Zn ion-exchanged Matrimid® HFs at modified polymer layer under high magnification (b) Zn ion-exchanged Matrimid® HFs under low magnification (c) Zn ion-exchanged Matrimid® HFs at unmodified polymer layer under high magnification

Figure 4.6a presents ATR-FTIR spectra of the bore side of pristine HFs and ZIF-8 seeded HFs (ZIF-8-S/HFs) obtained by PMMOF process. The pristine Matrimid® HFs exhibited characteristic ATR-FTIR peaks at 1364 cm^{-1} and 1718 cm^{-1}, which were assigned to C-N and asymmetric C=O vibration modes of imide groups, respectively.[155] Upon modification by KOH, the absorption peak corresponded to the C=O imide groups almost disappeared, resulting from imide ring cleavage by KOH solution. The hydrolyzed Matrimid® HFs exhibited several overlapping peaks at wavenumber between 1500 cm^{-1} - 1600 cm^{-1}, which are combination of N-H amide (1550 cm^{-1}), carboxyl-K ion complexes (1500 cm^{-1} - 1600 cm^{-1}), and C=O amide (1640 cm^{-1}) modes.[93] As shown in Figure 4.7, the ATR-FTIR spectra of KOH-treated and Zn ion-exchanged HFs were mostly

indistinguishable. Solvothermal reaction in a HmIm ligand solution led to formation of ZIF-8 seed crystals on the bore side of Matrimid® HFs, evidenced by the appearance of two new peaks at 421 cm^{-1} and 1145 cm^{-1}, which were assigned to Zn-N and C-N absorption bands of ZIF-8, respectively.[156]

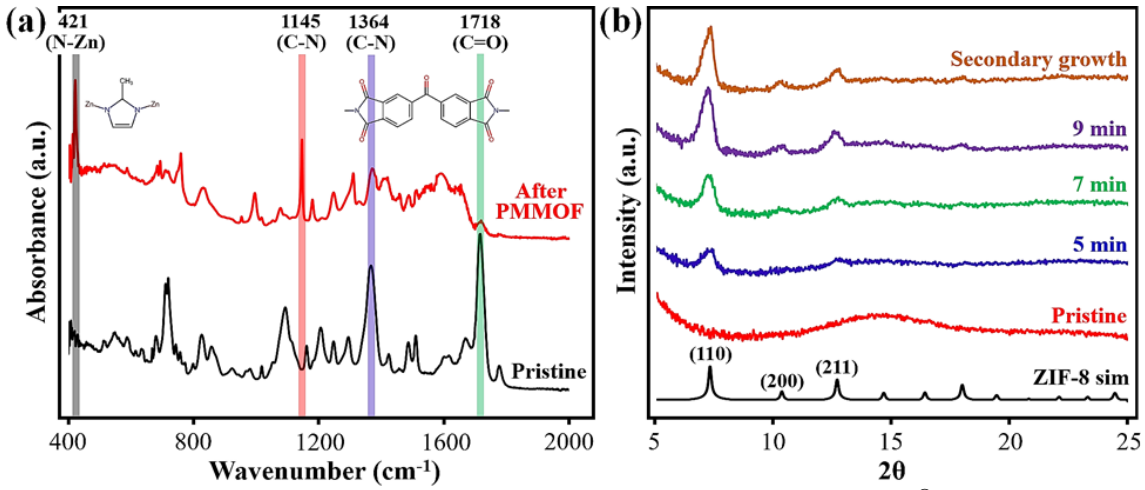

Figure 4.6 (a) ATR-FTIR spectra of the bore side of pristine Matrimid® HFs and ZIF-8-S/HFs after PMMOF process and (b) PXRD patterns of ZIF-8-S/HFs synthesized in different hydrolysis times in comparison with the simulated one

The corresponding PXRD patterns presented in Figure 4.6b further confirm the formation of pure phase ZIF-8 seed crystals. Interestingly, the intensities of characteristic (110) diffraction peaks of ZIF-8 increase as the KOH treatment time increases, indicating the formation of ZIF-8 crystals in greater number as hydrolysis reaction increases. An extended alkali treatment increases Zn ion content in the hydrophilic polymer layer, which led to an increase in ZIF-8 crystal formation. It is noted that Matrimid® HFs not subjected to a hydrolysis reaction did not form ZIF-8 crystals as evidenced from weak PXRD reflections as shown in Figure 4.8.[68]

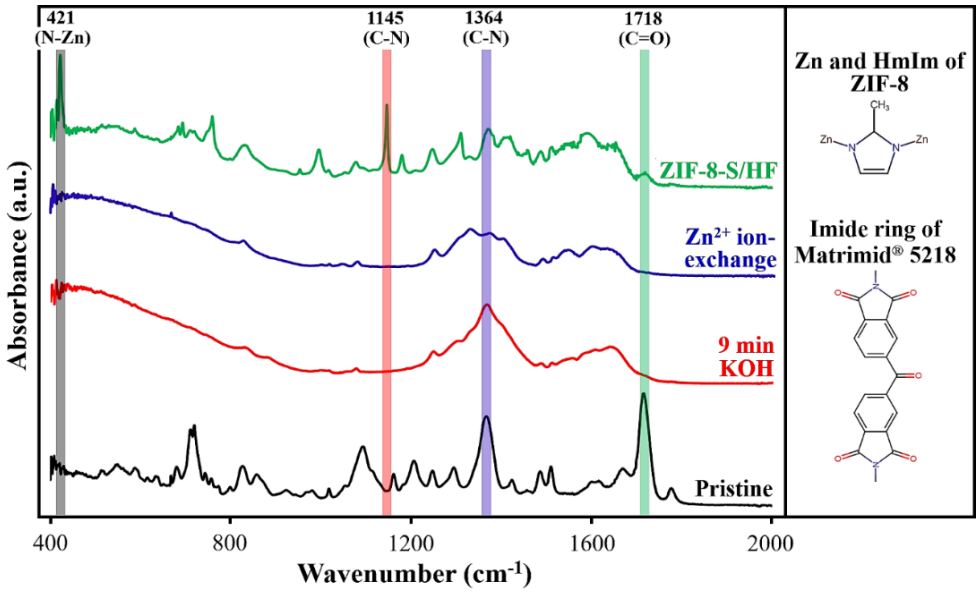

Figure 4.7 ATR-FTIR spectra of pristine, KOH-treated, Zn ion-exchanged, and ZIF-8 seed layers on Matrimid® HFs

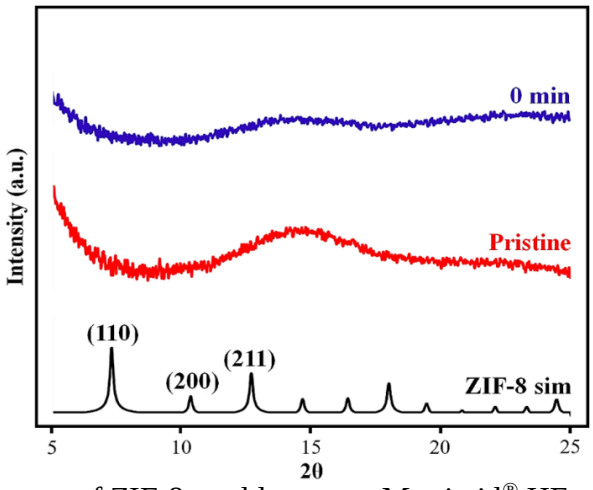

Figure 4.8 PXRD patterns of ZIF-8 seed layers on Matrimid® HFs not subjected to KOH treatment in comparison with pristine Matrimid® HFs and ZIF-8 simulated pattern

Since the quality of polycrystalline membranes prepared by secondary growth highly depends on quality of seed layers,[66, 154] we attempted to improve the quality of ZIF-8 seed layers on the bore side of Matrimid® HFs through systematic optimization of KOH treatment time. Figure 4.9 shows surface electron micrographs of ZIF-8-S/HFs after

PMMOF process. KOH treatment for 5 min led to poor quality ZIF-8 seed layers with low surface coverage. With an increase of KOH treatment time to 9 min, the ZIF-8 seed layers exhibited better surface coverage. As mentioned earlier, a longer KOH treatment time increases the number of Zn ions in polymer free volume as well as in ion-exchangeable sites, thereby leading to an enhancement in crystal formation.[68]

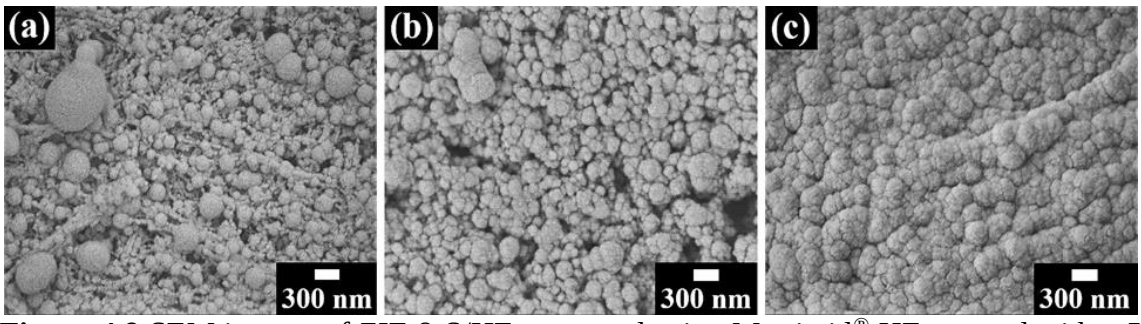

Figure 4.9 SEM images of ZIF-8-S/HFs prepared using Matrimid® HFs treated with a 5 M KOH for (a) 5 min (b) 7 min (c) 9 min

To further confirm the formation of ZIF-8 seed layers on bore side of Matrimid® HFs, a quick acid treatment were performed. As shown in Figure 4.10, after subjecting the seeded Matrimid® HF to a diluted HNO_3 (0.05 M) treatment for several minutes, ZIF-8 seed layers that were originally covering surface of the HFs was removed, exposing bare surfaces of the HFs.

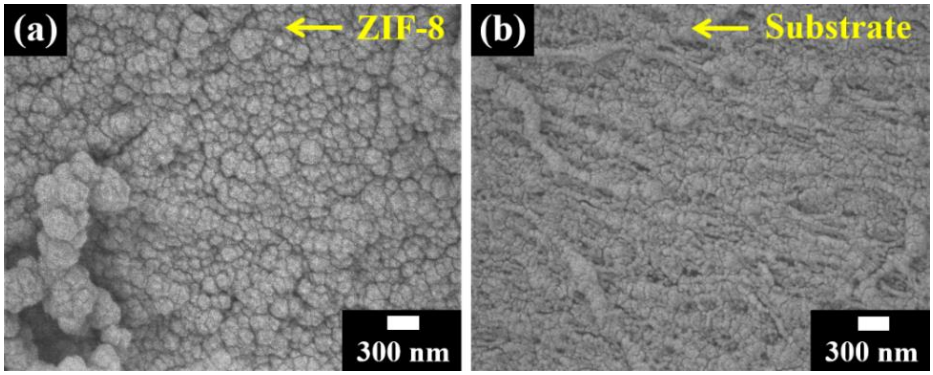

Figure 4.10 Top view of ZIF-8-S/HFs (a) before and (b) after HNO_3 treatment

Figure 4.11 presents microstructure of ZIF-8 seed layers after seeding optimization step. As oppose to the bore side, very few ZIF-8 crystals formed on the shell side even though a HmIm linker solution was provided from the shell side. To show site-selective feature of the PMMOF process, we attempted to form ZIF-8 seed layers and subsequently ZIF-8 membranes by performing the PMMOF method on the shell side of Matrimid® HFs. Figure 4.12 shows formation of high quality ZIF-8 seed layers and membranes on the shell side of Matrimid® HFs. Due to mechanical robustness and handling convenience during membrane synthesis and more importantly during module assembly, we focused on the synthesis of ZIF-8 membranes on bore side of Matrimid® HFs in this studies.

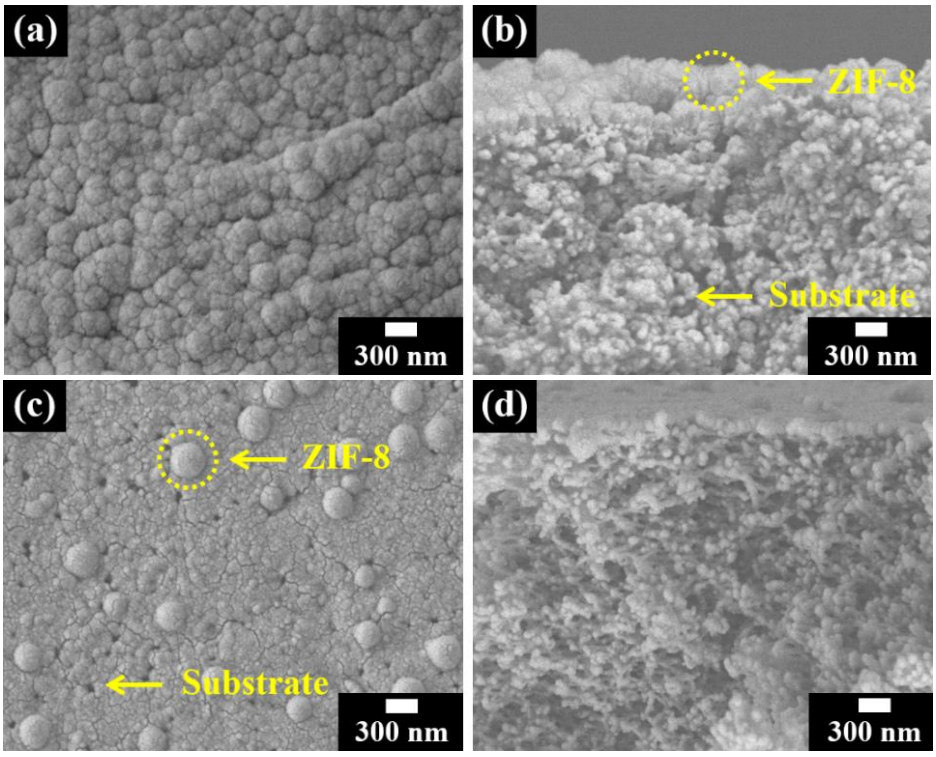

Figure 4.11 Top and cross section view of (a - b) bore and (c - d) shell side of ZIF-8-S/HFs after seed layer optimization step

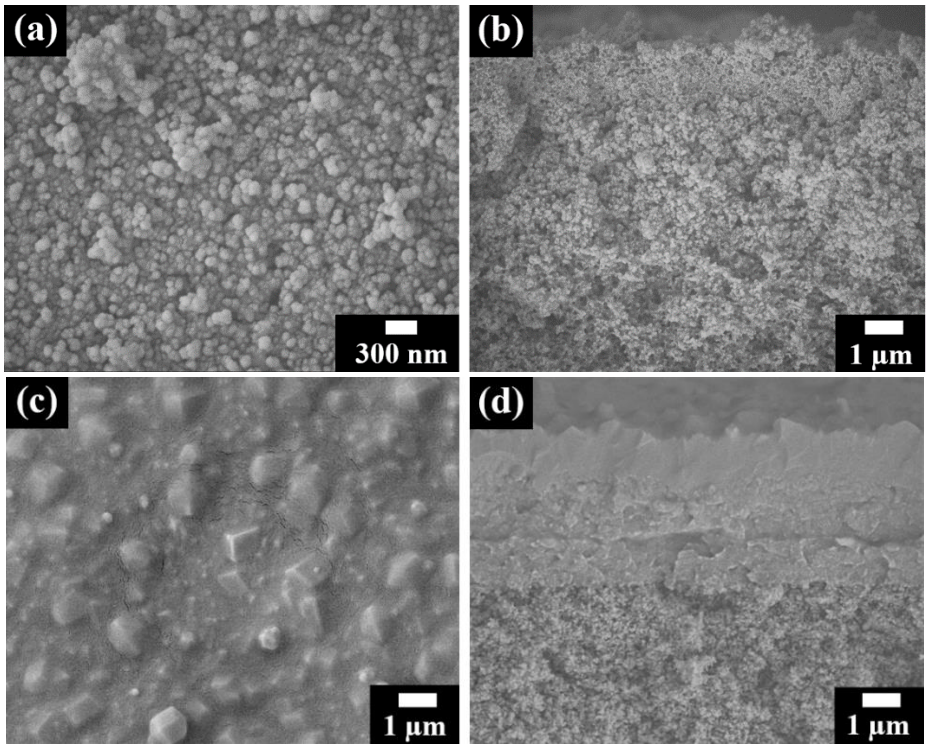

Figure 4.12 Top and cross section view of (a - b) ZIF-8-S/HFs (shell side) after PMMOF process and (c - d) ZIF-8-M-PDMS/HFs (shell side) after secondary growth

An optimized ZIF-8 seed layers on the bore side of Matrimid® HFs were then subjected to a continuous flow of growth solution to form high quality ZIF-8 membranes. As depicted in Figure 4.13(a - b), the secondarily grown ZIF-8 membranes were continuous, well-intergrown, and absent from any macroscopic defects such as cracks and pinholes. The thicknesses of the membranes were ~900 nm, comparable to the thickness of ZIF-8 membranes synthesized by our groups using microwave assisted seeding and microfluidic secondary growth technique.[10]

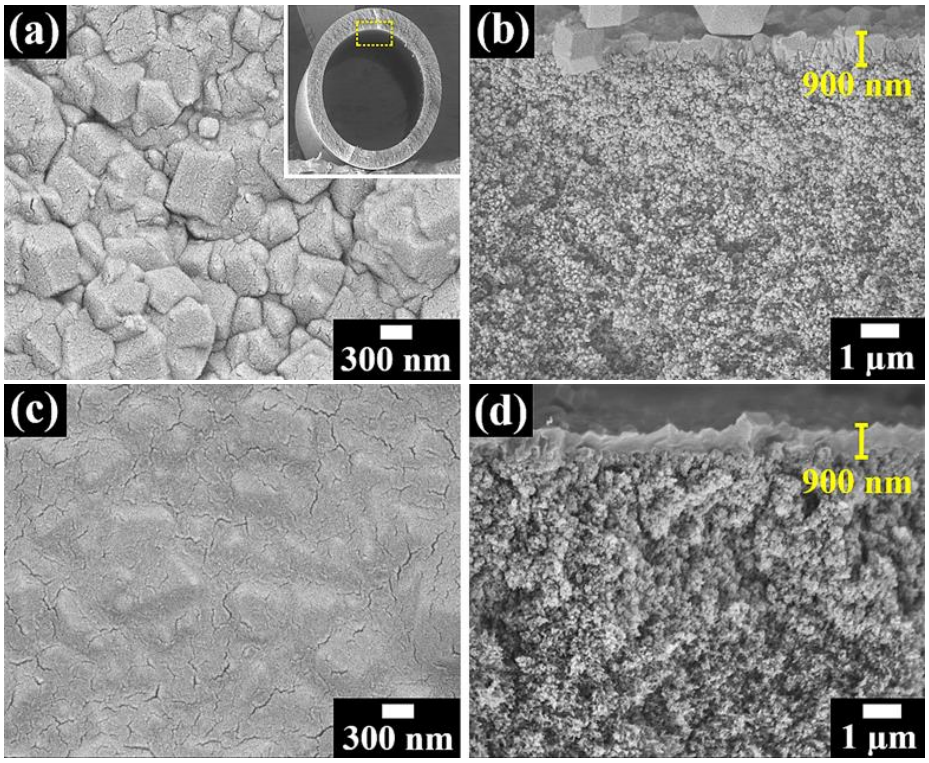

Figure 4.13 Top and cross section view of ZIF-8-M/HFs (a - b) before and (c - d) after PDMS coating step under high magnification. Inset image shows cross section of the ZIF-8-M/HFs under low magnification

Furthermore, ZIF-8 polycrystalline layer appears to be strongly adhered to the substrates, which is complete opposite to those prepared using ZIF-8 seed layers physically deposited on inner side of Matrimid® HFs to resemble conventional dip-coating method as presented in our earlier study.[10] Unlike the conventional dip-coating method, PMMOF seeding method enables the formation of ZIF-8 seed crystals with strong attachment to substrates surfaces, thereby resulting in ZIF-8 membranes that are strongly adhered to the HFs. We postulate that strong attachment of ZIF-8 polycrystalline layers to substrate surfaces is attributed to possible formation of chemical bonding between Zn ions coordinated to carboxylic groups of Matrimid® HFs and nitrogen of HmIm linkers.

Table 4.2 Binary propylene/propane separation performance of ZIF-8-M/HFs and ZIF-8-PDMS/HFs conducted at room temperature under atmospheric pressure

Sample	ZIF-8-M/HFs		ZIF-8-M-PDMS/HFs	
	Propylene permeance	**Separation factor**	**Propylene permeance**	**Separation factor**
M1	238.2	3.0	164.4	69.3
M2	265.3	1.6	148.4	54.4
M3	388.8	1.9	142.3	41.4
Avg.± stdev.	297.4 ± 80.2	2.2 ± 0.7	151.7 ± 11.4	55.0 ± 13.9

Propylene permeance unit: $\times 10^{-10}$ mol/(m^2•Pa•s)

Binary propylene/propane separation performances of ZIF-8 membranes on Matrimid® HFs (ZIF-8-M/HFs) were determined using a Wicke-Kallenbach setup conducted at room temperature under atmospheric pressure. The as-synthesized ZIF-8 membranes, unfortunately, showed poor propylene/propane separation performances (see Table 4.2) presumably due to poor membrane microstructures (i.e., ZIF-8 crystal grain boundary). It is well-known that gas transports through polycrystalline membranes are governed by selective diffusion through crystal grains (intra-crystalline diffusion) and non-selective diffusion through grain boundary (i.e., inter-crystalline diffusion). Sheng et al.[87] have demonstrated that these inter-crystalline grain boundary defects can be minimized or blocked by applying a thin layer of PDMS on top of a polycrystalline ZIF-8 layer. Defect reduction of ZIF-8 membranes result in significant improvement in propylene/propane separation performances. In addition, since PDMS is extremely permeable towards propylene, a thin PDMS coating is not expected to compromise propylene flux of the ZIF-8 membranes.[157]

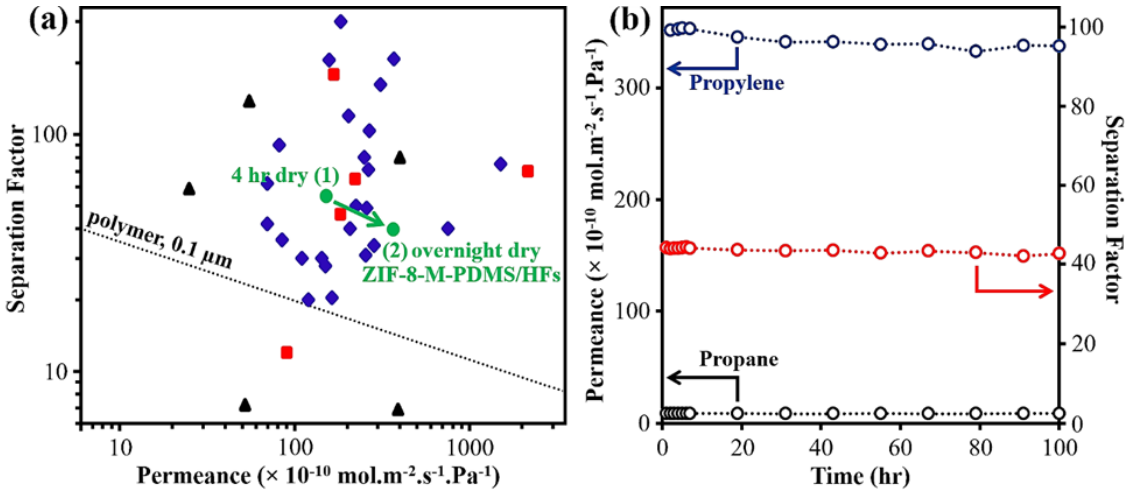

Figure 4.14 (a) propylene/propane separation performances of the ZIF-8-M-PDMS/HFs (●) in comparison to those reported in literature. The data includes ZIF-8 membranes grown on polymer HFs (■),[10, 78, 80, 81, 84] organic and inorganic flat discs (♦),[71, 87, 147, 59, 70, 116, 119, 145, 158-161] and inorganic tubes, capillaries, and HFs (▲).[148-151] The upper bound for polymer membrane was drawn based on work by Ma et al.[83] (b) long term permeation test conducted at room temperature under atmospheric pressure

To coat thin PDMS layer onto ZIF-8-M/HFs, a PDMS coating solution was flowed through the bore side of ZIF-8-M/HFs that were already packaged into test modules. Figure 4.13(c - d) shows the surface and cross section microstructures of the PDMS coated ZIF-8 membranes (ZIF-8-M-PDMS/HFs), showing a smooth and uniform PDMS layer coating the top of polycrystalline ZIF-8 layer. Thickness between PDMS coated and as-synthesized ZIF-8 membranes were identical, owing to extremely thin PDMS layer. After PDMS curing process, separation performances of the ZIF-8-M-PDMS/HFs were again tested under equal molar propylene/propane feed.

Figure 4.14a and Table 4.2 present separation performances of the ZIF-8-M-PDMS/HFs, showing average propylene/propane separation factor and propylene permeance of 55 and 152 × 10^{-10} mol/(m^2•Pa•s), respectively. The performances are comparable to those reported in literatures and most importantly they are within the

'commercially attractive' region for commercial propylene-selective membranes as proposed by Colling et al.[13] (see also Figure 4.15). The ability to *in-situ* seal or heal defective ZIF-8 membranes inside membrane modules using facile flow processing method is important for practical application as it provide new means to either improve or restore separation performances of the membranes after membrane module assembly or during actual operation.

For their practical applications, it is of great interest to enhance propylene permeances of ZIF-8 membranes.[147] We found that propylene permeances of the ZIF-8 membranes increases dramatically to $369 \pm 17 \times 10^{-10}$ mol/(m^2•Pa•s) when the seeded HFs (i.e., ZIF-8-S/HFs) are dried at 60^{o}C for prolonged time (i.e, overnight) prior to secondary growth. The propylene/propane separation factor decreases from 55 to 40 but the separation factor is still within an acceptable value. The enhancement in propylene permeance of our ZIF-8 membranes were surprising. We postulate that the improvement in propylene permeances may stem from the instability of the KOH-modified layer in methanol. As previously mentioned, only a portion of Matrimid® HFs (several μm thick) were hydrolyzed and then ion-exchanged to form Zn polyamate salts, and this Zn polyamate salts are believed to be slightly dissolved in methanol solvent.[162]

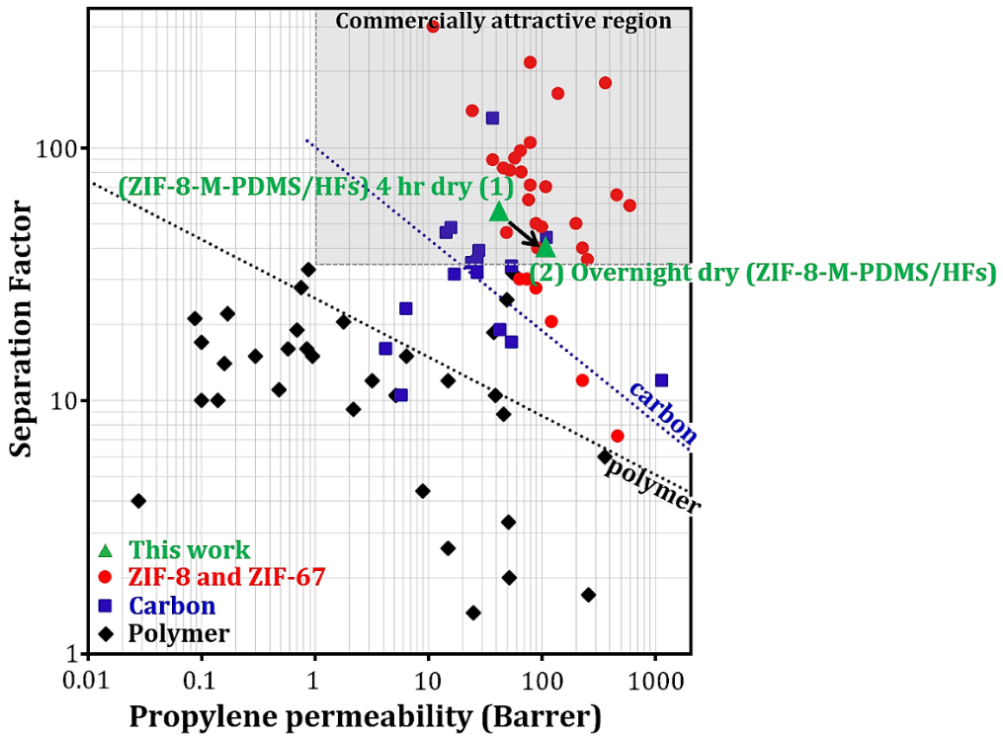

Figure 4.15 Propylene/propane separation performances of the ZIF-8-M-PDMS/HFs in comparison to those reported in literature, 1 Barrer = 3.348×10^{-16} mol•m/(m^2•Pa•s). The data includes polymer,[163-172] carbon,[172-174] and ZIF membranes,[10, 59, 70, 71, 78, 80, 81, 84, 87, 116, 118, 119, 142, 145, 147-151, 158-161, 175-178] (ZIF-8 and iso-structural ZIF-67 synthesized on either organic or inorganic substrates). The commercially attractive region, polymer upper bound, and carbon upper bound were drawn based on refs.[13, 163, 174]

Due to much shorter drying time (4 hrs.) after ZIF-8 seeding step, residual methanol in the pore of substrates might cause dissolution of a part of the Zn ion-exchanged layer which subsequently densifies, thereby leading to a reduced propylene permeance. As opposed to methanol, the Zn polyamate salt layers are insoluble in water as mentioned by Frost et al.,[179] therefore the use of water-based secondary growth solution during secondary growth step does not compromise the pore of substrates. Finally, long term stability of the ZIF-8 membranes is essential for their large scale applications. As shown in Figure 4.14b, ZIF-8-M-PDMS/HFs exhibit a relatively stable separation

performances over 100 hrs. of continuous flow of binary propylene/propane mixture. There were no significant deterioration in membrane performances observed during the long term permeation measurements.

4.4. Conclusion

We have successfully demonstrated a formation of submicron thick polycrystalline ZIF-8 membranes on the bore side of Matrimid® HFs using a secondary growth method. Nanometer-sized ZIF-8 seed crystals with uniform surface coverage were prepared using a polymer modification process followed by solvothermal reaction in a HmIm ligand solution. Location of ZIF-8 seed layers and membranes (i.e., shell or bore side) were readily controlled by adjusting the location of polymer modification. A subsequent microfluidic secondary growth conducted at room temperature resulted in continuous and well-intergrown submicron thick ZIF-8 membranes. The optimized ZIF-8 membranes, once coated with a thin PDMS layer, displayed an average propylene permeance and propylene/propane separation factor of 369×10^{-10} mol/(m^2•Pa•s) and 40, respectively. Furthermore, the membranes showed stable separation performances over continuous operation of 100 hrs. The current synthesis is expected applicable for facile preparation of ZIF-8 membrane modules by growing ZIF-8 films on off-the-shelf HF modules which is a significant step forwards towards commercialization of ZIF-8 membranes.

5. SYNTHESIS OF ULTRATHIN ZIF-8 MEMBRANES ON PVDF HOLLOW FIBERS USING BASE MODIFICATION STRATEGY

5.1. Introduction

Inorganic zeolites have been fabricated into polycrystalline membranes, however, high membrane fabrication cost estimated around $5,000 - $10,000 per sq. meter of assembled module limit their widespread uses in industry.[180] The majority of zeolite membrane cost (> 75%) is from the use of expensive ceramic substrates.[54] This issue would also be true for ZIF-8 membranes especially those grown on ceramic substrates. The fabrication cost of ZIF-8 membranes could be brought down, to some extent, by using polymer substrates as the cost of manufacture for polymer is significantly lower.

Our group has successfully developed two new ZIF-8 synthesis methods to prepare ZIF-8 membranes on bore side of Matrimid® HFs for propylene/propane separation: (1) microwave assisted seeding followed by microfluidic secondary growth[3] (2) PMMOF seeding followed by microfluidic secondary growth.[181] ZIF-8 membranes synthesized using these methods exhibited promising binary propylene/propane separation performances, exceeding the Robeson upper bound. In addition, their separation performances are within the 'commercially attractive' region required for propylene-selective membranes.[13] The use of inexpensive Matrimid® HFs as substrates for ZIF-8 membrane synthesis makes them attractive from economic point of view. We believe ZIF-8 membrane fabrication cost could be further reduced by using cheaper and more readily available polymers such as PVDF, polyethersulfone, polysulfone, cellulose acetate, etc.

PVDF is a semi-crystalline polymer with repeat unit of $-(CH_2-CF_2)_n-$.[182] PVDF has received significant interest as membrane material owing to its excellent mechanical strength, thermal stability, as well as inertness against various chemicals and solvents.[98] PVDF has been extensively used in water separation applications as microfiltration and ultrafiltration HF membranes and currently explored for bio-separation application. PVDF is soluble in common organic solvents such as dimethyl formamide, N-methyl-2-pyrrolidone, and N,N-dimetyl acetamide. Porous PVDF flat sheets or HFs can be prepared via simple phase inversion method, which is a common process in large scale membrane production.[183]

PVDF HFs have been used as substrates for the synthesis of ZIF-8 membranes. Unfortunately, PVDF tend to be chemically inert with few available nucleation sites which lead to unsatisfactorily low ZIF-8 nucleation densities on substrate surfaces.[86] Due to poor heterogeneous nucleation of ZIF-8 on the supports, chemical functionalization steps were often introduced. For example, Chen and co-workers[73, 74] have successfully synthesized well-intergrown 1 µm thick ZIF-8 membranes on PVDF HFs for hydrogen separation. The 3-aminopropyl-triethoxysilane-titania functionalized PVDF HFs were immersed in ZIF-8 synthesis solution for several hours to obtain a continuous ZIF-8 layer. Li et al.,[72] on the other hand, introduced ammonization-based chemical modification on PVDF HFs to prepare continuous ZIF-8 membranes for hydrogen separation.

As mentioned in Chapter 2, chemical reactions between PVDF and strong base (e.g., KOH, NaOH, etc.) led to dehydrofluorination and formation of C=C and -OH bonds. Active groups (i.e., -OH) on KOH-modified PVDF HFs act as nucleation sites thereby

promotes heterogeneous nucleation of ZIF-8.[184-187] By limiting PVDF dehydrofluorination reactions mostly on bore side of PVDF HFs, we can direct nucleation and growth of ZIF-8 crystals selectively on the bore side to create densely packed ZIF-8 seed layers. In addition, -OH groups of the KOH-modified PVDF HFs can form covalent bonds (Zn-O) with ZIF-8 frameworks to create strongly adhered ZIF-8 polycrystalline layers on the substrates.[184] Covalent linkages between substrates and ZIF-8 frameworks can improve mechanical stability of the membranes.

Herein, we report a new methodology for the synthesis of ultrathin ZIF-8 membranes on PVDF HFs based on PVDF dehydrofluration reactions. A new seeding steps, namely KOH-assisted solvothermal seeding was proposed to deposit high quality ZIF-8 seed layers on bore side of PVDF HFs. A warm KOH solution was used to modify PVDF polymer chains, creating abundance of -OH groups on PVDF surfaces. Hydroxyl groups on PVDF surfaces promote high heterogeneous nucleation density of ZIF-8. The proposed method is site-selective, allowing ZIF-8 seed layers to be deposited on preferred surfaces (i.e., bore or shell side of PVDF HFs). Microfluidic secondary growth carried out at room temperature led to formation of defect-free ZIF-8 membranes strongly adhered to substrate surfaces. A number of characterization tools were used to confirm formation of ZIF-8 seed crystals and membranes on the support. Electron diffraction and FTIR spectroscopy were used to determine crystallinities and chemical bonds of ZIF-8, respectively. Electron microscopy was used to analyze microstructures of ZIF-8 seed layers and membranes. Binary propylene/propane permeation measurements were carried out to assess quality of ZIF-8 membranes.

5.2. Experimental section

5.2.1. Materials

PVDF HF microfiltration membrane module (Microza® UMP-1047R) was purchased from Pall Corporation. Potassium hydroxide (KOH, reagent grade, VWR International) was used to chemically modify PVDF HF substrates. Zinc nitrate hexahydrate ($Zn(NO_3)_2 \cdot 6H_2O$, 98%, Sigma-Aldrich), 2-methylimidazole ($C_4H_6N_2$, 99%, Sigma-Aldrich, hereafter HmIm), sodium formate (HCOONa, 99%, Sigma-Aldrich), methanol (CH_3OH, > 99%, Alfa-Aesar), and deionized water were used to synthesize ZIF-8 seed layers and membranes. PDMS (Sylgard® 184, Dow Chemical) and hexane (C_6H_{14}, ACS grade, VWR International) were used to seal defective ZIF-8 membranes. Ethanol (C_2H_5OH, 94 - 96%, Alfa-Aesar) was used as solvent to clean PVDF HFs.

5.2.2. Methods

5.2.2.1. Preparation of PVDF HFs

PVDF HF membrane module was disassembled to obtain individual PVDF HF. The HF was then immersed in ethanol overnight to remove glycerin preservative from pore of the HF. Then, the HF was dried at 60°C overnight to remove ethanol solvent. Pristine PVDF HF has ID, OD, and average pore size of 1400 µm, 2200 µm, and 0.2 µm, respectively. Top and cross section micrographs of bore and shell side of pristine PVDF HF are shown in Figure 5.1. Preparation of PVDF HF setup 10 cm in length used for ZIF-8 seeding and secondary growth steps can be found in previous chapter (see section 4.2 in

Chapter 4). Since PVDF HF is slightly larger in diameter in comparison to Matrimid® HF, a much larger PTFE tubing (ID/OD, 4.76/6.35 mm) was used to house the PVDF HF.

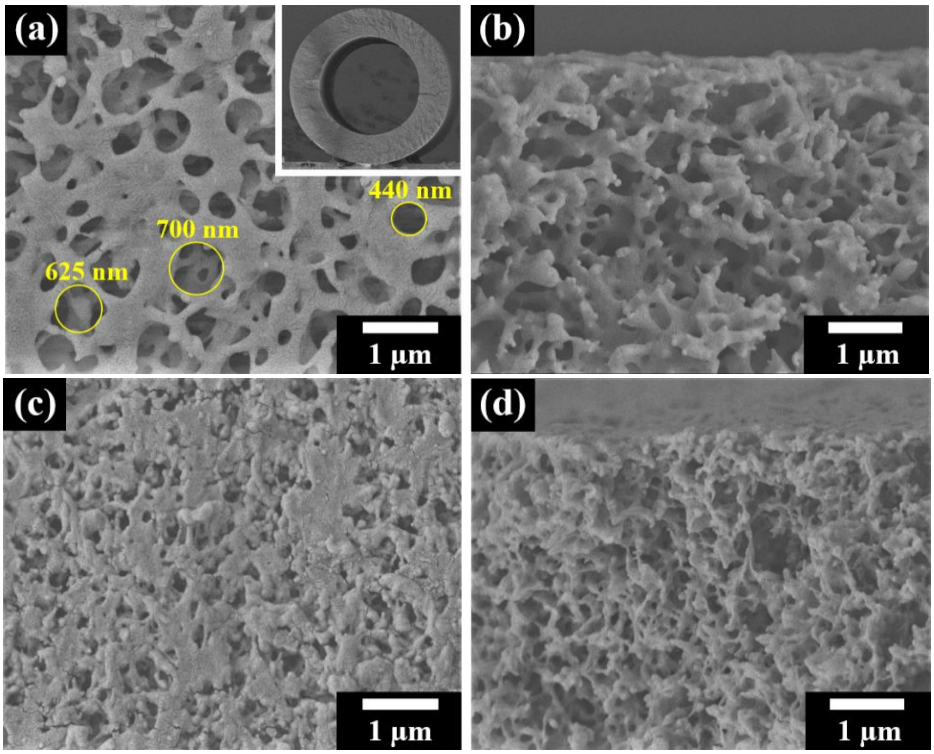

Figure 5.1 Top and cross section view of the (a - b) bore side and (c - d) shell side of pristine PVDF HFs. Inset SEM image shows cross section of the HFs under low magnification

5.2.2.2. Preparation of ZIF-8 seed layers on PVDF HFs

KOH solution was used to modify PVDF polymer chains. Using a syringe pump (Harvard Model 55-4152), a warm (50°C) KOH solution (5 M) was fed to the bore side of PVDF HF at a flow rate of 5.50×10^{-3} ml/s for different period of time. The KOH-treated PVDF HF (hereafter, PVDF-X, where X represent the KOH treatment time in min) was then saturated with a 100 mM of Zn solution at a flow rate of 5.50×10^{-3} ml/s for 1 hr (hereafter, PVDF-X-Zn). Excess KOH and Zn solutions were purged slowly with air and

dried with Kimwipes. Preparation of metal and linker precursor solutions and procedures to deposit ZIF-8 seed layers on PVDF HF (hereafter, PVDF-X-S) can be found in Chapter 4 (see section 4.2).

5.2.2.3. Preparation and defect sealing of ZIF-8 membranes on PVDF HFs

Synthesis of a well-intergrown ZIF-8 membrane on PVDF HF (hereafter, PVDF-X-M) and defect sealing of ZIF-8 membrane using PDMS (hereafter, PVDF-X-M-PDMS) were carried out following procedure found in Chapter 4 (see section 4.2).

5.2.2.4. Characterization

ATR-FTIR spectra were collected using a Nicolet iS5 FTIR Spectrometer equipped with iD7-ATR diamond accessory scanning from 400 cm^{-1} to 4000 cm^{-1}. PXRD patterns were collected using a Rigaku Miniflex II benchtop X-ray diffractometer with Cu-Kα radiation scanning from the 2θ range of 5 - 25 °. Electron micrographs were obtained using a JEOL JSM-7500F operating at acceleration voltage of 5 keV and working distance of 15 mm. Gas separation properties of the as-synthesized and PDMS coated ZIF-8 membranes were measured using the Wicke-Kallenbach method shown in Figure 5.2. Binary propylene/propane permeation measurements were performed under atmospheric pressure at room temperature (~22°C). Binary mixture of propylene and propane (6.67×10^{-1} ml/s) was fed to the bore side while argon sweep gas (6.67×10^{-1} ml/s) was flowed through the shell side of PVDF HF. Composition of propylene and propane in sweep gas was measured using Agilent GC 7890 A gas chromatography.

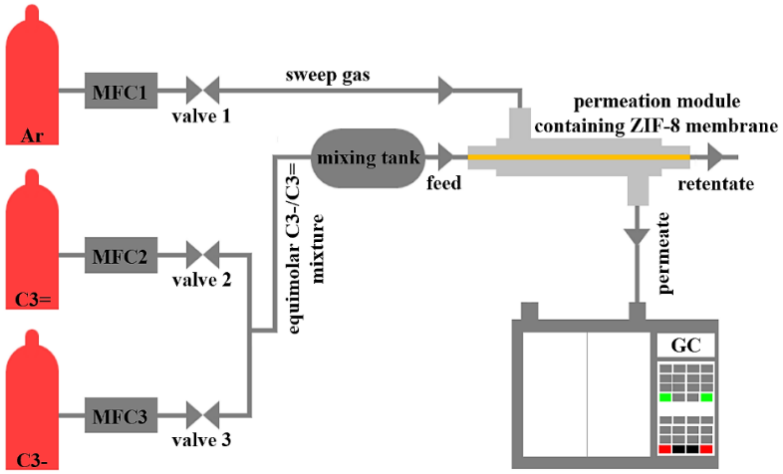

Figure 5.2 Schematic illustration of the Wicke-Kallenbach setup for binary propylene/propane permeation measurements

5.3. Result and discussion

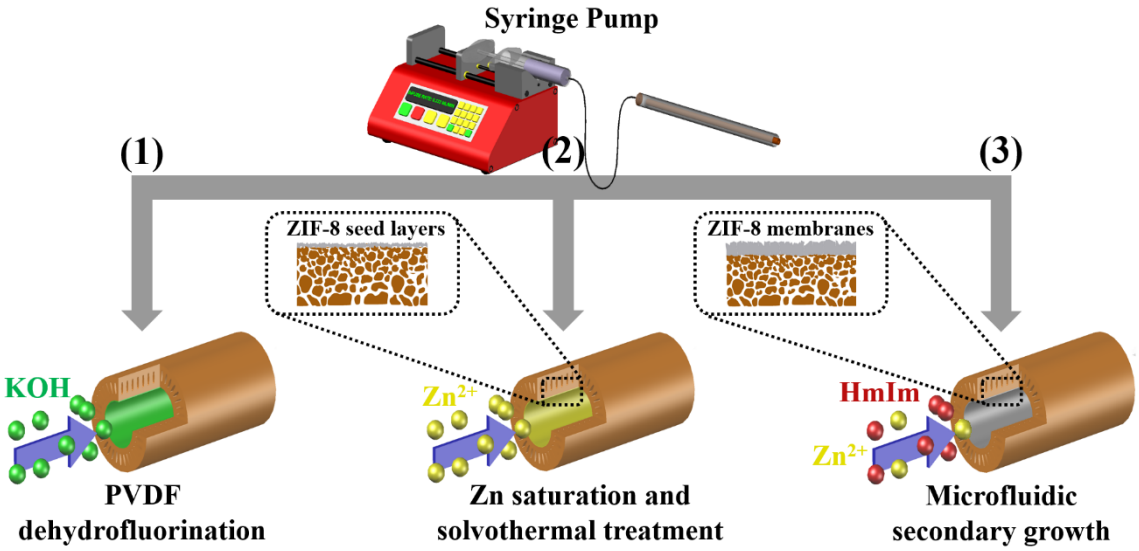

Figure 5.3 Schematic illustration of KOH-assisted solvothermal seeding followed by microfluidic secondary growth to prepare ultrathin ZIF-8 membranes on PVDF HFs

Figure 5.3 shows schematic of the KOH-assisted solvothermal seeding method to deposit densely packed ZIF-8 seed layers selectively on bore side of PVDF HF. This method is very much similar to the PMMOF seeding method described in Chapter 4 but it

involves different chemical reactions to modify polymer surface. In brief, a warm KOH solution provided to bore side of PVDF HF modifies PVDF polymer chains and creates C=C and -OH bonds that can act as nucleation sites for ZIF-8 crystals. Subsequent Zn saturation and solvothermal linker treatment steps led to formation of densely packed ZIF-8 seed layers on the bore side of PVDF HF. The ZIF-8 seed layers were then secondarily grown to form defect-free ZIF-8 membranes under continuous flow of growth solution.

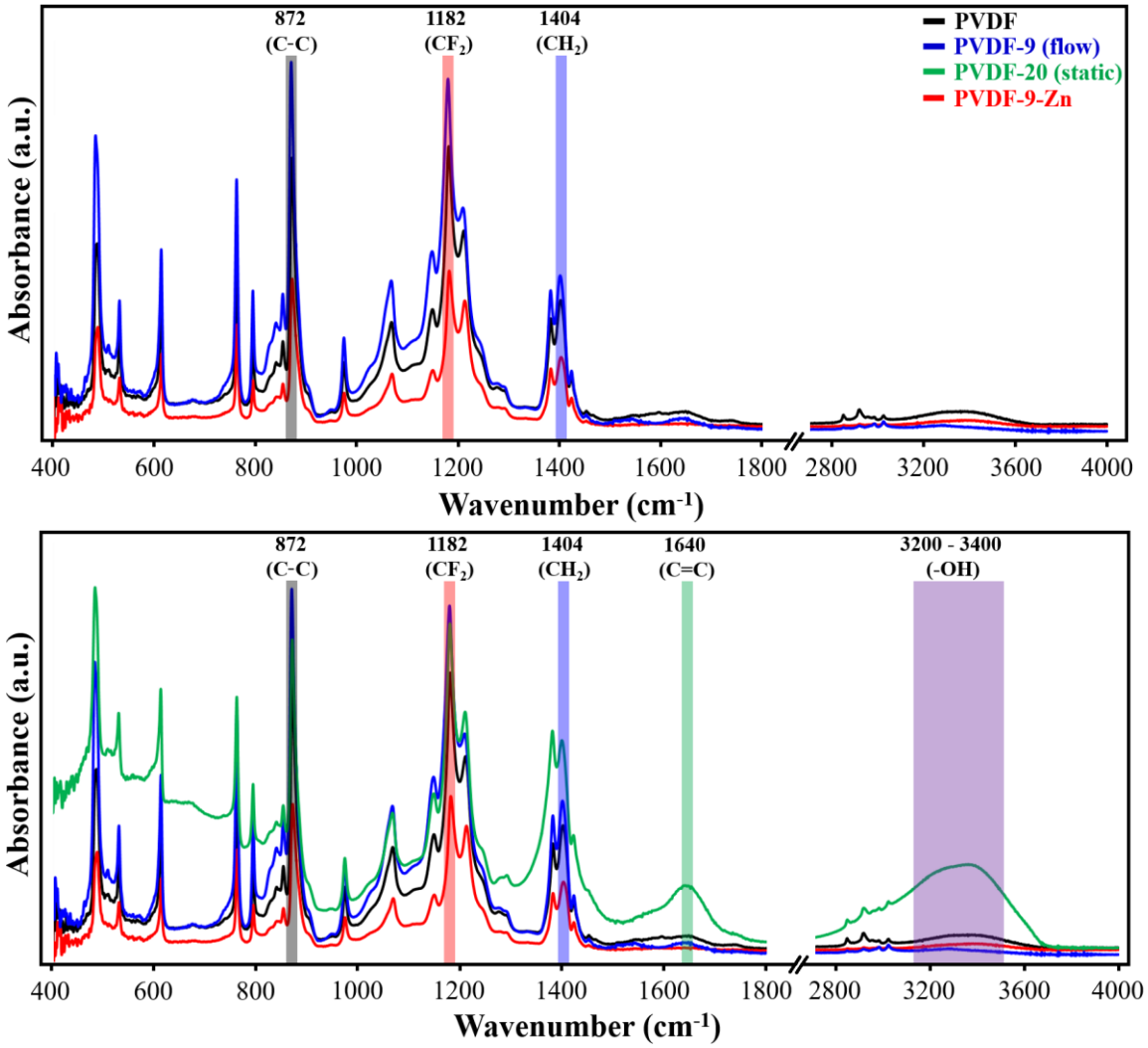

Figure 5.4 ATR-FTIR spectra of PVDF, PVDF-9 (microfluidic flow condition), PVDF-20 (static condition), and PVDF-9-Zn

Figure 5.4 shows ATR-FTIR spectra of pristine (PVDF), KOH-treated (PVDF-X), and Zn-saturated (PVDF-X-Zn) PVDF HFs. Pristine PVDF HF exhibits characteristic FTIR peaks at 872 cm^{-1}, 1182 cm^{-1}, and 1404 cm^{-1} that correspond to C-C, $-CF_2$, and $-CH_2$ stretching vibrations, respectively.[188] The FTIR spectra of pristine and KOH-modified (i.e., PVDF-9) were surprisingly identical. After KOH treatment, the absorption peaks that correspond to C=C (1640 cm^{-1}) and -OH (3000 cm^{-1} - 3400 cm^{-1}) bonds of the KOH-modified PVDF HF are expected appear but it is not the case under current modification condition (i.e., continuous microfluidic flow of KOH solution to the bore side of PVDF HF at flow rate 5.50×10^{-3} ml/s of for 9 min). The main reasoning behind this observation is most likely to due to limited dehydrofluorination reaction under microfluidic condition.

In order to validate our hypothesis that dehydrofluorination reaction is limited under microfluidic condition, we decided to expose the PVDF HF to a much harsher KOH treatment. The PVDF HF was immersed in 20 ml of KOH solution for 20 min under static condition and temperature of the solution was maintained at 50^{o}C throughout. ATR-FTIR analysis was taken on the shell side of PVDF HF instead of the bore side for easier access. As can be seen from Figure 5.4, the HF exposed to a more severe KOH treatment exhibit two new broad FTIR peaks at 1640 cm^{-1} and 3000 cm^{-1} - 3400 cm^{-1}, that can be assigned to C=C and -OH absorption bands of the chemically modified PVDF HF.[100] In addition, we also observed a slight discoloration of PVDF HF from white to light brown, consistent with previous observation.[98] We also obtained similar FTIR results when the PVDF HFs were subjected to static KOH treatment using only 3.0 ml KOH solution (equivalent to total volume of KOH solution used under microfluidic condition) for 9 min. Based on the

above findings, we have confirmed that PVDF dehyrofluorination reaction have indeed occurred, however, the extent of reaction under microfluidic flow condition may be limited in comparison to under static condition. PXRD patterns of PVDF, PVDF-9, and PVDF-9-Zn were illustrated in Figure 5.5a. For all cases, the PXRD patterns are identical and they possess two major diffraction peaks that correspond to α and β-phases of the PVDF.[189]

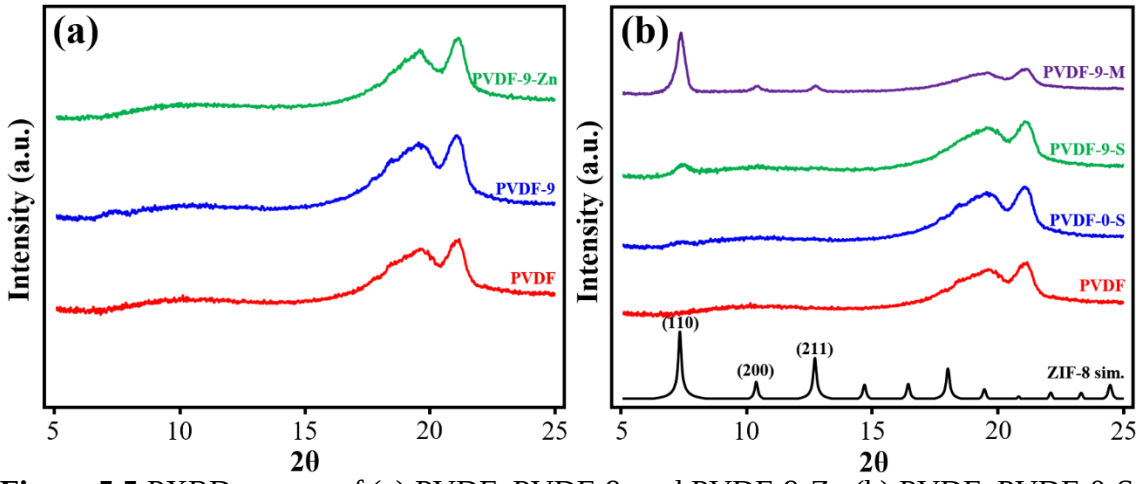

Figure 5.5 PXRD pattern of (a) PVDF, PVDF-9, and PVDF-9-Zn (b) PVDF, PVDF-0-S, PVDF-9-S, and PVDF-9-M in comparison with ZIF-8 simulated pattern

5.3.1. Synthesis of ZIF-8 seed layers (standard condition, X = 9)

To obtain densely packed ZIF-8 seed layers on bore side of PVDF HF, PVDF-9-Zn was subjected to a solvothermal treatment in HmIm linker solution for 1 hr, followed by cooldown to room temperature for 2 hrs. Please note that standard KOH treatment of 9 min was selected following the condition used in Chapter 4. However, the standard 9 min KOH treatment time used in ZIF-8 seeding step may or may not be an optimized condition. Optimization of ZIF-8 seeding step, by varying KOH treatment time will be discussed in detail in later section. For comparison, similar solvothermal treatment was also performed

on unmodified PVDF HF to highlight the importance of dehydrofluorination reaction required to obtain densely packed ZIF-8 seed layers. As shown in Figure 5.5b, both of the seeded HFs (i.e., PVDF-9-S and PVDF-0-S) exhibit characteristic diffraction peaks of ZIF-8 but PVDF HF not subjected to KOH treatment showed weaker diffraction intensity. This suggest that ZIF-8 seed crystals form in greater number when the PVDF HF was subjected to KOH treatment.

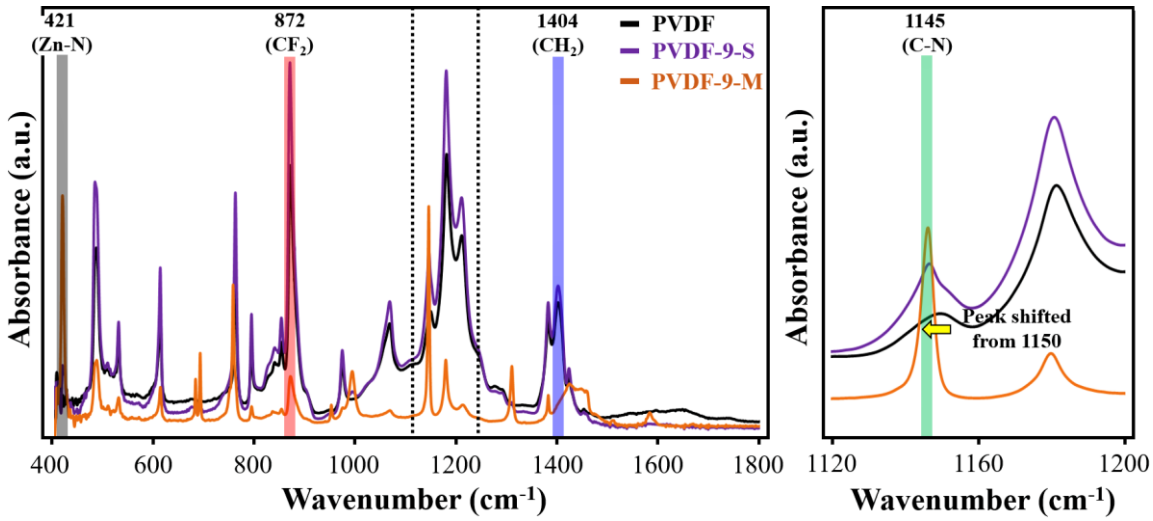

Figure 5.6 ATR-FTIR spectra of PVDF, PVDF-9, PVDF-20, and PVDF-9-Zn

After solvothermal HmIm treatment, two new absorption peaks at 421 cm^{-1} and 1145 cm^{-1} appeared and these peaks can be assigned to Zn-N and C-N bands of ZIF-8 seed crystals (Figure 5.6).[156] However, the FTIR peak intensities of ZIF-8, especially those at 421 cm^{-1} were relatively weak that sometimes indistinguishable from the pristine HFs. It is important to point out that the ATR-FTIR spectra in Figure 5.6 were taken on the bore side of PVDF HF instead of the shell side. The FTIR spectroscopy taken on shell side of the HF however did not show any peak signatures of ZIF-8 (result is not shown), indicating the majority of the ZIF-8 seed layers are deposited selectively on the bore side.

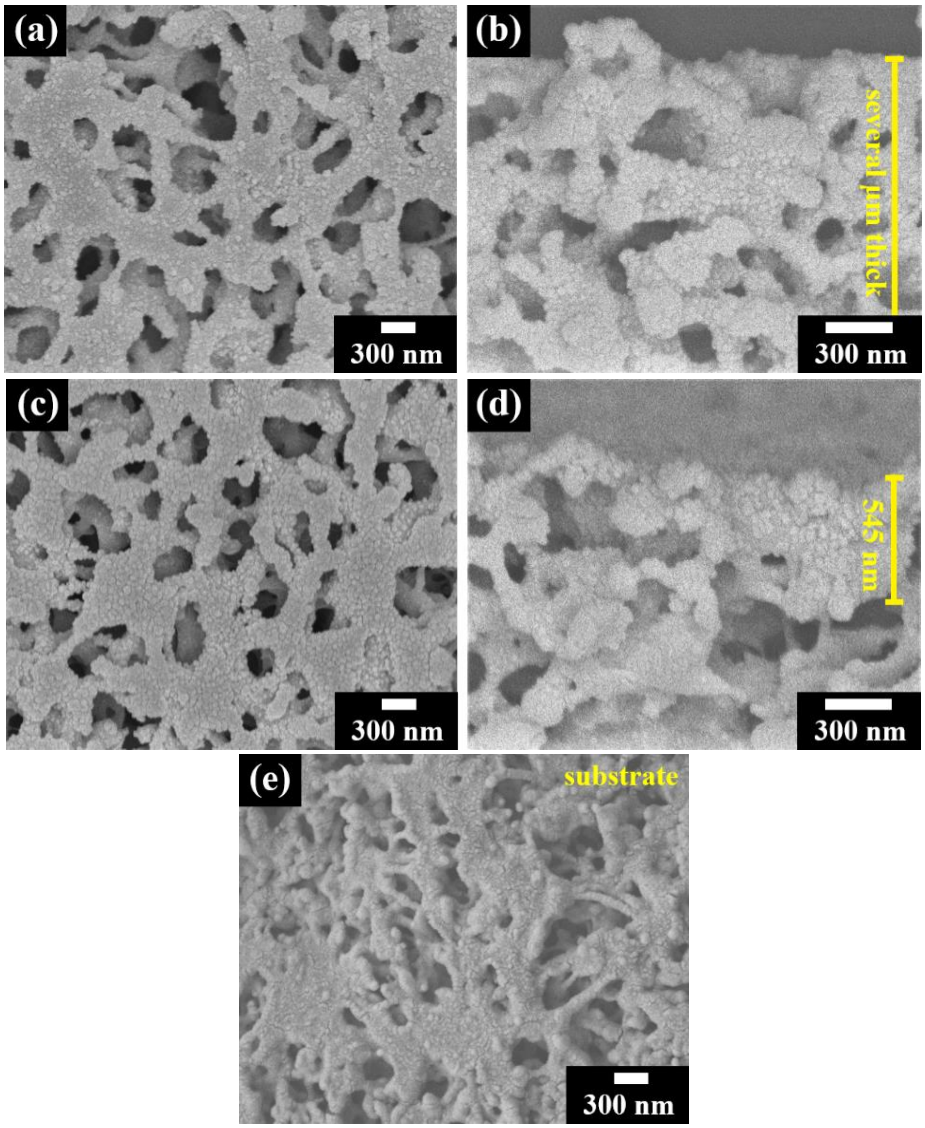

Figure 5.7 Top and cross section view of the bore side of (a - b) PVDF-9-S (c - d) PVDF-0-S (e) top view of the shell side of PVDF-9-S

Figure 5.7(a - b) show top and cross section electron micrographs of PVDF HFs after seeding step (i.e., PVDF-9-S). ZIF-8 seed nanocrystals roughly 60 nm in size were uniformly covering surface of the HFs. Cross section view revealed that ZIF-8 seed layers not only form on the very top surface of the HFs but also form several µm thick from the surface. During KOH treatment, KOH solution diffuse on both axial and radial direction

of the HFs modifying not only surface but also inside the substrates (modification up to several μm deep depending on the KOH treatment time). Abundance of -OH groups on PVDF surfaces act as nucleation sites for ZIF-8 crystals. As a result, PVDF HFs subjected to KOH treatment form ZIF-8 crystals in greater number than that of unmodified PVDFs. As oppose to bore side, there were no ZIF-8 crystals formed on the shell side of PVDF HFs even though linker solution was provided from the shell side, indicating site-selective nature of KOH-assisted solvothermal seeding step.

It is also critical to perform similar seeding steps using PVDF HFs that are not subjected to KOH treatment. Due to inertness of pristine PVDF HFs, very few ZIF-8 crystals are expected to form on substrate surfaces. As illustrated in Figure 5.7(c - d), the amount of ZIF-8 crystals deposited on the surface of PVDF-0-S is not as many (though not obvious) than those of PVDF-9-S. Based on this observation, eliminating KOH treatment during ZIF-8 seeding step and relying only on intrinsic surface properties of pristine PVDF HFs are not encouraged as the pristine HFs provide relatively low heterogeneous nucleation density of ZIF-8 which led to formation of poor quality ZIF-8 seed layers.

5.3.2. Synthesis of ZIF-8 membranes (standard condition, X = 9)

ZIF-8 membranes were prepared by subjecting ZIF-8 seed layers on PVDF HFs (i.e., PVDF-9-S) to continuous microfluidic flow of growth solution at flow rate of 1.67×10^{-3} ml/s at room temperature for 6 hrs. The resulting ZIF-8 membranes were continuous, well-intergrown, and free from any macroscopic defects such as cracks. The membranes

were relatively thin (~1.2 µm). The membranes were also free from delamination, indicating that ZIF-8 layers were strongly bonded to substrates. To minimize grain boundary defects, PDMS coating layers were applied on top of polycrystalline ZIF-8 layers. As shown in Figure 5.8, thin PDMS layers were successfully coated on top of ZIF-8 membranes. The thickness of PDMS coated ZIF-8 membranes was comparable to those of as-synthesized membranes, owing to extremely thin PDMS coating.

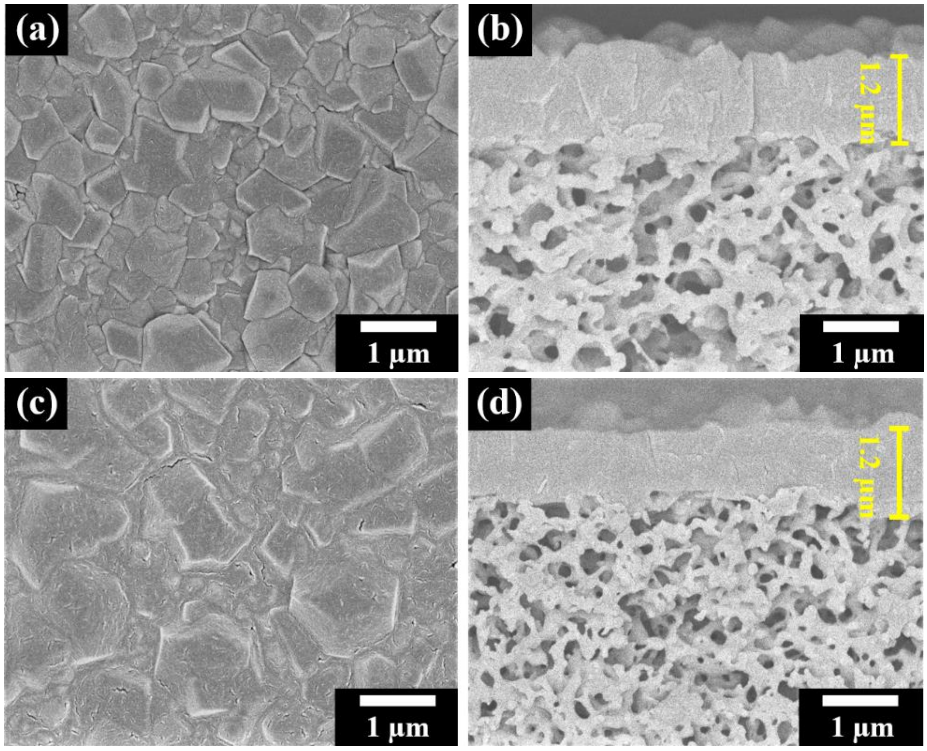

Figure 5.8 Top and cross section view of (a) PVDF-9-M (b) PVDF-9-M-PDMS

Several control experiments were carried out to highlight the importance of having good quality ZIF-8 seed layers prior to secondary growth. First control experiment is *in-situ* ZIF-8 membrane synthesis, where secondary growth solution was flowed through the bore side of PVDF HFs that have no pre-attached ZIF-8 seed crystals. Second control experiment is a typical secondary growth on PVDF-0-S, where secondary growth solution

was fed through the bore side of PVDF HFs containing poor quality ZIF-8 seed layers. Secondary growth conditions were maintained the same for both control experiment (i.e., secondary growth flow rate of 1.67×10^{-3} ml/s for 6 hrs.). Top and cross section electron micrographs of the secondarily grown ZIF-8 membranes are presented in Figure 5.9. Both of the membranes appear to be well-intergrown and defect-free, comparable to those synthesized using standard condition (i.e., PVDF-9-M). Therefore, we expect the propylene/propane separation performances of the membranes to be somewhat similar. However, propylene/propane permeation measurements revealed that these membranes possess markedly different separation performances (will be discussed in later section).

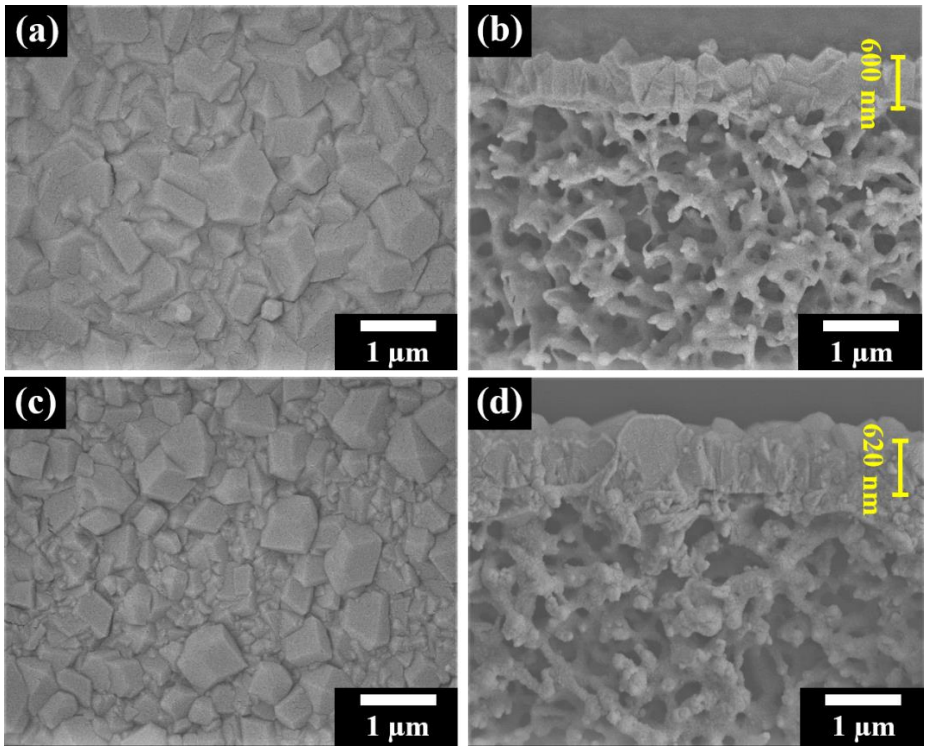

Figure 5.9 Top and cross section SEM images of (a) *in-situ* grown ZIF-8 membrane (b) PVDF-0-M

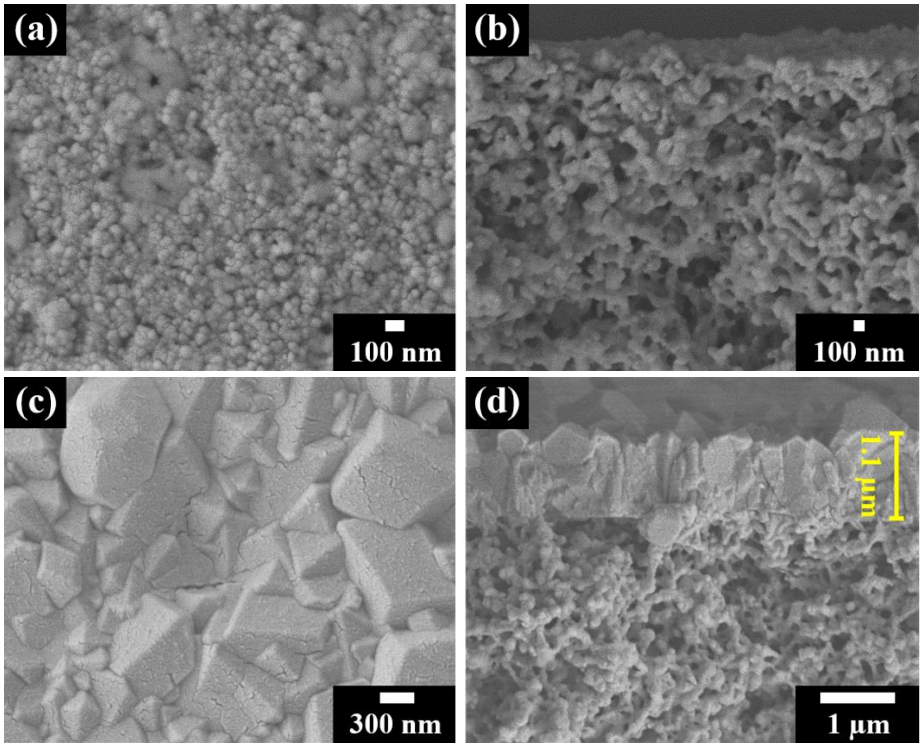

Figure 5.10 Top and cross section view of (a - b) ZIF-8 seed layers and (c - d) ZIF-8 membranes grown on the shell side of PVDF HFs

As previously mentioned, the KOH-assisted solvothermal seeding method is site-selective, enables us to grow ZIF-8 seed layers on either bore or shell side of the HFs. To demonstrate the site-selective nature of the process, KOH treatment, Zn saturation, and secondary growth steps were performed on shell side of the HFs, thereby forming ZIF-8 seed layers and membranes selectively on the shell side. Figure 5.10(a - b) shows that high quality ZIF-8 seed layers have been successfully deposited on the shell side of HFs using KOH-assisted solvothermal seeding method. Since ZIF-8 seed layers were deposited on the shell side of HFs, we thought it would be easier for us to perform secondary growth by immersing the seeded HFs in ZIF-8 synthesis solution. Secondary growth time, concentration, and temperature were maintained the same. As shown in Figure 5.10(c - d),

the resulting ZIF-8 membranes were also well-intergrown. The thickness of the membranes was around 1.1 µm, comparable to those synthesized on bore side of PVDF HFs under microfluidic condition. Due to handling convenience and ease of synthesis inside membrane module, we decided to focus on the preparation of ZIF-8 membranes on bore side of PVDF HFs for current study.

5.3.3. Separation performances of ZIF-8 membranes (standard condition, X = 9)

Prior to the permeation measurement, the as-synthesized ZIF-8 membranes were first assembled into membranes modules. Each module contains a single HF membrane with an active membrane length of 4 cm (effective membrane area of 1.75 cm^2). Pristine PVDF and PVDF-9-M were tested using Wicke-Kallenbach setup conducted at room temperature and atmospheric pressure. The pristine PVDF HF was not selective towards propylene and exhibited high propylene permeance of $4992 \pm 38 \times 10^{-10}$ mol/(m^2•Pa•s). On the other hand, the PVDF-9-M showed significantly lower propylene permeance. The membrane displayed an average propylene permeance and separation factor of $133 \pm 14 \times 10^{-10}$ mol/(m^2•Pa•s) and 2.5 ± 0.1, respectively. Even though separation factors of the membranes are unattractive, they are higher than Knudsen separation factor.[13]

Poor propylene/propane separation performances observed in PVDF-9-M is likely due to high concentration grain boundary defects, providing non-selective transport pathway for both propylene and propane gases. Sheng and co-workers[87] have demonstrated that these inter-crystalline grain boundary defects can be abated by applying thin PDMS layers on top of ZIF-8 layers. After PDMS coating steps, propylene/propane

separation factor of their ZIF-8 membranes improved from 3 to 55. Based on their findings, we believe if thin layer of PDMS were applied on top of our ZIF-8 membranes, we would observed similar improvement in propylene/propane separation factor.

Table 5.1 Binary propylene/propane separation performance of different ZIF-8 membranes

Samples	**Propylene permeance**	**Separation factor**
PVDF	4992 ± 38	1.0 ± 0.0
PVDF-0-M	722 ± 35	1.1 ± 0.1
PVDF-*in-situ*-M	207 ± 1.0	1.2 ± 0.3
PVDF-9-M	133 ± 14	2.5 ± 0.1
PVDF-9-M-PDMS	109 ± 2.7	4.5 ± 0.6

Propylene permeance unit: $\times 10^{-10}$ mol/(m^2•Pa•s)

To test our hypothesis, a thin layer of PDMS was applied on the PVDF-9-M by flowing a 5 wt.% PDMS/hexane solution through the bore side of HF followed by curing at room temperature for 48 hrs. under vacuum. After PDMS curing steps, separation performances of the PDMS coated ZIF-8 membranes on PVDF HFs (i.e., PVDF-9-M-PDMS) were again tested under equal molar propylene/propane feed. Table 5.1 present the separation performances of the PDMS coated membranes showing average propylene/propane separation factor and propylene permeance of 4.5 ± 0.6 and 109 ± 2.7× 10^{-10} mol/(m^2•Pa•s), respectively. To our surprise, the improvement in separation factor of our PDMS coated ZIF-8 membranes were marginal which are of complete opposite to our previous observation described in Chapter 4.

It is surmised that ZIF-8 membranes on PVDF HFs synthesized using KOH-assisted solvothermal seeding method possess poorer grain boundary structures that that of ZIF-8 membranes grown on Matrimid® HFs (see Chapter 4). There are a number of variables that can contribute to the poor separation performances of PVDF-9-M and PVDF-9-M-PDMS. First, pristine PVDF HFs possess average surface pores that are larger than that of pristine Matrimid® HFs (200 nm vs. 20 nm). In addition, PVDF HFs have larger ID (1400 µm vs. 465 µm) and possess different surface properties than Matrimid® HFs. As a result, ZIF-8 membranes grown on PVD HFs may possess poorer microstructures than that those grown of Matrimid® HFs. It is also important to note that the synthesis conditions which includes KOH-assisted solvothermal seeding, secondary growth, and PDMS coating have yet to be optimized. As a consequence, we ended up with ZIF-8 membranes with higher concentration grain boundary defects. Each of the synthesis steps need to be optimized in order to improve separation performances of the membrane.

We also have carried out propylene/propane permeation measurements on PVDF-0-M and *in-situ* grown ZIF-8 membranes (i.e., PVDF-*in-situ*-M). As shown in Table 5.1, separation performances of the membranes were much worse than PVDF-9-M indicating that membrane quality were not great. The main reasoning behind this observation is due to the use of poor quality seed layers during ZIF-8 membranes synthesis. This finding highlights importance of having high quality seed layers as a prerequisite for the synthesis of ZIF-8 membranes via secondary growth.

5.3.4. Improving propylene/propane separation performances of ZIF-8 membranes

Based on our initial finding, separation performances of ZIF-8 membranes synthesized using standard condition (i.e., PVDF-9-M), even after PDMS coating, are unsatisfactory. Microstructure optimization is believed to be the key to improve gas transport properties of ZIF-8 membranes on PVDF HFs. In this section, important synthesis variables are manipulated and their effect on membrane microstructures and separation performances are analyzed. Optimization of the synthesis steps are divided into three sections:

- PDMS coating step
- ZIF-8 seeding step
- Secondary growth step

5.3.4.1. Optimization of PDMS coating step

As described in earlier chapter, PDMS coating is merely used in membrane post-treatment to minimize grain boundary defects. Microstructures of ZIF-8 membranes synthesized using secondary growth are governed by ZIF-8 seeding conditions (affect microstructures of ZIF-8 seed layers) and secondary growth conditions (affect microstructures of ZIF-8 membranes). However, it is still important to perform control experiment to make sure that current PDMS coating conditions have already been optimized and no further changes in PDMS coating conditions are required. Table 5.2 shows standard PDMS coating conditions used to seal membrane grain boundary defects. We hypothesize by increasing number of coating layer, PDMS concentration, and coating

duration, the quality of PDMS coating layer will improve and this will lead to significant improvement in propylene/propane separation factor.

Table 5.2 Standard condition used to coat ZIF-8 membranes with PDMS

Variables	**Value**
Concentration of PDMS in hexane (wt.%)	5.0
PDMS flow rate (ml/s)	1.83×10^{-3}
Coating duration (s)	60
Number of PDMS coating layer	1.0
Curing time under vacuum (hrs.)	48

Table 5.3 provide a summary of binary propylene/propane separation performances of various PDMS coated ZIF-8 membranes (i.e., PVDF-9-M-PDMS). For each parameter investigated, other parameters were kept constant following the standard condition.

Table 5.3 Binary propylene/propane separation performance of different PDMS coated ZIF-8 membranes

Concentration of PDMS in hexane	**5 wt.%**	**10 wt.%**
Propylene permeance	109	105
Separation factor	4.4	4.9
Number of coating layer	**1 layer**	**2 layers**
Propylene permeance	105	102
Separation factor	5.1	5.0
Coating duration	**60 s**	**600 s**
Propylene permeance	111	110
Separation factor	4.0	4.0

Propylene permeance unit: $\times 10^{-10}$ mol/(m^2•Pa•s)

Based on the result shown in Table 5.3, no significant changes in propylene permeance and propylene/propane separation factor were observed. Decreasing trend in propylene permeance was observed due to slight increase in PDMS layer thickness. Based on these results, we conclude that standard PDMS coating conditions are sufficiently good and no further changes are required.

5.3.4.2. Optimization of ZIF-8 seeding steps

Even though the quality of ZIF-8 seed layers synthesized using standard condition (i.e., KOH treatment of 9 min) are considered as good, crystal densities and surface coverage of ZIF-8 crystals on substrate can further be improved. As shown in Figure 5.1, surface pores of pristine PVDF HFs are relatively large. In some cases the pore size can be as large as 700 nm. After ZIF-8 seeding step, densely packed ZIF-8 seeds 60 nm in size were deposited on polymer surfaces, however, the pores were not filled with ZIF-8 crystals. We have strong reason to believe that if these pores were to be filled with ZIF-8 crystals, we may be able to synthesize ZIF-8 membranes with better grain boundary structures. One possible way to fill the pores with ZIF-8 crystals is to promote higher heterogeneous nucleation density of ZIF-8 on PVDF surfaces.

To increase ZIF-8 nucleation rate, KOH treatment time was increased from 9 min to 15 min and later to 20 min. Longer KOH treatment increases the amount of C=C and -OH groups available on polymer surfaces which then promotes higher heterogeneous nucleation density of ZIF-8. As shown in Figure 5.11, sizes of ZIF-8 seed crystals for all cases were comparable (~60 nm). However, there are a few differences in microstructure

of the seed layers. As KOH treatment time was increased from 9 min to 15 min, more ZIF-8 crystals were deposited on the bore side of PVDF HF, however, they were still not enough to completely fill pore of PVDF. Further increasing KOH treatment to 20 min unfortunately did not led to higher ZIF-8 crystal formation due to pore enlargement. Pore enlargement from longer KOH treatment observed in this study was consistent with previous study by Rabuni et al.[190] and Xiao et al.[101] ZIF-8 seed layers synthesized using PVDF HFs subjected to 20 min KOH treatment were more discontinuous due to less surfaces for ZIF-8 seed crystals to attach to during ZIF-8 seeding step.

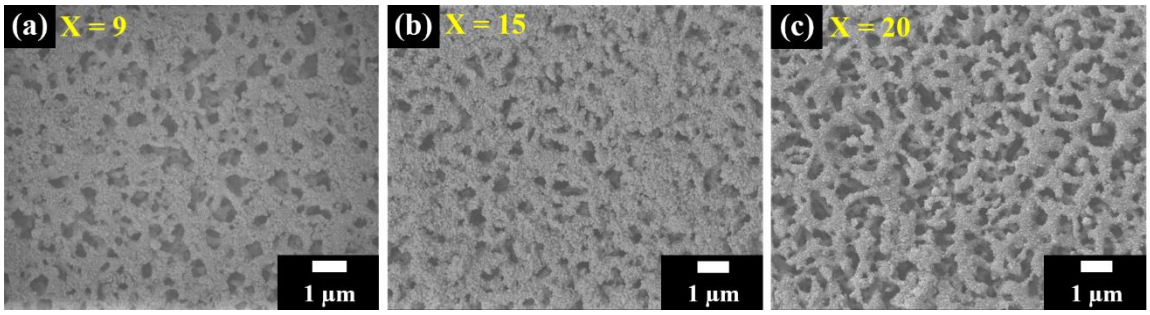

Figure 5.11 Top SEM images of seeded HF after subjected to KOH treatment (i.e., X) for (a) 9 min (b) 15 min (c) 20 min

The seeded PVDF HFs (i.e., PVDF-9-S, PVDF-15-S, and PVDF-20-S) were then secondarily grown into ZIF-8 membranes following similar standard secondary growth procedure described in earlier section. Binary propylene/propane separation performances of each membrane are presented in Table 5.4. PVDF-20-M displayed the worst separation performances. As previously explained, the pores of PVDF HF after 20 min KOH treatment were enlarged. In addition, ZIF-8 seed layers were more discontinuous with no ZIF-8 crystal filling in the pores. During secondary growth, ZIF-8 seed crystals have to grow and cover these large pores resulting in membranes with poorer grain boundary.

Table 5.4 Binary propylene/propane separation performance of ZIF-8 membranes synthesized using PVDF HFs treated in KOH for different period of time

KOH treatment (X min)	PVDF-X-M		PVDF-X-M-PDMS	
	Propylene permeance	Separation factor	Propylene permeance	Separation factor
9	123	2.6	109	4.4
15	162	2.3	107	5.9
20	360	1.9	380	1.7

Propylene permeance unit: $\times 10^{-10}$ mol/(m^2•Pa•s)

On the other hand, separation performances of PVDF-9-M and PVDF-15-M, without PDMS coating were comparable. After PDMS coating step, both of the membranes showed improvement in propylene/propane separation factor but the improvement were not great. PVDF-15-M-PDMS showed higher propylene/propane separation factor than PVDF-9-M-PDMS presumably due to better membrane microstructures, originating from higher ZIF-8 seed crystal density. Based on above result, we conclude that 9 min or 15 min KOH treatment time may be the best condition for seeding step. Prolonging PVDF dehydroxylation reaction longer than 15 min is not recommended as KOH further deteriorates and enlarges substrate's pores resulting in poorer quality ZIF-8 seed crystals and membranes.

5.3.4.3. Optimization of secondary growth steps (secondary growth flow rate)

To the best of our knowledge, we are the only group that works on synthesis of ZIF-8 membranes on bore side of polymer HFs using microfluidic secondary growth

method. There are little to no information on the effect of secondary growth flow rates on ZIF-8 membrane microstructures and their separation performances available in literature. Therefore, we are keen to know what effect secondary growth flow rates have on ZIF-8 membrane performances. We initially postulate that we may be able to obtain membranes with tighter grain boundary structures if the secondary growth flow rates were to be reduced. Our initial claim is based on the fact that most of ZIF-8 membranes with propylene/propane separation factor higher than 35 are synthesized on easily accessible external surface (i.e., flat disc) under static condition inside an autoclave. In this study, we decided to investigate three different secondary growth flow rates: (1) 1.67×10^{-3} ml/s (2) 1.67×10^{-4} ml/s (3) 1.67×10^{-5} ml/s. KOH treatment time of 9 min and secondary growth time of 6 hrs. are selected in this study.

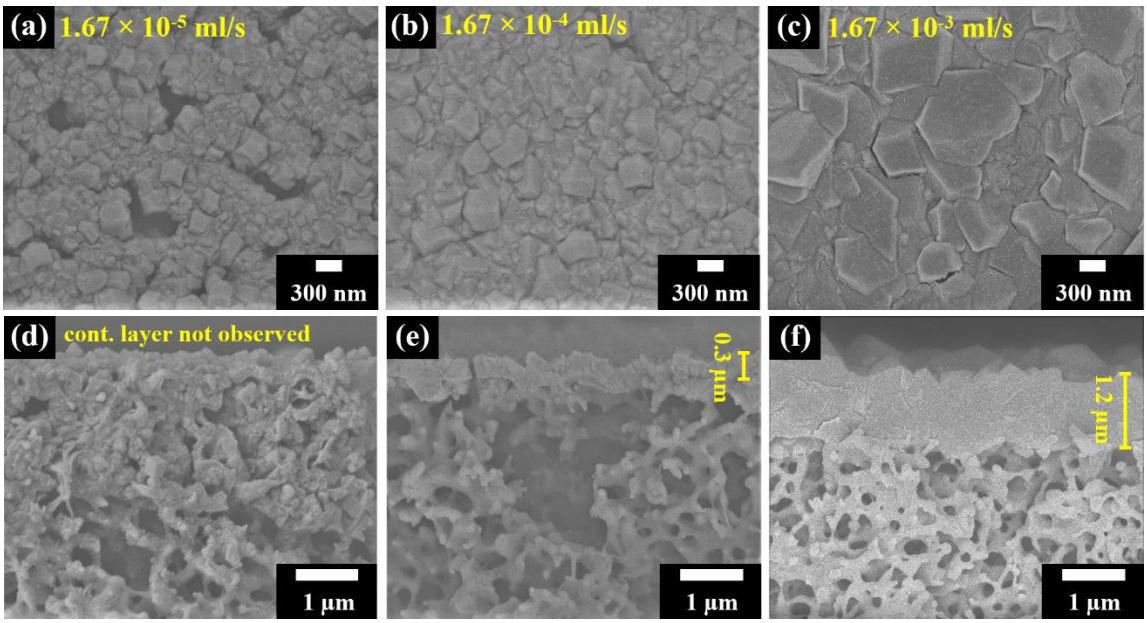

Figure 5.12 (a - c) top and (d - f) cross section SEM images of ZIF-8 membranes synthesized using different secondary growth flow rates

Figure 5.12 shows top and cross section microstructures of ZIF-8 membranes synthesized under different secondary growth flow rates. ZIF-8 membranes grown using secondary growth flow rate of 1.67×10^{-3} ml/s form thick (~1.2 μm), continuous, and well-intergrown polycrystalline layer. As shown in Figure 5.12b, reducing secondary growth flow rate by 10 times led to the formation of thinner ZIF-8 membranes (~300 nm thick). However, the membranes were barely covering the substrate surfaces. Further reducing the secondary growth flow rates by 100 times led to ZIF-8 membranes with large defects (large voids several hundred nanometer in size). Cross section SEM image of the membranes did not show formation of continuous polycrystalline layer (see Figure 5.12a and Figure 5.12d).

Nevertheless, both of the membranes (i.e., ZIF-8 membranes synthesized using secondary growth flow rates of 1.67×10^{-4} ml/s and 1.67×10^{-5} ml/s) possess many micro defects and most likely will not show good propylene/propane separation factor. Due to extremely low secondary growth flow rates, the ZIF-8 seed crystals on PVDF HFs were unable to fully grow into thick and well-intergrown membranes. Therefore, it is critical to perform secondary growth at higher flow rates to ensure sufficient growth nutrient is available for ZIF-8 seed layers to grow into continuous and defect-free membranes.

Binary propylene/propane separation performance of ZIF-8 membranes are presented in Table 5.5. As expected, ZIF-8 membranes synthesized using low secondary growth flow rates (i.e., 1.67×10^{-5} ml/s and 1.67×10^{-4} ml/s) have high propylene permeance and are not selective towards propylene. For comparison the propylene permeance of pristine PVDF HFs is $4992 \pm 38 \times 10^{-10}$ mol/(m^2•Pa•s). This result is

unsurprising because we observed a lot of large voids and pinhole defects on membrane surfaces. In this case, PDMS coating step are not performed because ZIF-8 membranes are too defective. Coating the membrane with PDMS is not going to improve performances of the membranes.

Table 5.5 Binary propylene/propane separation performance of ZIF-8 membranes synthesized using different secondary growth flow rate

Flow rate (ml/s)	PVDF-9-M		PVDF-9-M-PDMS	
	Propylene permeance	Separation factor	Propylene permeance	Separation factor
1.67×10^{-5}	2512	1.0	-	-
1.67×10^{-4}	4254	1.0	-	-
1.67×10^{-3}	123	2.6	109	4.4
3.34×10^{-3}	244	3.8	220	4.4

Propylene permeance unit: $\times 10^{-10}$ mol/(m^2•Pa•s)

Based on SEM analysis and propylene/propane permeation measurements, we conclude that it is necessary perform secondary growth under high flow rates to obtain continuous and well-intergrown ZIF-8 membranes. So, we decided to increase the secondary growth flow rates to 3.34×10^{-3} ml/s. The separation performances of the membranes are presented in Table 5.5. The membranes displayed propylene permeance of 244×10^{-10} mol/(m^2•Pa•s) and propylene/propane separation factor of 3.8. After PDMS coating step, propylene permeance and separation factor unfortunately does not increase as much (propylene permeance of 220×10^{-10} mol/(m^2•Pa•s) and separation factor of 4.4). We unfortunately could not further increase secondary growth flow rate beyond 3.34×10^{-3} ml/s due to limitation of syringe pumps.

5.3.4.4. Optimization of secondary growth steps (tertiary growth)

The basic idea behind tertiary growth is to further grow the existing ZIF-8 layers previously grown via secondary growth. Further crystal growth led to formation of thicker ZIF-8 membranes with larger grain sizes. By performing tertiary growth, we expect to obtain membranes with tighter grain boundary structures. Obviously, there will be a slight reduction in propylene permeance but propylene/propane separation factor may increase tremendously. To perform tertiary growth, the ZIF-8 membrane synthesized using secondary growth method was subjected to additional secondary growth cycle at similar flow rate for 6 hrs. A standard 9 min KOH treatment time was used for seeding step.

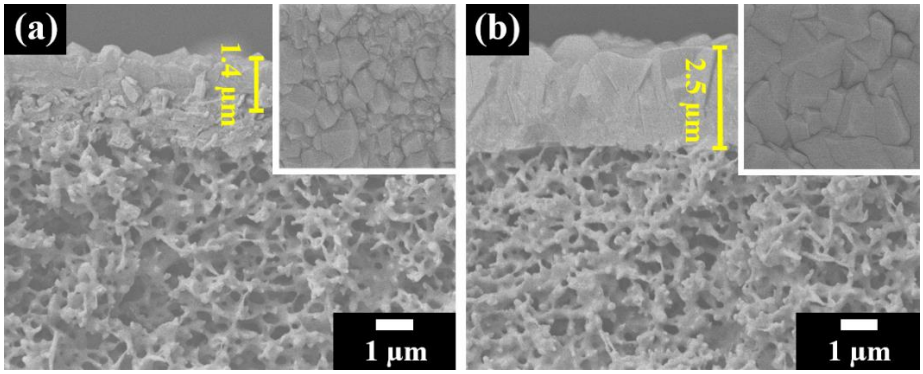

Figure 5.13 Cross section SEM images of ZIF-8 membrane on PVDF HF after (a) secondary growth (b) tertiary growth. Inset images shows the top view of the membranes

The microstructures of ZIF-8 membranes after tertiary grown are presented in Figure 5.13. Inset SEM images revealed that both membranes (i.e., after secondary and tertiary growth) were continuous and defect-free but tertiary grown ZIF-8 membranes have larger crystal grains due to further crystal growth. The thickness of the membrane increased from 1.4 µm to 2.5 µm. Based on quick microstructure analysis, we expect that

separation performances of ZIF-8 membranes after tertiary growth improves but unfortunately no improvement was observed (result not shown). Even though there are several more of secondary growth parameter that can be investigated, we decided not to pursue those area because we believe main issue is likely due to unsuitable pore size of PVDF HFs. Unless this issue is addressed first, whatever secondary growth optimization that we performed will not improve performances of the ZIF-8 membranes.

5.4. Conclusions

In summary, we have presented a new methodology for the preparation of ZIF-8 membranes on bore side of PVDF HFs using secondary growth method. This simple method enables us to transform the relatively cheap PVDF HF ultrafiltration membranes for water separation into high quality ZIF-8 membranes for propylene/propane separation. PVDF dehydroflorination reaction creates abundance of active groups to promote high heterogeneous nucleation of ZIF-8, resulting in formation of densely packed ZIF-8 seed layers on bore side of the HFs. Subsequent microfluidic secondary growth led to formation of continuous and well-intergrown 1.2 μm thick ZIF-8 membranes well anchored to PVDF substrates. Our best ZIF-8 membranes, after PDMS coating, displayed an average propylene permeance and separation factor as high as 107×10^{-10} mol/(m^2•Pa•s) and 5.9, respectively, which unfortunately are not that attractive. Microstructure control is required to synthesize ZIF-8 membranes with fewer micro-defects in order to improve propylene/propane separation performances of the membranes.

6. CONCLUSIONS AND FUTURE DIRECTIONS

6.1. Conclusion

In this dissertation, we discussed several challenges in synthesizing pure ZIF-8 membranes on scalable HF substrates for large scale propylene/propane separation. Although much progress has been made, difficulty in preparing large area ZIF-8 membranes on inorganic/organic substrates and expensive membrane processing (especially those grown on inorganic ceramic substrates) limit their widespread uses as gas separation membranes. Herein, we explored the prospect of using inexpensive polymer HF substrates for the synthesis of high quality ZIF-8 membranes intended for high performance propylene/propane separation. Two new ZIF-8 seeding strategies, namely PMMOF seeding and KOH-assisted solvothermal seeding have been developed with sole purpose of selective deposition of densely packed ZIF-8 seed layers on bore side of polymer HFs. Microfluidic secondary growth conducted at room temperature led to formation of defect-free ultrathin ZIF-8 membranes.

Our first objective was to study ZIF thin film formation using PMMOF method. Imide rings of polyimides were hydrolyzed with strong base and later doped with Zn ions. Subsequent solvothermal treatment in linker solution led to formation of high quality ZIF thin films. In addition to ZIF thin films, formation of ZIF/polymer mixed matrix layers was also observed, a microstructure that has never been previously observed. Metal ion doping can be simply changed, thereby enabling us to prepare a variety of ZIF thin films (i.e., ZIF-8, ZIF-67, and Zn/Co mixed metal ZIF-8). This simple yet versatile method

allows ZIF thin films to be grown on any polyimides. Ultrathin ZIF-8 thin films on different polyimide substrates (e.g., as Matrimid®, Kapton®, and Torlon®) with various geometries were demonstrated.

Our second objective was to synthesize ultrathin ZIF-8 membranes on polymer HFs for propylene/propane separation using the PMMOF method. Commercially available polyimide, Matrimid® HFs were chosen as substrates for membrane synthesis. Site-selective nature of PMMOF process enables formation of densely packed ZIF-8 seed nanocrystals selectively on bore side of Matrimid® HFs. Microfluidic secondary growth led to formation of defect-free ~900 nm thick ZIF-8 membranes. Facile PDMS coating minimizes grain boundary defects, resulting in an improvement of membrane performances (propylene permeability and separation factor of 99 Barrer and 40, respectively), satisfying commercial requirement for propylene-selective membranes.

Our final objective was to look for a novel method to prepare ultrathin ZIF-8 membranes on cheaper and more readily available PVDF ultrafiltration or microfiltration HF membranes commonly used in water separation. Facile KOH-assisted solvothermal seeding was proposed. KOH solution modified the PVDF polymer, created plenty of hydroxyl groups to enhance high heterogeneous nucleation of ZIF-8. KOH treatment of 9 min was found optimum to prepare high quality ZIF-8 seed layers. Similar to the PMMOF method, KOH-assisted seeding method was also site-selective, allowing ZIF-8 seed layers to be deposited on bore side of PVDF HFs and later grown into well-intergrown membranes. Propylene/propane separation performances of the ~1.2 μm thick ZIF-8 membranes were unsatisfactory even after PDMS coating (ZIF-8 membranes with best

separation performances: propylene permeance of 107 × 10^{-10} mol/(m^2•Pa•s) and separation factor of 5.9), indicating poor membrane microstructures.

6.2. Future directions

6.2.1. Optimization and microstructure control of ZIF-8 membranes

As described in Chapter 4 and 5, propylene/propane separation performances of ZIF-8 membranes on both Matrimid® and PVDF HFs, without PDMS coating were poor, presumably due to high concentration of grain boundary defects. Although applying thin layer of PDMS improves separation performances of the membranes, it adds unnecessary steps to the already complex ZIF-8 membrane formation process. Rather than relying on PDMS coating layer to improve separation performances of the as-synthesized ZIF-8 membranes, controlling membrane microstructures through systematic optimization of seeding and secondary growth could be a better solution.

To best of our knowledge, we are the only group (Hamid et al.[181] and Lee et al.[10]) that work on synthesis of ZIF-8 membranes on bore side of polymer HFs via microfluidic secondary growth for propylene/propane separation. Currently there has been no follow up studies to improve microstructures of our ZIF-8 membranes. Establishing solid fundamentals on microstructure-property relationship of ZIF-8 membranes on polymer HFs prepared under microfluidic condition is therefore necessary. In this section, we proposed several future works to improve membrane microstructures for high resolution propylene/propane separation.

Among ZIF-8 membranes reported in literature, those with propylene/propane separation factor greater than 35 are mostly grown under static and tightly regulated condition (e.g., Kwon et al.[118] and Lee et al.[158] to list a few). Autoclave-based synthesis provides uniform and vibration free environment for ZIF-8 seed nanocrystals to grow into well-intergrown membranes with better grain boundary structures. For the synthesis of ZIF-8 membranes on polymer HFs using microfluidic secondary growth, a number of non-ideal growth conditions that may affect growth of ZIF-8 crystals exist (e.g., vibration from open environment, occasional non-uniform flow, and concentration gradients along HF length). We hypothesized that if similar static secondary growth condition can be replicated, the resulting ZIF-8 membranes may possess tighter grain boundary. Therefore, we proposed a simple secondary growth flow protocol where static and continuous flow of growth solution is alternated. Static secondary growth enables the ZIF-8 crystals to grow uninterrupted under static condition while continuous flow helps to replenish depleted growth nutrient.

As mentioned in Chapter 5, ZIF-8 membranes grown on PVDF HFs unfortunately displayed very little improvement in separation factor even though ZIF-8 seeding and secondary growth optimization have been carried out. This led us to look into the possibility that surface pores of pristine PVDF HF may be unsuitable for preparation of high quality ZIF-8 membranes. As shown in Figure 5.1a, pores on bore side of pristine PVDF HFs are relatively large (sometimes reaching up to 700 nm in diameter). Even though densely packed ZIF-8 seed layers have been successfully deposited on the PVDF surface, in order to form continuous polycrystalline layers, these seed nanocrystals have

to grow and cover large gaps between two neighboring pores. We have a reason to believe that ZIF-8 grain boundary structures across the pores are not as good compared to those on the surfaces due to low ZIF-8 crystal density as illustrated in Figure 6.1. Defect density of the membranes would be even higher especially when ultrathin membranes are prepared. To test this hypothesis, we propose that these empty pores to be filled with ZIF-8 nanocrystals to form a continuous ZIF-8 seed layers. These seed layers can later be grown into ZIF-8 membranes following similar secondary growth mentioned in Chapter 5. Of course, a much simpler option would be to use PVDF HFs with smaller pores.

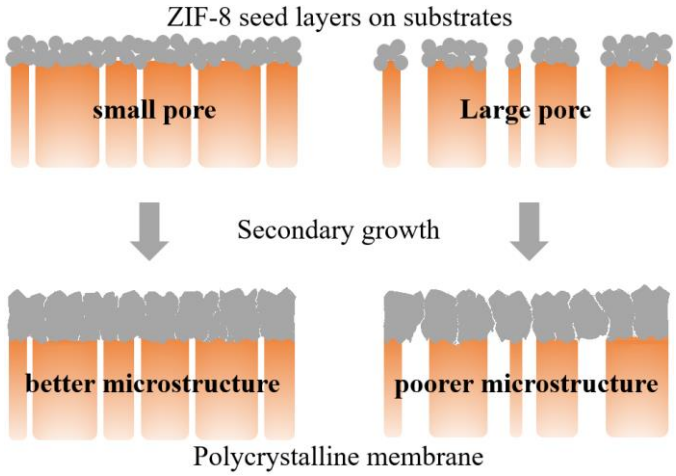

Figure 6.1 Schematic of ZIF-8 membranes grown on large and small pore substrates. It is hypothesized that ZIF-8 membranes grown on large pore substrates possess poorer grain boundary structures because ZIF-8 seed crystals have to cover large pores in order to create continuous ZIF-8 layers

6.2.2. Synthesis of high productivity ZIF-8 membranes

For practical application, increasing propylene productivity of ZIF-8 membranes is important to justify high membrane cost.[180] Productivity of ZIF-8 membranes can be improved by using high surface-to-volume ratio substrates and reducing membrane thickness. As described in Chapter 4 and 5, we have successfully demonstrated the

formation of ultrathin ZIF-8 membranes on high surface-to-volume ratio substrates (i.e., polymer HFs). To further reduce membrane thicknesses, we propose thickness control strategy through simple manipulation of secondary growth flow rates. Our initial study showed that thickness of ZIF-8 membranes can be reduced by decreasing the flow rate of secondary growth solution. Unlike our previously reported work that utilized post-synthetic linker exchange to effectively reduce effective membrane thickness,[147] the proposed method is much simpler.

6.2.3. ZIF-8 membrane testing under a more realistic condition

It is worth highlighting that propylene/propane permeation measurements of ZIF-8 membranes were carried out at room temperature and atmospheric pressure, which are considered too ideal for separation membranes. In petrochemical industry, propylene/propane mixtures output of refinery steam crackers or reactor purge are under pressure between 15 - 30 bar depending on plant condition.[153, 191, 192] Before considering membrane scale-up, it is therefore, critical to evaluate ZIF-8 membranes true separation potentials under high pressure conditions. For that, we propose to perform high pressure (i.e., 15 bar) propylene/propane permeation measurements and investigate membrane long term stability under this condition.

6.2.4. Scaling-up ZIF-8 membranes (membrane module formation)

Today's gas separation plants require between 1,000 - 500,000 sq. meter of membrane area, depending on scale of separation.[193] Despite a few laboratory/small scale

success, scaling-up the synthesis of polycrystalline ZIF-8 membranes on polymer HFs to meet commercial scale separation requirement is a daunting task. To date, most of research works on the synthesis of ZIF-8 membranes on polymer HFs focus on single fiber synthesis and single fiber testing because they can be performed with relative ease. To evaluate the feasibility of scaling-up ZIF-8 membrane synthesis, it would be best to start considering multiple HF synthesis with larger dimension (i.e., length).

As shown in Figure 6.2, one can start transitioning from small to medium size modules that are capable to house single HF but twice the length. Then, one can move from medium to large modules that can accommodate up to 5 PVDF HFs. Identifying important engineering and technical challenges in synthesizing multiple ZIF-8 membranes on polymer HFs would be beneficial to membrane community. One possible issue that most likely to occur is inconsistency of separation properties in each fibers. Ability to pinpoint defective ZIF-8 membranes and heal the membranes among multiple HFs is hugely important.

Figure 6.2 Optical photograph of different module sizes used for the synthesis of ZIF-8 membranes on polymer HFs

A commercial membrane module, depending on fiber dimension and packing density, contains tens of thousands of HFs inside.[194] One can expect that packaging the

relatively fragile and brittle ZIF-8 membranes on polymer HFs into membrane module element would be extremely challenging. Rather than following conventional route of preparing ZIF-8 membranes prior to membrane module assembly, preparing ZIF-8 membranes inside preformed membrane module is less complicated. Benefit of this method is that one can decouple pure polymer HF packaging into module (which can be done with relative ease on commercial scale) and ZIF-8 membrane synthesis altogether. Of course this requires creative and unconventional ZIF-8 membranes fabrication strategies.

To the best of our knowledge, there are only two research groups that have successfully demonstrated synthesis of multiple ZIF-8 membranes on polymer HFs inside preformed membrane modules.[78, 84] We believe that our PMMOF and KOH-assisted solvothermal seeding method could also be used to prepare ZIF-8 membranes inside preformed membrane modules. The ability to prepare ZIF-8 membranes inside preformed membrane modules using either PMMOF method or KOH-assisted solvothermal seeding method is a significant step forward towards commercialization of ZIF-8 membranes.

REFERENCES

1. Eldridge, R. B., Olefin/paraffin separation technology: a review. *Ind. Eng. Chem. Res.* **1993**, *32*, 2208-2212.

2. Das, M.; Koros, W. J., Performance of 6FDA-6FpDA polyimide for propylene/propane separations. *J. Membr. Sci.* **2010**, *365*, 399-408.

3. Hamid, M. R. A.; Jeong, H.-K., Recent advances on mixed-matrix membranes for gas separation: Opportunities and engineering challenges. *Korean J. Chem. Eng.* **2018**, *35*, 1577-1600.

4. Baker, R. W., Future directions of membrane gas separation technology. *Ind. Eng. Chem. Res.* **2002**, *41*, 1393-1411.

5. Li, J.-R.; Kuppler, R. J.; Zhou, H.-C., Selective gas adsorption and separation in metal-organic frameworks. *Chem. Soc. Rev.* **2009**, *38*, 1477-1504.

6. Furukawa, H.; Cordova, K. E.; O'Keeffe, M.; Yaghi, O. M., The chemistry and applications of metal-organic frameworks. *Science* **2013**, *341*, 1230444.

7. Park, K. S.; Ni, Z.; Côté, A. P.; Choi, J. Y.; Huang, R.; Uribe-Romo, F. J.; Chae, H. K.; O'Keeffe, M.; Yaghi, O. M., Exceptional chemical and thermal stability of zeolitic imidazolate frameworks. *Proc. Natl. Acad. Sci. U.S.A.* **2006**, *103*, 10186-10191.

8. Phan, A.; Doonan, C. J.; Uribe-Romo, F. J.; Knobler, C. B.; O'keeffe, M.; Yaghi, O. M., Synthesis, structure, and carbon dioxide capture properties of zeolitic imidazolate frameworks. *Acc. Chem. Res.* **2009**, *43*, 58-67.

9. Banerjee, R.; Phan, A.; Wang, B.; Knobler, C.; Furukawa, H.; O'Keeffe, M.; Yaghi, O. M., High-throughput synthesis of zeolitic imidazolate frameworks and application to CO2 capture. *Science* **2008**, *319*, 939-943.

10. Lee, M. J.; Hamid, M. R. A.; Lee, J.; Kim, J. S.; Lee, Y. M.; Jeong, H.-K., Ultrathin zeolitic-imidazolate framework ZIF-8 membranes on polymeric hollow fibers for propylene/propane separation. *J. Membr. Sci.* **2018**, *559*, 28-34.

11. Zhang, C.; Lively, R. P.; Zhang, K.; Johnson, J. R.; Karvan, O.; Koros, W. J., Unexpected Molecular Sieving Properties of Zeolitic Imidazolate Framework-8. *J. Phys. Chem. Lett.* **2012**, *3*, 2130-2134.

12. Li, K.; Olson, D. H.; Seidel, J.; Emge, T. J.; Gong, H.; Zeng, H.; Li, J., Zeolitic Imidazolate Frameworks for Kinetic Separation of Propane and Propene. *J. Am. Chem. Soc.* **2009**, *131*, 10368-10369.

13. Colling, C. W.; Huff Jr, G. A.; Bartels, J. V., Processes using solid perm-selective membranes in multiple groups for simultaneous recovery of specified products from a fluid mixture. International Patent WO2004002609A3, 2004.

14. Koros, W. J.; Mahajan, R., Pushing the limits on possibilities for large scale gas separation: which strategies? *J. Membr. Sci.* **2000**, *175*, 181-196.

15. Amghizar, I.; Vandewalle, L. A.; Van Geem, K. M.; Marin, G. B., New trends in olefin production. *Engineering* **2017**, *3*, 171-178.

16. Torres Galvis, H. M.; de Jong, K. P., Catalysts for production of lower olefins from synthesis gas: a review. *ACS Catal.* **2013**, *3*, 2130-2149.

17. Galadima, A.; Muraza, O., Recent developments on silicoaluminates and silicoaluminophosphates in the methanol-to-propylene reaction: a mini review. *Ind. Eng. Chem. Res.* **2015**, *54*, 4891-4905.

18. Blay, V.; Epelde, E.; Miravalles, R.; Perea, L. A., Converting olefins to propene: Ethene to propene and olefin cracking. *Catal. Rev.* **2018**, *60*, 278-335.

19. Akah, A.; Al-Ghrami, M., Maximizing propylene production via FCC technology. *Appl. Petrochem. Res.* **2015**, *5*, 377-392.

20. Energy, U. S. D. o. *Hydrocarbon Gas Liquids (HGL): Recent Market Trends and Issues*; U.S. Department of Energy: Washington, DC, 2014; pp 1 - 34.

21. Angelini, P.; Armstrong, T.; Counce, R.; Griffith, W.; LKlasson, T.; Muralidharan, G.; Narula, C.; Sikka, V.; Closset, G.; Keller, G. *Materials for separation technologies: Energy and emission reduction opportunities*; Department of Energy's Office of Energy Efficiency and Renewable Energy: Washington, DC, 2005; p 103.

22. Sholl, D. S.; Lively, R. P., Seven chemical separations to change the world. *Nat. News* **2016**, *532*, 435.

23. Ho, W.; Sirkar, K., *Membrane handbook*. Springer: New York, NY, 2012.

24. Ravanchi, M. T.; Kaghazchi, T.; Kargari, A., Application of membrane separation processes in petrochemical industry: a review. *Desalination* **2009**, *235*, 199-244.

25. Meindersma, G.; Kuczynski, M., Implementing membrane technology in the process industry: problems and opportunities. *J. Membr. Sci.* **1996**, *113*, 285-292.

26. Freeman, B. D., Basis of permeability/selectivity tradeoff relations in polymeric gas separation membranes. *Macromolecules* **1999**, *32*, 375-380.

27. Ladewig, B.; Al-Shaeli, M. N. Z., *Fundamentals of membrane bioreactors*. Springer: East Singapore, Singapore, 2017.

28. Bernardo, P.; Drioli, E.; Golemme, G., Membrane gas separation: a review/state of the art. *Ind. Eng. Chem. Res.* **2009**, *48*, 4638-4663.

29. Galizia, M.; Chi, W. S.; Smith, Z. P.; Merkel, T. C.; Baker, R. W.; Freeman, B. D., 50th anniversary perspective: Polymers and mixed matrix membranes for gas and vapor separation: A review and prospective opportunities. *Macromolecules* **2017**, *50*, 7809-7843.

30. Baker, R. W., *Membrane technology and applications*. John Wiley & Sons: West Sussex, United Kingdom, 2012.

31. Hilal, N.; Ismail, A. F.; Wright, C., *Membrane fabrication*. CRC Press: Boca Raton, FL, 2015.

32. Vanherck, K.; Koeckelberghs, G.; Vankelecom, I. F., Crosslinking polyimides for membrane applications: a review. *Prog. Polym. Sci.* **2013**, *38*, 874-896.

33. Robeson, L. M., The upper bound revisited. *J. Membr. Sci.* **2008**, *320*, 390-400.

34. Goh, P.; Ismail, A.; Sanip, S.; Ng, B.; Aziz, M., Recent advances of inorganic fillers in mixed matrix membrane for gas separation. *Sep. Purif. Technol.* **2011**, *81*, 243-264.

35. Koros, W. J., Some opportunities & challenges for our membrane community to consider-with an Emphasis on gas separations. *Membr. Sci. Technol.* **2006**, *26*, 1-5.

36. Hunger, K.; Schmeling, N.; Jeazet, H. B.; Janiak, C.; Staudt, C.; Kleinermanns, K., Investigation of cross-linked and additive containing polymer materials for membranes

with improved performance in pervaporation and gas separation. *Membranes* **2012**, *2*, 727-763.

37. Sehgal, R.; Brinker, C. J., Supported inorganic membranes. U.S. Patent US5772735A, 1998.

38. Kluiters, S. *Status review on membrane systems for hydrogen separation*; Energy research Centre of the Netherlands ECN: Petten, Netherlands, 2004; p 29.

39. Caro, J., Hierarchy in inorganic membranes. *Chem. Soc. Rev.* **2016**, *45*, 3468-3478.

40. Tavolaro, A.; Drioli, E., Zeolite membranes. *Adv. Mater.* **1999**, *11*, 975-996.

41. Lin, Y.; Duke, M. C., Recent progress in polycrystalline zeolite membrane research. *Curr. Opin. Chem. Eng.* **2013**, *2*, 209-216.

42. Gascon, J.; Kapteijn, F.; Zornoza, B.; Sebastian, V.; Casado, C.; Coronas, J., Practical approach to zeolitic membranes and coatings: state of the art, opportunities, barriers, and future perspectives. *Chem. Mater.* **2012**, *24*, 2829-2844.

43. Carreon, M. A.; Li, S.; Falconer, J. L.; Noble, R. D., Alumina-supported SAPO-34 membranes for CO_2/CH_4 separation. *J. Am. Chem. Soc.* **2008**, *130*, 5412-5413.

44. Yang, S.; Cao, Z.; Arvanitis, A.; Sun, X.; Xu, Z.; Dong, J., DDR-type zeolite membrane synthesis, modification and gas permeation studies. *J. Membr. Sci.* **2016**, *505*, 194-204.

45. White, J. C.; Dutta, P. K.; Shqau, K.; Verweij, H., Synthesis of ultrathin zeolite Y membranes and their application for separation of carbon dioxide and nitrogen gases. *Langmuir* **2010**, *26*, 10287-10293.

46. Lee, T.; Choi, J.; Tsapatsis, M., On the performance of c-oriented MFI zeolite Membranes treated by rapid thermal processing. *J. Membr. Sci.* **2013**, *436*, 79-89.

47. Koros, W. J.; Zhang, C., Materials for next-generation molecularly selective synthetic membranes. *Nat. Mater.* **2017**, *16*, 289.

48. HÄGG, M. B.; Lie, J. A.; Lindbråthen, A., Carbon molecular sieve membranes: a promising alternative for selected industrial applications. *Ann. N. Y. Acad. Sci.* **2003**, *984*, 329-345.

49. Vu, D. Q.; Koros, W. J.; Miller, S. J., High pressure CO_2/CH_4 separation using carbon molecular sieve hollow fiber membranes. *Ind. Eng. Chem. Res.* **2002**, *41*, 367-380.

50. Kim, Y. K.; Park, H. B.; Lee, Y. M., Preparation and characterization of carbon molecular sieve membranes derived from BTDA-ODA polyimide and their gas separation properties. *J. Membr. Sci.* **2005**, *255*, 265-273.

51. Tseng, H.-H.; Itta, A. K., Modification of carbon molecular sieve membrane structure by self-assisted deposition carbon segment for gas separation. *J. Membr. Sci.* **2012**, *389*, 223-233.

52. Choi, J.; Jeong, H.-K.; Snyder, M. A.; Stoeger, J. A.; Masel, R. I.; Tsapatsis, M., Grain boundary defect elimination in a zeolite membrane by rapid thermal processing. *Science* **2009**, *325*, 590-593.

53. Xomeritakis, G.; Lai, Z.; Tsapatsis, M., Separation of xylene isomer vapors with oriented MFI membranes made by seeded growth. *Ind. Eng. Chem. Res.* **2001**, *40*, 544-552.

54. Caro, J., Are MOF membranes better in gas separation than those made of zeolites? *Curr. Opin. Chem. Eng.* **2011**, *1*, 77-83.

55. Vu, D. Q.; Koros, W. J.; Miller, S. J., Mixed matrix membranes using carbon molecular sieves: I. Preparation and experimental results. *J. Membr. Sci.* **2003**, *211*, 311-334.

56. Chen, B.; Yang, Z.; Zhu, Y.; Xia, Y., Zeolitic imidazolate framework materials: recent progress in synthesis and applications. *J. Mater. Chem. A* **2014**, *2*, 16811-16831.

57. Yao, J.; Wang, H., Zeolitic imidazolate framework composite membranes and thin films: synthesis and applications. *Chem. Soc. Rev.* **2014**, *43*, 4470-4493.

58. Li, Y.; Liang, F.; Bux, H.; Yang, W.; Caro, J., Zeolitic imidazolate framework ZIF-7 based molecular sieve membrane for hydrogen separation. *J. Membr. Sci.* **2010**, *354*, 48-54.

59. Kwon, H. T.; Jeong, H.-K., In situ synthesis of thin zeolitic–imidazolate framework ZIF-8 membranes exhibiting exceptionally high propylene/propane separation. *J. Am. Chem. Soc.* **2013**, *135*, 10763-10768.

60. Huang, A.; Bux, H.; Steinbach, F.; Caro, J., Molecular-sieve membrane with hydrogen permselectivity: ZIF-22 in LTA topology prepared with 3-aminopropyltriethoxysilane as covalent linker. *Angew. Chem. Int. Ed.* **2010**, *49*, 4958-4961.

61. Liu, Y.; Hu, E.; Khan, E. A.; Lai, Z., Synthesis and characterization of ZIF-69 membranes and separation for CO_2/CO mixture. *J. Membr. Sci.* **2010**, *353*, 36-40.

62. Huang, A.; Dou, W.; Caro, J. r., Steam-stable zeolitic imidazolate framework ZIF-90 membrane with hydrogen selectivity through covalent functionalization. *J. Am. Chem. Soc.* **2010**, *132*, 15562-15564.

63. Hobday, C. L.; Bennett, T. D.; Fairen-Jimenez, D.; Graham, A. J.; Morrison, C. A.; Allan, D. R.; Düren, T.; Moggach, S. A., Tuning the swing effect by chemical functionalization of zeolitic imidazolate frameworks. *J. Am. Chem. Soc.* **2017**, *140*, 382-387.

64. Drioli, E.; Giorno, L., *Encyclopedia of Membranes*. Springer: Berlin, Germany, 2015.

65. Yampolskii, Y.; Freeman, B., *Membrane gas separation*. John Wiley and Sons: West Sussex, United Kingdom, 2010.

66. Shah, M.; McCarthy, M. C.; Sachdeva, S.; Lee, A. K.; Jeong, H.-K., Current Status of Metal-Organic Framework Membranes for Gas Separations: Promises and Challenges. *Ind. Eng. Chem. Res.* **2012**, *51*, 2179-2199.

67. Zhu, Y.; Liu, Q.; Caro, J.; Huang, A., Highly hydrogen-permselective zeolitic imidazolate framework ZIF-8 membranes prepared on coarse and macroporous tubes through repeated synthesis. *Sep. Purif. Technol.* **2015**, *146*, 68-74.

68. Abdul Hamid, M. R.; Park, S.; Kim, J. S.; Lee, Y. M.; Jeong, H.-K., In situ formation of zeolitic-imidazolate framework thin films and composites using modified polymer substrates. *J. Mater. Chem. A* **2019**, *7*, 9680-9689.

69. Snyder, M. A.; Tsapatsis, M., Hierarchical nanomanufacturing: from shaped zeolite nanoparticles to high-performance separation membranes. *Angew. Chem. Int. Ed.* **2007**, *46*, 7560-7573.

70. Kwon, H. T.; Jeong, H.-K., Highly propylene-selective supported zeolite-imidazolate framework (ZIF-8) membranes synthesized by rapid microwave-assisted seeding and secondary growth. *Chem. Commun.* **2013**, *49*, 3854-3856.

71. Pan, Y.; Lai, Z., Sharp separation of C_2/C_3 hydrocarbon mixtures by zeolitic imidazolate framework-8 (ZIF-8) membranes synthesized in aqueous solutions. *Chem. Commun.* **2011**, *47*, 10275-10277.

72. Li, W.; Meng, Q.; Zhang, C.; Zhang, G., Metal-Organic Framework/PVDF Composite Membranes with High H_2 Permselectivity Synthesized by Ammoniation. *Chem.: Eur. J.* **2015**, *21*, 7224-7230.

73. Hou, J.; Sutrisna, P. D.; Wang, T.; Gao, S.; Li, Q.; Zhou, C.; Sun, S.; Yang, H.-C.; Wei, F.; Ruggiero, M. T.; Zeitler, J. A.; Cheetham, A. K.; Liang, K.; Chen, V., Unraveling the Interfacial Structure-Performance Correlation of Flexible Metal-Organic Framework Membranes on Polymeric Substrates. *ACS Appl. Mater. Interfaces* **2019**, *11*, 5570-5577.

74. Hou, J.; Sutrisna, P. D.; Zhang, Y.; Chen, V., Formation of ultrathin, continuous metal-organic framework membranes on flexible polymer substrates. *Angew. Chem. Int. Ed.* **2016**, *55*, 3947-3951.

75. Kong, L.; Zhang, G.; Liu, H.; Zhang, X., APTES-assisted synthesis of ZIF-8 films on the inner surface of capillary quartz tubes via flow system. *Mater. Lett.* **2015**, *141*, 344-346.

76. Cacho-Bailo, F.; Catalan-Aguirre, S.; Etxeberria-Benavides, M.; Karvan, O.; Sebastian, V.; Tellez, C.; Coronas, J., Metal-organic framework membranes on the inner-

side of a polymeric hollow fiber by microfluidic synthesis. *J. Membr. Sci.* **2015**, *476*, 277-285.

77. Marti, A. M.; Wickramanayake, W.; Dahe, G.; Sekizkardes, A.; Bank, T. L.; Hopkinson, D. P.; Venna, S. R., Continuous Flow Processing of ZIF-8 Membranes on Polymeric Porous Hollow Fiber Supports for CO_2 Capture. *ACS Appl. Mater. Interfaces* **2017**, *9*, 5678-5682.

78. Brown, A. J.; Brunelli, N. A.; Eum, K.; Rashidi, F.; Johnson, J.; Koros, W. J.; Jones, C. W.; Nair, S., Interfacial microfluidic processing of metal-organic framework hollow fiber membranes. *Science* **2014**, *345*, 72-75.

79. Echaide-Górriz, C.; Clément, C.; Cacho-Bailo, F.; Téllez, C.; Coronas, J., New strategies based on microfluidics for the synthesis of metal–organic frameworks and their membranes. *J. Mater. Chem. A* **2018**, *6*, 5485-5506.

80. Eum, K.; Ma, C.; Rownaghi, A.; Jones, C. W.; Nair, S., ZIF-8 membranes via interfacial microfluidic processing in polymeric hollow fibers: efficient propylene separation at elevated pressures. *ACS Appl. Mater. Interfaces* **2016**, *8*, 25337-25342.

81. Eum, K.; Rownaghi, A.; Choi, D.; Bhave, R. R.; Jones, C. W.; Nair, S., Fluidic Processing of High-Performance ZIF-8 Membranes on Polymeric Hollow Fibers: Mechanistic Insights and Microstructure Control. *Adv. Funct. Mater.* **2016**, *26*, 5011-5018.

82. Biswal, B. P.; Bhaskar, A.; Banerjee, R.; Kharul, U. K., Selective interfacial synthesis of metal-organic frameworks on a polybenzimidazole hollow fiber membrane for gas separation. *Nanoscale* **2015**, *7*, 7291-7298.

83. Ma, X.; Kumar, P.; Mittal, N.; Khlyustova, A.; Daoutidis, P.; Mkhoyan, K. A.; Tsapatsis, M., Zeolitic imidazolate framework membranes made by ligand-induced permselectivation. *Science* **2018**, *361*, 1008.

84. Li, W.; Su, P.; Li, Z.; Xu, Z.; Wang, F.; Ou, H.; Zhang, J.; Zhang, G.; Zeng, E., Ultrathin metal-organic framework membrane production by gel-vapour deposition. *Nat. Commun.* **2017**, *8*, 406.

85. Li, W.; Wu, W.; Li, Z.; Shi, J.; Xia, Y., Sol-gel asynchronous crystallization of ultra-selective metal-organic framework membranes for gas separation. *J. Mater. Chem. A* **2018**, *6*, 16333-16340.

86. Zhang, C.; Wu, B.-H.; Ma, M.-Q.; Wang, Z.; Xu, Z.-K., Ultrathin metal/covalent-organic framework membranes towards ultimate separation. *Chem. Soc. Rev.* **2019**, *48*, 3811-3841.

87. Sheng, L.; Wang, C.; Yang, F.; Xiang, L.; Huang, X.; Yu, J.; Zhang, L.; Pan, Y.; Li, Y., Enhanced C_3H_6/C_3H_8 separation performance on MOF membranes through blocking defects and hindering framework flexibility by silicone rubber coating. *Chem. Commun.* **2017**, *53*, 7760-7763.

88. Henis, J. M.; Tripodi, M. K., Multicomponent membranes for gas separations. U.S. Patent US4230463A, 1980.

89. Pinnau, I.; He, Z., Pure- and mixed-gas permeation properties of polydimethylsiloxane for hydrocarbon/methane and hydrocarbon/hydrogen separation. *J. Membr. Sci.* **2004**, *244*, 227-233.

90. Fang, M.; Wu, C.; Yang, Z.; Wang, T.; Xia, Y.; Li, J., ZIF-8/PDMS mixed matrix membranes for propane/nitrogen mixture separation: Experimental result and permeation model validation. *J. Membr. Sci.* **2015**, *474*, 103-113.

91. Hirayama, Y.; Yoshinaga, T.; Kusuki, Y.; Ninomiya, K.; Sakakibara, T.; Tamari, T., Relation of gas permeability with structure of aromatic polyimides I. *J. Membr. Sci.* **1996**, *111*, 169-182.

92. Akamatsu, K.; Ikeda, S.; Nawafune, H.; Deki, S., Surface Modification-Based Synthesis and Microstructural Tuning of Nanocomposite Layers: Monodispersed Copper Nanoparticles in Polyimide Resins. *Chem. Mater.* **2003**, *15*, 2488-2491.

93. Li, Y.; Lu, Q.; Qian, X.; Zhu, Z.; Yin, J., Preparation of surface bound silver nanoparticles on polyimide by surface modification method and its application on electroless metal deposition. *Appl. Surf. Sci.* **2004**, *233*, 299-306.

94. Mu, S.; Wu, Z.; Wang, Y.; Qi, S.; Yang, X.; Wu, D., Formation and characterization of cobalt oxide layers on polyimide films via surface modification and ion-exchange technique. *Thin Solid Films* **2010**, *518*, 4175-4182.

95. Lee, K. W.; Kowalczyk, S. P.; Shaw, J. M., Surface modification of PMDA-oxydianiline polyimide. Surface structure-adhesion relationship. *Macromolecules* **1990**, *23*, 2097-2100.

96. Lee, K. W.; Kowalczyk, S. P.; Shaw, J. M., Surface modification of BPDA-PDA polyimide. *Langmuir* **1991**, *7*, 2450-2453.

97. Tsuruoka, T.; Kumano, M.; Mantani, K.; Matsuyama, T.; Miyanaga, A.; Ohhashi, T.; Takashima, Y.; Minami, H.; Suzuki, T.; Imagawa, K. J. C. G., Interfacial Synthetic

Approach for Constructing Metal-Organic Framework Crystals Using Metal Ion-Doped Polymer Substrate. *Cryst. Growth Des.* **2016**, *16*, 2472-2476.

98. Liu, F.; Hashim, N. A.; Liu, Y.; Abed, M. M.; Li, K., Progress in the production and modification of PVDF membranes. *J. Membr. Sci.* **2011**, *375*, 1-27.

99. Wongchitphimon, S.; Wang, R.; Jiraratananon, R., Surface modification of polyvinylidene fluoride-co-hexafluoropropylene (PVDF-HFP) hollow fiber membrane for membrane gas absorption. *J. Membr. Sci.* **2011**, *381*, 183-191.

100. Al-Gharabli, S.; Mavukkandy, M. O.; Kujawa, J.; Nunes, S. P.; Arafat, H. A., Activation of PVDF membranes through facile hydroxylation of the polymeric dope. *J. Mater. Res.* **2017**, *32*, 4219-4231.

101. Xiao, L.; Davenport, D. M.; Ormsbee, L.; Bhattacharyya, D., Polymerization and functionalization of membrane pores for water related applications. *Ind. Eng. Chem. Res.* **2015**, *54*, 4174-4182.

102. Komaki, Y., Growth of fine holes by the chemical etching of fission tracks in polyvinylidene fluoride. *Nucl. Tracks* **1979**, *3*, 33-44.

103. Shinohara, H., Fluorination of polyhydrofluoroethylenes. II. Formation of perfluoroalkyl carboxylic acids on the surface region of poly(vinylidene fluoride) film by oxyfluorination, fluorination, and hydrolysis. *J. Polym. Sci.: Polym. Chem. Ed.* **1979**, *17*, 1543-1556.

104. Brewis, D.; Mathieson, I.; Sutherland, I.; Cayless, R.; Dahm, R., Pretreatment of poly (vinyl fluoride) and poly (vinylidene fluoride) with potassium hydroxide. *Int. J. Adhes. Adhes.* **1996**, *16*, 87-95.

105. Sun, C.; Feng, X., Enhancing the performance of PVDF membranes by hydrophilic surface modification via amine treatment. *Sep. Purif. Technol.* **2017**, *185*, 94-102.

106. Bottino, A.; Capannelli, G.; Monticelli, O.; Piaggio, P., Poly (vinylidene fluoride) with improved functionalization for membrane production. *J. Membr. Sci.* **2000**, *166*, 23-29.

107. Murray, L. J.; Dincă, M.; Long, J. R., Hydrogen storage in metal-organic frameworks. *Chem. Soc. Rev.* **2009**, *38*, 1294-1314.

108. Li, J.-R.; Sculley, J.; Zhou, H.-C., Metal-organic frameworks for separations. *Chem. Rev.* **2011**, *112*, 869-932.

109. Kreno, L. E.; Leong, K.; Farha, O. K.; Allendorf, M.; Van Duyne, R. P.; Hupp, J. T., Metal-organic framework materials as chemical sensors. *Chem. Rev.* **2011**, *112*, 1105-1125.

110. Lee, J.; Farha, O. K.; Roberts, J.; Scheidt, K. A.; Nguyen, S. T.; Hupp, J. T., Metal-organic framework materials as catalysts. *Chem. Soc. Rev.* **2009**, *38*, 1450-1459.

111. Wang, B.; Côté, A. P.; Furukawa, H.; O'Keeffe, M.; Yaghi, O. M., Colossal cages in zeolitic imidazolate frameworks as selective carbon dioxide reservoirs. *Nature* **2008**, *453*, 207.

112. Czaja, A. U.; Trukhan, N.; Müller, U., Industrial applications of metal-organic frameworks. *Chem. Soc. Rev.* **2009**, *38*, 1284-1293.

113. Silva, P.; Vilela, S. M.; Tomé, J. P.; Paz, F. A. A., Multifunctional metal-organic frameworks: from academia to industrial applications. *Chem. Soc. Rev.* **2015**, *44*, 6774-6803.

114. Shekhah, O.; Liu, J.; Fischer, R.; Wöll, C., MOF thin films: existing and future applications. *Chem. Soc. Rev.* **2011**, *40*, 1081-1106.

115. Liu, J.; Wöll, C., Surface-supported metal-organic framework thin films: fabrication methods, applications, and challenges. *Chem. Soc. Rev.* **2017**, *46*, 5730-5770.

116. Pan, Y.; Li, T.; Lestari, G.; Lai, Z., Effective separation of propylene/propane binary mixtures by ZIF-8 membranes. *J. Membr. Sci.* **2012**, *390*, 93-98.

117. Shah, M.; Kwon, H. T.; Tran, V.; Sachdeva, S.; Jeong, H.-K., One step in situ synthesis of supported zeolitic imidazolate framework ZIF-8 membranes: Role of sodium formate. *Microporous Mesoporous Mater.* **2013**, *165*, 63-69.

118. Kwon, H. T.; Jeong, H.-K.; Lee, A. S.; An, H. S.; Lee, J. S., Heteroepitaxially grown zeolitic imidazolate framework membranes with unprecedented propylene/propane separation performances. *J. Am. Chem. Soc.* **2015**, *137*, 12304-12311.

119. Shamsaei, E.; Lin, X.; Low, Z.-X.; Abbasi, Z.; Hu, Y.; Liu, J. Z.; Wang, H., Aqueous phase synthesis of ZIF-8 membrane with controllable location on an asymmetrically porous polymer substrate. *ACS Appl. Mater. Interfaces* **2016**, *8*, 6236-6244.

120. Cacho-Bailo, F.; Seoane, B.; Téllez, C.; Coronas, J., ZIF-8 continuous membrane on porous polysulfone for hydrogen separation. *J. Membr. Sci.* **2014**, *464*, 119-126.

121. Li, W.; Yang, Z.; Zhang, G.; Fan, Z.; Meng, Q.; Shen, C.; Gao, C., Stiff metal-organic framework-polyacrylonitrile hollow fiber composite membranes with high gas permeability. *J. Mater. Chem. A* **2014**, *2*, 2110-2118.

122. Brown, A. J.; Johnson, J.; Lydon, M. E.; Koros, W. J.; Jones, C. W.; Nair, S., Continuous polycrystalline zeolitic imidazolate framework-90 membranes on polymeric hollow fibers. *Angew. Chem. Int. Ed.* **2012**, *51*, 10615-10618.

123. Ge, L.; Zhou, W.; Du, A.; Zhu, Z., Porous polyethersulfone-supported zeolitic imidazolate framework membranes for hydrogen separation. *J. Phys. Chem. C* **2012**, *116*, 13264-13270.

124. Barankova, E.; Pradeep, N.; Peinemann, K.-V., Zeolite-imidazolate framework (ZIF-8) membrane synthesis on a mixed-matrix substrate. *Chem. Commun.* **2013**, *49*, 9419-9421.

125. Neelakanda, P.; Barankova, E.; Peinemann, K.-V., Polymer supported ZIF-8 membranes by conversion of sputtered zinc oxide layers. *Microporous Mesoporous Mater.* **2016**, *220*, 215-219.

126. Meilikhov, M.; Yusenko, K.; Schollmeyer, E.; Mayer, C.; Buschmann, H.-J.; Fischer, R. A., Stepwise deposition of metal organic frameworks on flexible synthetic polymer surfaces. *Dalton Trans.* **2011**, *40*, 4838-4841.

127. Li, Y.; Wee, L. H.; Volodin, A.; Martens, J. A.; Vankelecom, I. F., Polymer supported ZIF-8 membranes prepared via an interfacial synthesis method. *Chem. Commun.* **2015**, *51*, 918-920.

128. Centrone, A.; Yang, Y.; Speakman, S.; Bromberg, L.; Rutledge, G. C.; Hatton, T. A., Growth of metal-organic frameworks on polymer surfaces. *J. Am. Chem. Soc.* **2010**, *132*, 15687-15691.

129. Yao, J.; Dong, D.; Li, D.; He, L.; Xu, G.; Wang, H., Contra-diffusion synthesis of ZIF-8 films on a polymer substrate. *Chem. Commun.* **2011**, *47*, 2559-2561.

130. Nagaraju, D.; Bhagat, D. G.; Banerjee, R.; Kharul, U. K., In situ growth of metal-organic frameworks on a porous ultrafiltration membrane for gas separation. *J. Mater. Chem. A* **2013**, *1*, 8828-8835.

131. Tsuruoka, T.; Mantani, K.; Miyanaga, A.; Matsuyama, T.; Ohhashi, T.; Takashima, Y.; Akamatsu, K., Morphology control of metal–organic frameworks based on paddle-wheel units on ion-doped polymer substrate using an interfacial growth approach. *Langmuir* **2016**, *32*, 6068-6073.

132. Ohhashi, T.; Tsuruoka, T.; Fujimoto, S.; Takashima, Y.; Akamatsu, K., Controlling the Orientation of Metal–Organic Framework Crystals by an Interfacial Growth Approach Using a Metal Ion-Doped Polymer Substrate. *Cryst. Growth Des.* **2018**, *18*, 402-408.

133. Woo, K. T.; Lee, J.; Dong, G.; Kim, J. S.; Do, Y. S.; Jo, H. J.; Lee, Y. M., Thermally rearranged poly(benzoxazole-co-imide) hollow fiber membranes for CO_2 capture. *J. Membr. Sci.* **2016**, *498*, 125-134.

134. Yang, S.; Wu, D.; Qi, S.; Cui, G.; Jin, R.; Wu, Z., Fabrication of Highly Reflective and Conductive Double-Surface-Silvered Layers Embedded on Polymeric Films through All-Wet Process at Room Temperature. *J. Phys. Chem. B* **2009**, *113*, 9694-9701.

135. Ikeda, S.; Akamatsu, K.; Nawafune, H.; Nishino, T.; Deki, S., Formation and Growth of Copper Nanoparticles from Ion-Doped Precursor Polyimide Layers. *J. Phys. Chem. B* **2004**, *108*, 15599-15607.

136. Huang, X. D.; Bhangale, S. M.; Moran, P. M.; Yakovlev, N. L.; Pan, J., Surface modification studies of Kapton® HN polyimide films. *Polym. Int.* **2003**, *52*, 1064-1069.

137. Wang, M.; Jiang, L.; Kim, E. J.; Hahn, S. H., Electronic structure and optical properties of $Zn(OH)_2$: LDA+U calculations and intense yellow luminescence. *RSC Adv.* **2015**, *5*, 87496-87503.

138. Pradhan, D.; Sindhwani, S.; Leung, K. T., Template-Free Electrochemical Growth of Single-Crystalline Zinc Nanowires at an Anomalously Low Temperature. *J. Phys. Chem. C* **2009**, *113*, 15788-15791.

139. Mu, S.; Wu, D.; Qi, S.; Wu, Z., Preparation of polyimide/zinc oxide nanocomposite films via an ion-exchange technique and their photoluminescence properties. *J. Nanomater.* **2011**, *2011*, 38.

140. Stoffel, N. C.; Hsieh, M.; Chandra, S.; Kramer, E. J., Surface Modification Studies of Polyimide Films Using Rutherford Backscattering and Forward Recoil Spectrometry. *Chem. Mater.* **1996**, *8*, 1035-1041.

141. Tsuruoka, T.; Miyanaga, A.; Ohhashi, T.; Hata, M.; Takashima, Y.; Akamatsu, K., Rational composition control of mixed-lanthanide metal-organic frameworks by an interfacial reaction with metal ion-doped polymer substrates. *J. Solid State Chem.* **2017**, *253*, 43-46.

142. Wang, C.; Yang, F.; Sheng, L.; Yu, J.; Yao, K.; Zhang, L.; Pan, Y., Zinc-substituted ZIF-67 nanocrystals and polycrystalline membranes for propylene/propane separation. *Chem. Commun.* **2016**, *52*, 12578-12581.

143. Eum, K.; Jayachandrababu, K. C.; Rashidi, F.; Zhang, K.; Leisen, J.; Graham, S.; Lively, R. P.; Chance, R. R.; Sholl, D. S.; Jones, C. W.; Nair, S., Highly Tunable Molecular Sieving and Adsorption Properties of Mixed-Linker Zeolitic Imidazolate Frameworks. *J. Am. Chem. Soc.* **2015**, *137*, 4191-4197.

144. Huang, L.; Xue, M.; Song, Q.; Chen, S.; Pan, Y.; Qiu, S., Carbon dioxide selective adsorption within a highly stable mixed-ligand Zeolitic Imidazolate Framework. *Inorg. Chem. Commun.* **2014**, *46*, 9-12.

145. Hillman, F.; Zimmerman, J. M.; Paek, S.-M.; Hamid, M. R. A.; Lim, W. T.; Jeong, H.-K., Rapid microwave-assisted synthesis of hybrid zeolitic-imidazolate frameworks with mixed metals and mixed linkers. *J. Mater. Chem. A* **2017**, *5*, 6090-6099.

146. Tsuruoka, T.; Matsuyama, T.; Miyanaga, A.; Ohhashi, T.; Takashima, Y.; Akamatsu, K., Site-selective growth of metal–organic frameworks using an interfacial growth approach combined with VUV photolithography. *RSC Adv.* **2016**, *6*, 77297-77300.

147. Lee, M. J.; Kwon, H. T.; Jeong, H.-K., High-Flux Zeolitic Imidazolate Framework Membranes for Propylene/Propane Separation by Postsynthetic Linker Exchange. *Angew. Chem. Int. Ed.* **2018**, *57*, 156-161.

148. Sun, J.; Yu, C.; Jeong, H.-K., Propylene-Selective Thin Zeolitic Imidazolate Framework Membranes on Ceramic Tubes by Microwave Seeding and Solvothermal Secondary Growth. *Crystals* **2018**, *8*, 373.

149. Huang, K.; Wang, B.; Chi, Y.; Li, K., High Propylene Selective Metal-Organic Framework Membranes Prepared in Confined Spaces via Convective Circulation Synthesis. *Adv. Mater. Interfaces* **2018**, *5*, 1800287.

150. Hara, N.; Yoshimune, M.; Negishi, H.; Haraya, K.; Hara, S.; Yamaguchi, T., Diffusive separation of propylene/propane with ZIF-8 membranes. *J. Membr. Sci.* **2014**, *450*, 215-223.

151. Hara, N.; Yoshimune, M.; Negishi, H.; Haraya, K.; Hara, S.; Yamaguchi, T., ZIF-8 membranes prepared at miscible and immiscible liquid-liquid interfaces. *Microporous Mesoporous Mater.* **2015**, *206*, 75-80.

152. Kang, Z.; Fan, L.; Sun, D., Recent advances and challenges of metal-organic framework membranes for gas separation. *J. Mater. Chem. A* **2017**, *5*, 10073-10091.

153. Ma, X.; Liu, D., Zeolitic Imidazolate Framework Membranes for Light Olefin/Paraffin Separation. *Crystals* **2018**, *9*.

154. Lovallo, M. C.; Gouzinis, A.; Tsapatsis, M., Synthesis and characterization of oriented MFI membranes prepared by secondary growth. *AIChE J.* **1998**, *44*, 1903-1913.

155. Tin, P. S.; Chung, T. S.; Liu, Y.; Wang, R.; Liu, S. L.; Pramoda, K. P., Effects of cross-linking modification on gas separation performance of Matrimid membranes. *J. Membr. Sci.* **2003**, *225*, 77-90.

156. Huang, D.; Xin, Q.; Ni, Y.; Shuai, Y.; Wang, S.; Li, Y.; Ye, H.; Lin, L.; Ding, X.; Zhang, Y., Synergistic effects of zeolite imidazole framework@graphene oxide composites in humidified mixed matrix membranes on CO_2 separation. *RSC Adv.* **2018**, *8*, 6099-6109.

157. Sadrzadeh, M.; Amirilargani, M.; Shahidi, K.; Mohammadi, T., Gas permeation through a synthesized composite PDMS/PES membrane. *J. Membr. Sci.* **2009**, *342*, 236-250.

158. Lee, M. J.; Kwon, H. T.; Jeong, H.-K., Defect-dependent stability of highly propylene-selective zeolitic-imidazolate framework ZIF-8 membranes. *J. Membr. Sci.* **2017**, *529*, 105-113.

159. Pan, Y.; Liu, W.; Zhao, Y.; Wang, C.; Lai, Z., Improved ZIF-8 membrane: Effect of activation procedure and determination of diffusivities of light hydrocarbons. *J. Membr. Sci.* **2015**, *493*, 88-96.

160. Liu, D.; Ma, X.; Xi, H.; Lin, Y. S., Gas transport properties and propylene/propane separation characteristics of ZIF-8 membranes. *J. Membr. Sci.* **2014**, *451*, 85-93.

161. Kwon, H. T.; Jeong, H.-K., Improving propylene/propane separation performance of Zeolitic-Imidazolate framework ZIF-8 Membranes. *Chem. Eng. Sci.* **2015**, *124*, 20-26.

162. Ding, Y.; Bikson, B.; Nelson, J. K., Polyimide Membranes Derived from Poly(amic acid) Salt Precursor Polymers. 1. Synthesis and Characterization. *Macromolecules* **2002**, *35*, 905-911.

163. Burns, R. L.; Koros, W. J., Defining the challenges for C_3H_6/C_3H_8 separation using polymeric membranes. *J. Membr. Sci.* **2003**, *211*, 299-309.

164. Krol, J. J.; Boerrigter, M.; Koops, G. H., Polyimide hollow fiber gas separation membranes: preparation and the suppression of plasticization in propane/propylene environments. *J. Membr. Sci.* **2001**, *184*, 275-286.

165. Bai, S.; Sridhar, S.; Khan, A. A., Metal-ion mediated separation of propylene from propane using PPO membranes. *J. Membr. Sci.* **1998**, *147*, 131-139.

166. Sridhar, S.; Khan, A. A., Simulation studies for the separation of propylene and propane by ethylcellulose membrane. *J. Membr. Sci.* **1999**, *159*, 209-219.

167. Staudt-Bickel, C.; Koros, W. J., Olefin/paraffin gas separations with 6FDA-based polyimide membranes. *J. Membr. Sci.* **2000**, *170*, 205-214.

168. Shimazu, A.; Ikeda, K.; Hachisuka, H., Method of selectively separating unsaturated hydrocarbon. U.S. Patent US5749943A, 1998.

169. Tanaka, K.; Taguchi, A.; Hao, J.; Kita, H.; Okamoto, K., Permeation and separation properties of polyimide membranes to olefins and paraffins. *J. Membr. Sci.* **1996**, *121*, 197-207.

170. Swaidan, R. J.; Ghanem, B.; Swaidan, R.; Litwiller, E.; Pinnau, I., Pure- and mixed-gas propylene/propane permeation properties of spiro- and triptycene-based microporous polyimides. *J. Membr. Sci.* **2015**, *492*, 116-122.

171. Okamoto, K.; Noborio, K.; Jianqiang, H.; Tanaka, K.; Kita, H., Permeation and separation properties of polyimide membranes to 1,3-butadiene and n-butane. *J. Membr. Sci.* **1997**, *134*, 171-179.

172. Okamoto, K.-i.; Kawamura, S.; Yoshino, M.; Kita, H.; Hirayama, Y.; Tanihara, N.; Kusuki, Y., Olefin/Paraffin Separation through Carbonized Membranes Derived from an Asymmetric Polyimide Hollow Fiber Membrane. *Ind. Eng. Chem. Res.* **1999**, *38*, 4424-4432.

173. Chng, M. L.; Xiao, Y.; Chung, T.-S.; Toriida, M.; Tamai, S., Enhanced propylene/propane separation by carbonaceous membrane derived from poly (aryl ether ketone)/2,6-bis(4-azidobenzylidene)-4-methyl-cyclohexanone interpenetrating network. *Carbon* **2009**, *47*, 1857-1866.

174. Hayashi, J.-i.; Mizuta, H.; Yamamoto, M.; Kusakabe, K.; Morooka, S.; Suh, S.-H., Separation of Ethane/Ethylene and Propane/Propylene Systems with a Carbonized BPDA-pp‘ODA Polyimide Membrane. *Ind. Eng. Chem. Res.* **1996**, *35*, 4176-4181.

175. Zhou, S.; Wei, Y.; Li, L.; Duan, Y.; Hou, Q.; Zhang, L.; Ding, L.-X.; Xue, J.; Wang, H.; Caro, J., Paralyzed membrane: Current-driven synthesis of a metal-organic framework with sharpened propene/propane separation. *Sci. Adv.* **2018**, *4*, eaau1393.

176. Lee, J. H.; Kim, D.; Shin, H.; Yoo, S. J.; Kwon, H. T.; Kim, J., Zeolitic imidazolate framework ZIF-8 films by ZnO to ZIF-8 conversion and their usage as seed layers for propylene-selective ZIF-8 membranes. *J. Ind. Eng. Chem.* **2019**, *72*, 374-379.

177. Tanaka, S.; Okubo, K.; Kida, K.; Sugita, M.; Takewaki, T., Grain size control of ZIF-8 membranes by seeding-free aqueous synthesis and their performances in propylene/propane separation. *J. Membr. Sci.* **2017**, *544*, 306-311.

178. Ramu, G.; Lee, M.; Jeong, H.-K., Effects of zinc salts on the microstructure and performance of zeolitic-imidazolate framework ZIF-8 membranes for propylene/propane separation. *Microporous Mesoporous Mater.* **2018**, *259*, 155-162.

179. Frost, L.; Scala, L., Method for forming reverse osmosis membranes composed of polyamic acid salts. U.S. Patent US3835207A, 1974.

180. Tsapatsis, M., Toward high-throughput zeolite membranes. *Science* **2011**, *334*, 767-768.

181. Abdul Hamid, M. R.; Park, S.; Kim, J. S.; Lee, Y. M.; Jeong, H.-K., Synthesis of Ultrathin Zeolitic Imidazolate Framework ZIF-8 Membranes on Polymer Hollow Fibers

Using a Polymer Modification Strategy for Propylene/Propane Separation. *Ind. Eng. Chem. Res.* **2019**, *58*, 14947 - 14953.

182. Kang, G.-d.; Cao, Y.-m., Application and modification of poly(vinylidene fluoride) (PVDF) membranes - A review. *J. Membr. Sci.* **2014**, *463*, 145-165.

183. Ji, J.; Liu, F.; Hashim, N. A.; Abed, M. R. M.; Li, K., Poly(vinylidene fluoride) (PVDF) membranes for fluid separation. *React. Funct. Polym.* **2015**, *86*, 134-153.

184. Huang, A.; Liu, Q.; Wang, N.; Caro, J., Highly hydrogen permselective ZIF-8 membranes supported on polydopamine functionalized macroporous stainless-steel-nets. *J. Mater. Chem. A* **2014**, *2*, 8246-8251.

185. Huang, A.; Liu, Q.; Wang, N.; Zhu, Y.; Caro, J. r., Bicontinuous zeolitic imidazolate framework ZIF-8@ GO membrane with enhanced hydrogen selectivity. *J. Am. Chem. Soc.* **2014**, *136*, 14686-14689.

186. Ruan, X.; Zhang, X.; Zhou, Z.; Jiang, X.; Dai, Y.; Yan, X.; He, G., ZIF-8 heterogeneous nucleation and growth mechanism on Zn(II)-doped polydopamine for composite membrane fabrication. *Sep. Purif. Technol.* **2019**, *214*, 95-103.

187. Liu, Q.; Wang, N.; Caro, J. r.; Huang, A., Bio-inspired polydopamine: a versatile and powerful platform for covalent synthesis of molecular sieve membranes. *J. Am. Chem. Soc.* **2013**, *135*, 17679-17682.

188. Yu, Z.; Pan, Y.; He, Y.; Zeng, G.; Shi, H.; Di, H., Preparation of a novel anti-fouling β-cyclodextrin-PVDF membrane. *RSC Adv.* **2015**, *5*, 51364-51370.

189. Meng, N.; Priestley, R. C. E.; Zhang, Y.; Wang, H.; Zhang, X., The effect of reduction degree of GO nanosheets on microstructure and performance of PVDF/GO hybrid membranes. *J. Membr. Sci.* **2016**, *501*, 169-178.

190. Rabuni, M.; Nik Sulaiman, N.; Aroua, M.; Hashim, N. A., Effects of alkaline environments at mild conditions on the stability of PVDF membrane: an experimental study. *Ind. Eng. Chem. Res.* **2013**, *52*, 15874-15882.

191. Alcheikhhamdon, Y.; Pinnau, I.; Chen, B.; Hoorfar, M., Propylene-Propane separation using Zeolitic-Imidazolate Framework (ZIF-8) membranes: Process techno-commercial evaluation. *J. Membr. Sci.* **2019**, 117252.

192. Baker, R. W.; Da Costa, A. R.; Daniels, R., Membrane-augmented manufacture of propylene derivatives. U.S. Patent US6414202B1, 2002.

193. Baker, R. W.; Low, B. T., Gas Separation Membrane Materials: A Perspective. *Macromolecules* **2014**, *47*, 6999-7013.

194. Li, D.; Wang, R.; Chung, T.-S., Fabrication of lab-scale hollow fiber membrane modules with high packing density. *Sep. Purif. Technol.* **2004**, *40*, 15-30.